ABSTRACT

JAMES RIVAS, ARTHUR MC CARTY. Simultaneous Biochar and Syngas Production in a Top-Lit Updraft Biomass Gasifier. (Under the direction of Dr. Wenqiao Yuan and Dr. Michael Boyette.)

Biomass materials can be converted to a wide variety of products, e.g., biochar and syngas through thermochemical conversions. In this study, the thermochemical conversion of biomass residues was carried out in a top-lit updraft gasifier. This gasifier type has been extensively used in developing countries to reduce air pollutants in biomass burning while cooking. However, little literature is found related to the quality and quantification of the products. **The goal of this study was to investigate top-lit updraft gasification as a potential alternative to the production of biochar and syngas from biomass residues**. **The first objective** was to understand the effect of the airflow rate and insulation on the overall top-lit updraft gasification process through the quantification of the products and co-products. The results showed that increasing the airflow rate from 8 to 20 lpm proportionally increased the reaction temperature up to 868^{o}C. This increase in temperature negatively impacted the produced biochar which decreased (e.g., from 39.3% to 31.3%, rice hulls – with insulation) with the increase in airflow rate. Little effect in the syngas composition was noticed when varying the airflow, but significant reduction of the tar content (e.g., from 58.7 to 11.8 g/m3, wood chips – without insulation) was observed with the addition of insulation and increase of airflow, enhancing the quality of the produced biochar. **The second objective** was to investigate the effect of airflow rate and insulation on the properties of the produced biochar. The properties of the biochar were significantly affected by the airflow and the insulation, but their variations were also governed by the properties of the biomass. Due to the large amount of ash in rice hulls (23%), biochar presented decreasing carbon content as the air flow increased, which was

opposite to wood chips biochar because of the low ash content in the untreated wood chips (0.57%). In addition, the BET surface area of the biochar increased up to 332 m^2/g when increasing the airflow, but it further increased to 405 m^2/g with the addition of insulation. **The third objective** was to evaluate the effect of variation of the physical properties of biomass on the products and co-products of top-lit updraft gasification, and on the properties of the biochar. Variation of the moisture content, particle size and density of the biomass mainly affected the biochar yield, reaction temperature, biochar physiochemical properties and tar content in the syngas. For instance, when the particle size was increased, the yield of biochar was higher, but the reaction temperature was reduced, promoting tar production. **The fourth objective** was to investigate the effect of the airflow and physical properties of biomass on the surface chemistry of biochar. The variation of the airflow produced basic biochars (pH>7.0) that presented increasing basic functional group and CEC. However, the variation of the physical properties of the biomass produced a more diversified biochar. For instance, when increasing the biomass compactness from 0 to 3 kg, the biochar presented decreasing pH (from 12 to 0.95) that caused increase in the carboxylic functional group (from 0 to 0.016 mmol g^{-1}) and decrease in the basic functional group (from 0.115 to 0.073 mmol g^{-1}). Finally, **the fifth objective** was to develop a kinetic model to predict the yield of biochar, syngas and tar in a top-lit updraft gasifier. The model developed model considered the three main zone of the gasifier, pyrolysis, incomplete combustion and reduction zone. The validation of the model was found to qualitatively predict the product distribution of biochar, hydrogen, carbon monoxide, and tar in syngas at different airflow rates, moisture contents, particle sizes and biomass compactness.

Simultaneous Biochar and Syngas Production in a Top-Lit Updraft Biomass Gasifier

by
Arthur Mc Carty James Rivas

A dissertation submitted to the Graduate Faculty of
North Carolina State University
in partial fulfillment of the
requirements for the Degree of
Doctor of Philosophy

Biological and Agricultural Engineering

Raleigh, North Carolina

2015

APPROVED BY:

_____	_____
Dr. Wenqiao Yuan	Dr. Michael Boyette
Committee Co-chair	Committee Co-chair
_____	_____
Dr. Praveen Kolar	Dr. Tiegang Fang

_____
Dr. Brian Jackson

DEDICATION

…and whatever you do, whether in word or deed, do it all in the name of the Lord Jesus, giving thanks to God the Father through him. Colossians 3.17 (NIV).

…y todo lo que hagan, de palabra o de obra, háganlo en el nombre del Señor Jesús, dando gracias a Dios el Padre por medio de él. Colosenses 3.17 (NVI). [in Spanish]

BIOGRAPHY

Arthur Mc Carty James Rivas was born in Panama City, Panama. As a teenager he dreamed to be a scientist. As a result, he pursued a bachelor degree in Mechanical Engineering in the Technological University of Panama and graduated in 2007. After working for 1 year as Building Mechanical System designer, he applied for an IFARHU-SENACYT scholarship (Panamanian Government) that he received in spring 2009. In spring 2010, he enrolled in a Master program in Biological and Agricultural Engineering in Kansas State University, and graduated in spring 2012. Shortly after, in fall 2012, he joined NC State University to pursue a Ph.D. in Biological and Agricultural Engineering.

ACKNOWLEDGMENTS

I would like to thank my advisor Dr. Wenqiao Yuan for his outstanding support and guidance during my MS and Ph. D. studies. I also would like to thank Dr. Mike Boyette for sharing his research ideas and encouraging me. I thank my committee members, Dr. Kolar, Dr. Jackson and Dr. Tiegang for their helpful comments and suggestions to improve my work. Thanks to Dr. Wang from Kansas State University and Dr. Kumar from Oklahoma State University for analyzing biochar and biomass samples. Many thanks to Adam Rushing, Meghan Porter and Ty Prentice for their assistance in gasification experiments and biochar analyses. Thanks to Justin Macialek for technical support during experiments and building the top-lit updraft gasifier. I want to specially thank my wife Nimia Itzela for her love, patience and support during this journey. Thanks to all my friends everywhere in the world and in RDU, you have a special place in my heart. Many thanks to all my family, specially my mom (Beatriz), sisters (Nelva and Berta), brother (Abraham) and father and mother-in-law (Ariel and Itzela) for all their prayers and support. I also want to thank Dr. Marcelo Coronado for encouraging me to pursue a Ph.D. in the U.S. and his family (Deyka, Alan, Alec, Reggy and Andres) for welcoming me as part of their family in my first years in the U.S. Finally, I want to thank the Panamanian government for their partial financial support through my IFARHU-SENACYT scholarship.

TABLE OF CONTENTS

LIST OF TABLES

LIST OF FIGURES

CHAPTER 1 - Introduction

Biomass is the organic matter of biological organisms (Wood and Kellogg, 1988). It is considered one of the major target products for energy and chemicals production. The National Renewable Energy Laboratory reported that in the U.S. annually produce more than 248 million dry tonnes of biomass wastes. In addition to 60 thousand dry tonnes of energy crops. For instance, switch grass and hybrid poplar that are specially used to produce bioenergy (Milbrandt, 2005). The importance of producing energy from biomass relies on its carbon source which is the CO_2 from the atmosphere (Lal, 2004). The utilization of carbon from biomass to produce bioenergy and bio-products contributes to reduce the concentration levels of carbon dioxide in the atmosphere (Matovic, 2011). This is achieved through the sequestration of carbon and the neutral production of carbon from biomass-based fuels (Brick and Lytse, 2010). The production of chemicals from biomass is another way to reduce the dependency on fossil fuels in developing countries as well as developed countries. Pyrolysis, gasification and hydrothermal conversion are some examples of thermochemical process to convert biomass into useful products (e.g. biochar, syngas, bio-oil) which can be further processed and implemented in industrial applications (Goyal et al., 2008). Although different processes present their advantages and disadvantages, researchers worldwide are working on optimizing and evaluating biomass conversion processes to improve quality and performance of biomass-based production of fuels and chemicals.

Biomass gasification is the partial oxidation of biomass at high temperatures (Li et al., 2004). In this thermochemical process, biomass and air react to produce biochar and a gas mixture of hydrogen and carbon monoxide known as syngas (Knoef, 2005). Biochar is a carbon-rich

material that is produced at temperatures lower than 700ºC in an oxygen-free atmosphere (Lehmann and Joseph, 2009). Despite the fact that gasifiers are not designed to produce biochar, most gasification units are reported to produce less than 10% biochar that is considered a byproduct of the process and known to represent lack of carbon conversion (Bridgwater, 2012; Cao et al., 2006). This is because the configuration of gasification systems require maximize the yield of gas products rather than carbon production (Cao et al., 2006). In contrast, slow pyrolysis is the most common method for the production of biochar (Jameel et al., 2010). This process maximizes the yield of solid and/or liquid products due to the reaction of biomass at relatively high temperature. However, pyrolysis process often require energy input that decrease the efficiency of the process due to the elevated temperatures and heating rates (Demirbas, 2004; Yaman, 2004). Therefore, if the simultaneous production of syngas and quality biochar from biomass gasification is achieved. Biochar could be produce at a high efficiency because of the generation of exothermic heat for carbonization reactions and the parallel production of syngas.

1.1. Problem Statement

This project was focused on the production of biochar and syngas using biomass gasification process. The utilization of biomass gasification for syngas production has been widely studied. Moreover, since this process is oriented on the production of gases, it is not generally presented as a feasible way for biochar production. The hypothesis of this project is that top-lit updraft (TLUD) gasification could be an alternative for the simultaneous production of biochar and syngas. This process can generate syngas while producing relatively high yields of biochar. However, despite the promising yields of biochar, little work has been done to comprehend the

mechanisms of product generation and physiochemical properties of biochar. In order to understand this process, evaluation of the operational parameters, gasifier design and properties of the biomass need to be correlated with the biochar yield, biochar properties and syngas production. Because of the disadvantage of tar production in gasification systems, tar content in syngas needs to be monitored and quantified; in order to identify primary methods (e.g. such as increase in reaction temperature) that discourage its production in top-lit updraft gasifiers.

1.2. Research objective

The study of the production mechanisms of TLUD helped not only to better understand this gasification process, but also to select appropriate operational conditions for the clean production of syngas, and generation of quality biochar for various applications. As part of this project a kinetic model for the prediction of TLUD products based on the properties of the biomass was developed.

This work was divided into five main objectives:

1) To understand the effect of airflow and insulation on syngas and biochar generations of rice hulls and woodchips in a top-lit updraft gasifier
2) To characterize key properties of biochar from TLUD and correlate such properties to airflow, insulation and biomass properties
3) To examine the effect of physical properties of biomass on the yield and properties of TLUD products
4) To investigate the effect of the airflow and physical properties of biomass on the surface chemistry of biochar.

5) To develop a kinetic model for the prediction of the yield of biochar, syngas and tar in a top-lit updraft gasifier.

1.3. References

Brick, S., & Lyutse, S. (2010). Biochar: Assessing the promise and risks to guide US policy. *Natural Resources Defense Council Issue Paper.Available at:Http://www.Nrdc.org/energy/files/biochar_paper.Pdf (Accessed 3 November 2012),*

Bridgwater, A. V. (2012). Review of fast pyrolysis of biomass and product upgrading. *Biomass and Bioenergy, 38*(0), 68-94. doi:10.1016/j.biombioe.2011.01.048

Cao, Y., Wang, Y., Riley, J. T., & Pan, W. (2006). A novel biomass air gasification process for producing tar-free higher heating value fuel gas. *Fuel Processing Technology, 87*(4), 343-353.

Demirbas, A. (2004). Effects of temperature and particle size on bio-char yield from pyrolysis of agricultural residues. *Journal of Analytical and Applied Pyrolysis, 72*(2), 243-248. doi:10.1016/j.jaap.2004.07.003

Goyal, H., Seal, D., & Saxena, R. (2008). Bio-fuels from thermochemical conversion of renewable resources: A review. *Renewable and Sustainable Energy Reviews, 12*(2), 504-517.

Jameel, H., Keshwani, D. R., Carter, S., Treasure, T., & Cheng, J. (2010). Thermochemical conversion of biomass to power and fuels. *Biomass to Renewable Energy Processes,* , 437-491.

Lal, R. (2004). Soil carbon sequestration to mitigate climate change. *Geoderma, 123*(1), 1-22.

Lehmann, J., & Joseph, S. (2009). In edited by Johannes Lehmann and Stephen Joseph., Lehmann J.,Dr. (Eds.), *Biochar for environmental management : Science and technology*. London: Earthscan. Retrieved from http://www2.lib.ncsu.edu/catalog/record/NCSU2333980

Li, X. T., Grace, J. R., Lim, C. J., Watkinson, A. P., Chen, H. P., & Kim, J. R. (2004). Biomass gasification in a circulating fluidized bed. *Biomass and Bioenergy, 26*(2), 171-193. doi:http://dx.doi.org/10.1016/S0961-9534(03)00084-9

Matovic, D. (2011). Biochar as a viable carbon sequestration option: Global and canadian perspective. *Energy, 36*(4), 2011-2016. doi:http://dx.doi.org.prox.lib.ncsu.edu/10.1016/j.energy.2010.09.031

Milbrandt, A. (2005). *A geographic perspective on the current biomass resource availability in the united states* United States. Department of Energy.

Wood, W. A., & Kellogg, S. T. (1988). *Biomass* Academic Press.

Yaman, S. (2004). Pyrolysis of biomass to produce fuels and chemical feedstocks. *Energy Conversion and Management, 45*(5), 651-671. doi:10.1016/S0196-8904(03)00177-8

CHAPTER 2 – Review of literature

2.1 Syngas production from biomass

Synthetic gas (Syngas) is a gas mixture of carbon monoxide and hydrogen, it could also contain CO_2, N_2, CH_4 if the selected gasification agent is air. This gas is the result of the partial combustion of carbon-based materials at high temperatures (600-1200^oC) (Yong et al., 2014; Richardson et al., 2015). The utilization of gasification to produce syngas has been known for few centuries; it was used to illuminate the streets of London in 1800's (Woolcock and Brown, 2013). The production of syngas involves several zones within the biomass gasifier's bed such as drying, combustion, gasification (or reduction) and pyrolysis zones (Knoef, 2005). These zones can be represented in different locations of the gasifier depending on its design and configuration (Reed and Das, 1988), Fig. 1. In the drying zone, moisture is removed from the biomass particles; this moisture is reacted in other thermochemical reactions to produce hydrogen (Hasan et al., 2010). Moreover, in the combustion zone, exothermic reactions of the carbon and some volatiles from the biomass produce carbon monoxide and carbon dioxide. These gases are used in the gasification reactions to increase the concentration of carbon monoxide and hydrogen in the gas mixture. The pyrolysis zone is the responsible for the formation of condensable aromatic hydrocarbons known as tars (Knoef, 2005). Depending on the gasifier's design, these aromatic hydrocarbons can help to fuel the combustion reactions or to decrease the quality of the syngas due to tar removal by the gas stream (Vreugdenhil and Zwart, 2009). Table 2.1 presents the major reactions occurring in every zone of the gasifier.

Table 2.1. Reactions during gasification of biomass (de Souza-Santos, 2010; Richardson et al., 2015)

Nº	Reactions	Name of reaction
	Drying	
1	Wet biomass + heat → biomass + moisture	Dehydration
	Combustion	
2	$C + ½ O_2 \rightarrow CO + 111$ kJ/mol	Partial combustion
3	$C + O_2 \rightarrow CO_2 + 394$ kJ/mol	Total combustion
4	$C_nH_m + (n/2)O_2 \rightarrow nCO + (m/2)H_2$	Tar partial oxidation
	Gasification	
5	$C + H_2O + 131$ kJ/mol $\rightarrow CO + H_2$	
6	$C + CO_2 + 173$ kJ/mol $\leftrightarrow 2CO$	Boudouard reaction
7	$C + 2H_2 \rightarrow CH_4 + 75$ kJ/mol	Hydrogen gasification
8	$CO_2 + H_2 + 40.9$ kJ/mol $\leftrightarrow CO + H_2O$	Water shift reaction
9	$CO + ½ O_2 \rightarrow CO_2 + 283$ kJ/mol	Carbon monoxide oxidation
10	$H_2 + ½ O_2 \rightarrow H_2O + 285$ kJ/mol	H_2 oxidation
11	$CH_4 + H_2O \rightarrow CO + 3H_2$	Methanation reaction
	Pyrolysis	
12	C_nH_m (tar) + heat → C	Secondary char formation
13	$C_aH_bO_c$(biomass) + heat → C (biochar) + volatiles	Devolatilization
14	Volatiles → gases ($CO + CO_2 + H_2 + CH_4$) + C_nH_m(tar)	

Fixed bed and fluidized bed gasifiers are the two major categories of biomass gasifiers (Richardson et al, 2015). Examples of fixed bed gasifiers are the downdraft, updraft and top-lit updraft. These gasifiers can produce syngas of similar heating value that ranges from 4.5 to 6 MJ/m^3, but their concentrations highly depends on the feedstock and operational parameters (Fremaux et al., 2015; Knoef, 2005). In packed bed gasifiers, the exothermical heat from the combustion zone provides the heat for other thermochemical reactions. Reaction 2 and 3 are examples of exothermic reactions. The combustion zone temperature in updraft gasifiers can

increase up to 1000ºC while in downdraft gasifiers ranges from 1000-1400ºC (Richardson et al, 2015; McKendry, 2002). In fixed bed gasifier, the internal distribution of the zones within the gasifier depends on the location of the combustion zone, the gasification-agent flow direction (e.g. air, oxygen) and the biomass feeding location. The location of the combustion zone in the gasifier can affect the quality of the syngas because of the increase in tar content (Reed and Das, 1988). Tar can cause downstream problems in gasification systems. It has been reported to block pipelines and create solid deposits in system components (Devi et al., 2003; Han and Kim, 2008). In a later section, tar production and minimization are addressed. Updraft gasifiers produce higher quantities of tar when compared with all other gasification technologies. This is because the flow direction of the gasification agent in this gasifier. As presented in figure 2.1A, air flows from the bottom within the combustion, reduction, pyrolysis and drying zones. Tar in this gasifier is mainly formed in the pyrolysis zone from which the syngas stream carries tar. Updraft gasifiers are reported to produce up to 100g/m^3 of tar (Milne et al., 1998). In contrast, downdraft gasifiers have a different configuration that grant them to produce relatively low tar content, since pyrolysis products are burned in the combustion zone, Fig. 2.1B. Downdraft gasifiers are reported to produce tar concentrations from 0.015 to 0.5 g/m^3 (Knoef, 2005). Therefore, downdraft gasifiers can be used to produce gas fuel for heat and power generation applications without major tar cleaning systems (Richardson et al, 2015). However, the utilization of fixed bed reactors for the production of syngas is restricted to small scale applications because of unpredictable variations in the temperature distribution of the gasification bed. Due to temperature instability, hot spots of exothermic reactions cause variation in the syngas composition. The effect of the temperature fluctuation can be

minimized be the utilization of biomass of uniform particle distribution; sizes ranging from 8mm to 50mm are recommended. Ash produced during gasification is also a major problem because when it melts at different ranges of temperature, it causes ash fusion on the grates creating blockages (Warnecke, 2000). All these problems increase as increasing the size of packed bed reactors; limiting downdraft and updraft gasifiers to applications with demands lower than 5 MWe and 20MWe, respectively (Knoef, 2005).

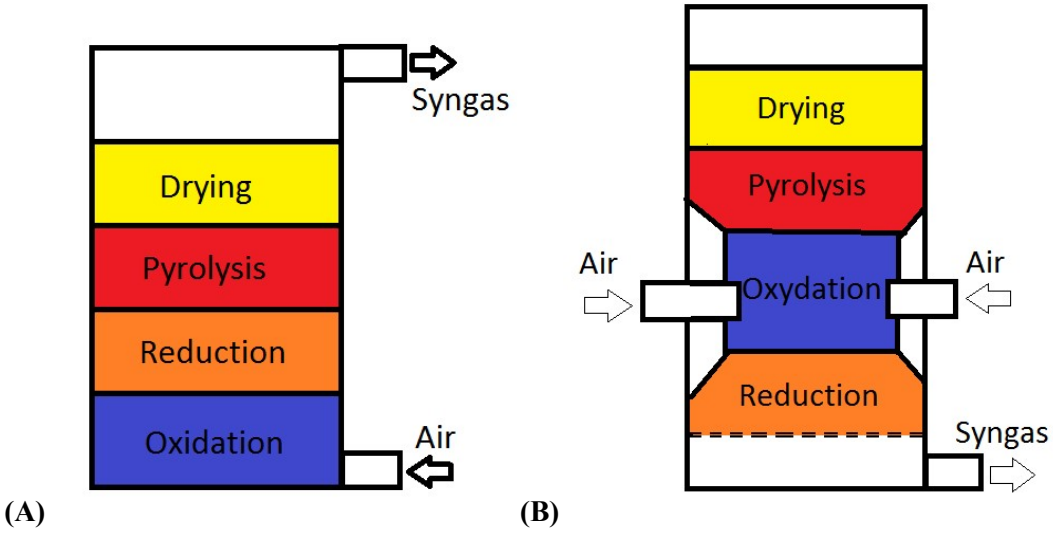

Fig. 2.1. (A) Updraft gasifier and (B) downdraft gasifier, source: (Knoef, 2005)

Fluidized bed gasifiers also produce syngas by the partial combustion of biomass (Lv et al., 2004). However, this reactor works differently compared with fixed bed gasifiers. In operation, biomass is carried from bottom to the top by an air stream injected from the bottom of the reactor. In order to provide the head for reaction, the air could be preheated or external heating devices can transfer heat within the reactor's wall. This reactor usually works in a range of temperature from 750 to 900ºC. The suspended biomass particles are dehydrated and

devolatilize because of the increasing temperatures in the gasifier that promote internal and surface reactions in the biomass. As the biomass particles are carried towards the top of the gasifier; they also release heat due to combustion reactions. This helps maintain a uniform temperature across this reactor (Hasan et al., 2010). Syngas from fluidized bed gasifiers presents similar range of heating value (3.0-5.0 MJ/m^3) compared with fixed bed gasifiers (Cao et al., 2006). Moreover, fluidized bed gasifiers have been reported to produce an average tar concentration of 10 g/m^3 which is between the production levels of updraft and downdraft gasifiers (Milne et al, 1998). However, despite their moderate tar content, fluidized bed gasifiers are more suitable for large scale applications because their uniform temperature distribution and high efficiency that contributes to uniform syngas production (Warnecke, 2000). These facts grant fluidized bed gasifiers to be scale-up to generate syngas for applications up to 100 MWe (Snip et al, 1996).

2.2 Applications of syngas from biomass gasification

The syngas produced from biomass gasification can be used in a wide number of applications including high-value chemical production, and heat and power generation. High concentrations of hydrogen in syngas can be used to produce high-value products (Lv et al, 2007). This can be achieved by steam reforming of syngas. In this process, syngas react with steam at high temperatures (e.g. 800^{o}C); this reforms the syngas increasing its hydrogen and carbon monoxide concentrations. These gases are further used for the production of selective hydrocarbons, diesel, methanol and ammonia (Blasi and Fiorenza, 2013). Fischer Tropsch is an example of a process to use syngas. This process is commonly used for the production of

synthetic crude and light olefins or heavy hydrocarbons. It takes place at temperatures between 200-350^{o}C at high pressures (25-60 bar) using a catalyst such as iron (Knoef, 2005). The possibility of using biomass gasification for the production of hydrocarbons via Fischer Tropsch has been explored; however, required cleaning of syngas is a major disadvantage. The syngas used for this process needs to be cleaned from tars and upgraded to a H_2:CO ratio of 2:1 (Tijmensen et al., 2002). Another potential end application of syngas is Ammonia synthesis. This chemical is highly used for the production of fertilizers (Winsley, 2007). It is produced by the reaction of one mole of nitrogen and 3 moles of hydrogen using iron-based catalysts. The production of hydrogen using biomass can lower the carbon release to the atmosphere when producing ammonia because of the use of renewable materials for its production and nitrogen from the air (Knoef, 2005). Current ammonia production is derived from fossil hydrocarbons by the synthesis of natural gas, naphtha or heavy residual oils (Menon, 1995). Syngas can be also used as a source for the production of hydrogen to upgrade heavy hydrocarbon fractions for the production of transportation fuels in the refinery industry. This could reduce the current dependency on natural gas for the production of hydrogen; however, this technology is still under development (Thengane et al., 2014) due to challenges in the production of clean syngas. Heat and/or power generation are the most developed end applications for syngas from biomass gasification (Hasler and Nussbaumer, 1999; Difs et al., 2010). For instance, despite the contaminants in tar, thousands of biomass gasifiers were used during World War II to power internal combustion engines in vehicles (Reed and Das, 1988). Nowadays, biomass gasifiers are also used for industrial power and heat generation. Large

scale units are being tested in different parts of the world and are capable to produce up to 100 MWe (Morris et al., 2005).

2.3 Production and elimination of tar in biomass gasification

Tars are the organic materials generated during thermochemical oxidation of biomass (Milne and Evan, 1998). The production of tar in gasifiers can be characterized by the formation of different species at different temperatures. Primary tars are derived from the reactions of elemental components of biomass at 500-800^{o}C. These include furfural, acetates, and methoxyphenols. Secondary tars are phenolic and olefin based; higher concentrations of secondary tars are formed at 700-800^{o}C. In addition, alkyl and condensed tertiary components are identified as tars including toluene, naphthalene, pyrene; their concentration increase at temperatures higher than 800^{o}C (Evan and Milne 1997). However, as increasing the reaction temperature, the concentration of most tar species in the syngas are reduced (Baker et al., 1988). These complex hydrocarbons not only cause downstream problems during syngas production, but also can represent permanent damage to industrial equipment depending on the concentration of tar (Richardson, et al., 2015). Therefore, tar limits have been set for the utilization of syngas in industrial equipment. For example, internal combustion engines are required to operate with 20-500 mg/Nm^3 of tar content (Corella, 1996), while industrial gas turbines require tar concentrations lower than 50 mg/Nm^3 (Stevens, 2001).

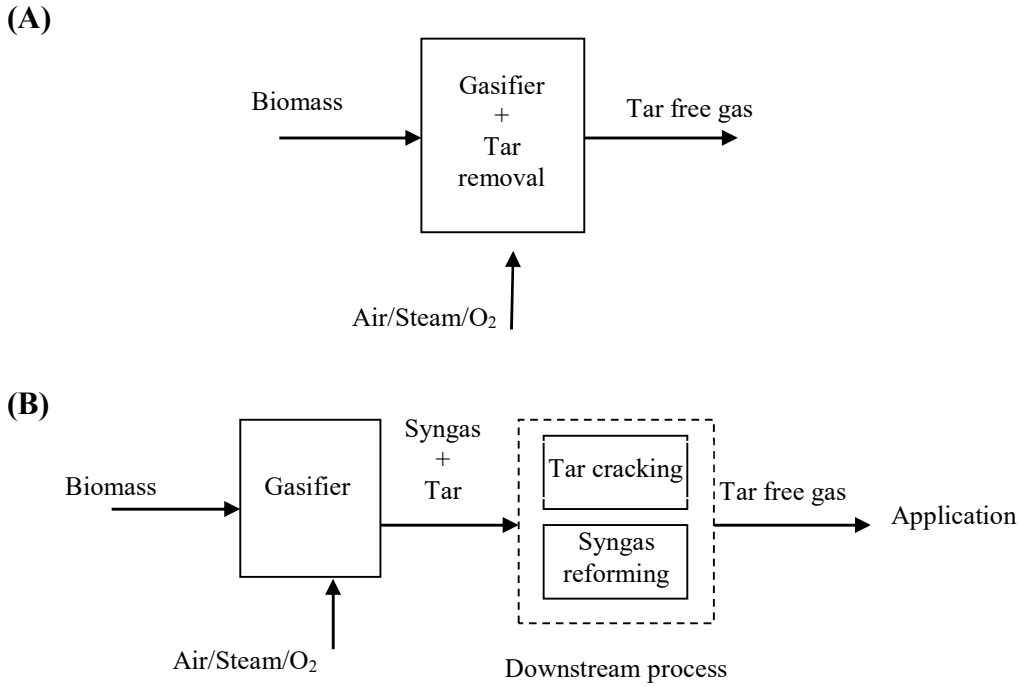

Fig. 2.2. (A) Primary method and (B) Secondary method for tar reduction (Modified from: Devi et al. 2003)

Methods for the reduction and destruction of tars in syngas have been developed. These methods are classified in two groups; primary methods and secondary methods. Primary methods are focused on reducing the production of tar during gasification, Fig. 2.2A. Identification of optimum operational parameters, in-bed catalyst and modification of gasifier design are some examples of the implementation of primary methods (Devi et al., 2003). Cao et al, (2006) studied the performance of a fluidized bed gasifier; the results showed that increasing the reaction temperature from 650 to 840ºC decreased the tar content from 1.2 to 0.3 g/Nm^3. In the same way, Kinoshita et al. (1994) found that increase in the reaction temperature from 700 to 900ºC discourage the formation of tar species in the gasification of sawdust. Narvaez et al. (1996) studied the effect of using calcined dolomite as in-bed catalyst;

additionally, the equivalent ratio effect on gasification performance was evaluated. The results presented that tar was reduced 50 wt% by increasing the equivalent ratio from 0.2 to 0.45. As a result of the subsequent increase in the reaction temperature because of the increasing equivalent ratio. The advantage of the primary methods is the elimination of downstream systems that can add complexity to the gasification process (Richardson et al., 2012). In contrast, the secondary methods are oriented to the post-treatments to remove tar or reform syngas, Fig. 2.2B. This represents the addition of a tar removal/cracking stage at the end of the gasification process. Examples of secondary methods are the physical removal of tar (e.g. filtration), utilization of high temperature reactors and catalytic reactors for tar cracking. The physical removal of tar using methods such as condensation or filtration helps to clean the gas, but it also suggests the collection and disposal of this byproduct (Milne et al., 1998). The utilization of heat to crack tar has been tested; Brandt and Henriksen (2000) used an aluminum oxide reactor to test its potential to crack tars. Reaction temperatures from 1200 to 1290ºC at residence time of 0.5-second was used. It was found that the utilization of this unit could decrease tar content to levels of 12-15 mg/Nm^3. However, even this low levels of tar would need further treatment since some industrial applications might require lower levels of tar content. The use of catalytic reactors is presented as another alternative for tar removal. This is because these reactors not only reduce the amount of tar by cracking it, but also reform the syngas by converting tar to more simple molecules such as hydrogen and carbon monoxide (Han and Kim, 2008; Richardson et al., 2012). Alkali metal catalyst and nickel based catalyst are some examples of chemical medium for tar cracking/reforming. James et al. (2014) studied the utilization of nickel-char catalyst to crack tar and reform syngas in a biomass updraft

gasifier. The results showed that tar decreased by 95% and the heating value of the syngas increased up to 36%. Nickel based catalyst have been extensively studied showing potential for tar conversion efficiencies from 71 to 99.7% and increase in hydrogen and carbon monoxide composition to 61 and 32%, respectively (Rivas, 2012).

2.4 Biochar production in biomass gasification

The utilization of biomass gasification for the production of biochar is a challenging task due to the low yield of biochar in this process. Several studies have reported biochar yields lower than 10% for biomass gasifiers units (Bridgewater, 2012; Brick and Lyutse, 2010). In recent experiments, Qian et al. (2013) studied the production of biochar in a fluidized bed reactor of 102 mm diameter and 1.1 m height. Equivalent ratios of 0.2, 0.25, and 0.3 at temperature of 700, 750 and 800ºC were studied. It was found that the properties of the biochar were affected by the variation of the operational properties. However, the yield of biochar for each parameter was not reported because of the inability of the system to completely collect all the biochar. An average yield of biochar of 12% was reported. Gasifiers are design to maximize the production of gases; as result, they produce low yield of biochar (Manya, 2012). A potential alternative for the production of biochar in biomass gasifiers is the top-lit updraft biomass gasifier (Peterson and Jackson, 2014; Brown, 2009). Due to its simple construction and relatively high yield of biochar, top-lit updraft gasifiers could be implemented in biochar production (Saravanakumar et al., 2007). However, most studies of this reactor have focused on the production of gas products for cooking purposes. A complete study considering product and byproduct quantification of this reactor has not been yet reported. Partial investigations

revealed that this gasifier can produce quality syngas for heat production in developing countries (Mukunda et al., 2010). The top-lit updraft reactor is composed of a vertical chamber with an air plenum at the bottom. Once filled, the top layer of biomass is ignited and then air flows from the bottom to the top. In contact with the fire, the incomplete combustion of the biomass produces enough exothermic heat to increase the combustion temperature. The increase in temperature leads to the production of pyrolysis gases from the biomass below the combustion zone. These pyrolysis gases are used to fuel the combustion zone as the flame moves towards the bottom. On the top of the combustion zone, part of the carbon in the biochar reacts with the gases produced generating hydrogen and carbon monoxide (Saravanakumar et al., 2007). Top-lit updraft gasifiers have been reported to produce yields of biochar of 20-25% (Reed and Larson, 1997). However, higher yield could be also achieved, Birzer (2014) reported biochar yields of up to 40% when carbonizing cow manure in a lab-scale TLUD gasifier. In another study, Huangfu et al. 2014 studied the performance of a small-scale TLUD; the moisture content of the biomass was varied from 5.9% to 22.1%. The results showed that biochar yield decreased with the addition of moisture from 26% to 22%. Despite the reduction in biochar yield, overall high yield of biochar was achieved in this reactor when compared with fluidized bed reactors. TLUDs are promoted in developing countries for cooking purposes due to their low pollutant emissions and high efficiency (Birzer et al., 2013). In addition, these reactors are capable to work with different types of biomass with low energy input (Tryner et al, 2014). As result of collaborative research, several projects have developed a wide variation of TLUD gasifiers for their utilization in developing countries (Reed and Larson, 1997; Anderson, 2009; Anderson and Reed, 2004). However, these projects did not reported product

generation as function of the variation of the gasification parameters and biomass physical and chemical properties.

2.5 Applications of biochar from biomass gasification

Due to its high carbon content, biochar has the potential to be used in a number of applications including soil conditioning, activated carbon production and high value chemical manufacture (Manya, 2012). The application of biochar to soil contributes to the sequestration of carbon from the atmosphere since carbon captured from the environment by the biomass is retained in the soil. Wood contains around 50% of carbon that is increased to 70-80% once the biomass is carbonized. All this carbon can be stored from the atmosphere when applied to the soil (Winsley, 2007). In addition, the utilization of biochar improves the quality of the soil because of its sorption qualities that help to retain nutrients and nitrogen (Ippolito et al., 2012). This technique promotes the growth of microorganisms in the soil. Biochar can also increase water retention, reduce leaching of nutrients and lower the acidity of the soil (Downie et al., 2009; Winsley, 2007). Laird (2010) studied the effect of using hardwood biochar in Midwestern soil. The results showed that the utilization of biochar in the soil improved its quality and reduced leaching of the plants nutrients; nitrogen and phosphorous lost were reduced by 11% and 69%, respectively. Due to its high surface area, biochar can promote the retention of nutrients such as fertilizer within its micro-pores. As result, the needed rate of fertilizer is dramatically decreased; this impacts positively the environment since the risk of nitrogen leaching into rivers and streams is reduced (Baum and Weitner, 2006). Yao (2012) investigated the utilization of peanut hull biochar in sandy soil; biochar produced using slow

pyrolysis at 600ºC was tested. It was found that compared with soil alone, biochar reduced the leaching of nitrates, ammonium and phosphate by 34, 34.7 and 20.6%, respectively. The utilization of biochar had also been tested for heavy metals retention. Uchimiya (2012) investigated the capacity of biochar to retain impurities such as Pb, Cu, Ni, and Cd. Manure biochar produced at 350 and 700ºC was used; the results showed that biochar improved the retention of heavy metals in the soil helping to retain potential contaminants.

Other application of biochar is the production of activated carbon for water purification, gas purification, and solvent recovery among others applications. The concept of activated carbon indicates that this material has undergone through a series of chemical or physical treatments to increase its absorption capacity (Emrich, 1985). Asargohar and Dalai (2006) investigated the utilization of biochar as activated carbon precursor; biochar samples were activated using potassium hydroxide at activation temperatures between 550 to 800ºC. The results showed that by increasing the activation temperature, the biochar surface area increased from 582 to 1210 m^2/g which was found to be 50 times greater than the initial surface area of the un-activated biochar. As result, the biochar can be used to reduce pollutants in different applications. In a similar study, Ahmad et al, 2007 tested the production of activated carbon from oil-palm wood for methylene blue adsorption. Biochar was produced in a slow pyrolysis unit at 390ºC. The use of limestone as activation agent at 806ºC increased the surface area of biochar to 1084 m^2/g. The adsorption experiments revealed that this activated carbon could adsorb up to 90.9 mg/g of methylene blue. Finally, in a different approach, Kutahyah and Eral (2004) investigated the adsorption capacity of activated carbon from biochar using uranium because of the need to clean this chemical in several stages of nuclear plants. The activation

process was carried out using zinc chloride at temperatures varying from 500 to 700ºC. The results showed that the activated carbon from biochar had 92% uranium absorption efficiency which represents a high adsorption capacity. All this suggests that the utilization of biomass feedstocks as raw material is a convenient and relatively low cost alternative to produce biochar for a wide number of applications.

2.6 References

Anderson, P. (2009). Construction plans for the "Champion-2008" TLUD gasifier cookstove (including operational instructions). United States of America. Available at: http://www.bioenergylists.org/files/Construction%20Plans%202009-03-11.pdf (Last accessed October 12th, 2015).

Ahmad, A., Loh, M., & Aziz, J. (2007). Preparation and characterization of activated carbon from oil palm wood and its evaluation on methylene blue adsorption. Dyes and Pigments, 75(2), 263-272.

Anderson, P. S., Reed, T. B., & Wever, P. W. (2007). Micro-gasification: What it is and why it works. Boiling Point, 53(3)

Azargohar, R. & Dalai, A. 2006, "Biochar as a precursor of activated carbon", *Twenty-Seventh Symposium on Biotechnology for Fuels and Chemicals*Springer, pp. 762.

Baker, E., Brown, M., Elliott, D. & Mudge, L. 1988, *Characterization and treatment of tars and biomass gasifiers*.

Baum, E. & Weitner, S. 2006, "Biochar application on soils and cellolosic ethanol production", *Clean Air Task Force, Washington*.

Birzer, C., Medwell, P., MacFarlane, G., Read, M., Wilkey, J., Higgins, M. & West, T. 2014, "A Biochar-producing, Dung-burning Cookstove for Humanitarian Purposes", *Procedia Engineering,* vol. 78, pp. 243-249.

Blasi, A., Fiorenza, G. & Freda, C. 2013, "Steam reforming of biofuels for the production of hydrogen-rich gas".

Brandt, P., Larsen, E. & Henriksen, U. 2000, "High tar reduction in a two-stage gasifier", *Energy & Fuels,* vol. 14, no. 4, pp. 816-819.

Brick, S. & Lyutse, S. 2010, "Biochar: Assessing the promise and risks to guide US policy", *Natural Resources Defense Council Issue Paper.Available at: http://www.nrdc.org/energy/files/biochar_paper.pdf (accessed 3 November 2012)*.

Bridgwater, A.V. 2012, "Review of fast pyrolysis of biomass and product upgrading", *Biomass and Bioenergy,* vol. 38, no. 0, pp. 68-94.

Brown, R. 2009, "Biochar production technology", *Biochar for environmental management: Science and technology*, pp. 127-146.

Cao, Y., Wang, Y., Riley, J.T. & Pan, W. 2006, "A novel biomass air gasification process for producing tar-free higher heating value fuel gas", *Fuel Processing Technology,* vol. 87, no. 4, pp. 343-353.

Corella, J. 1996, "Criteria for selection of dolomites and catalysts for tar elimination from biomass gasification gas; kinetic constants". *Fuel and Energy Abstracts*, 38(1), 36.

Cui, Y., Liang, J., Wang, Z., Zhang, X., Fan, C., Liang, D. & Wang, X. 2014, "Forward and reverse combustion gasification of coal with production of high-quality syngas in a simulated pilot system for in situ gasification", *Applied Energy,* vol. 131, no. 0, pp. 9-19.

de Souza-Santos, M.L. 2010, *Solid Fuels Combustion and Gasification: Modeling, Simulation,* CRC Press.

Devi, L., Ptasinski, K.J. & Janssen, F.J.J.G. 2003, "A review of the primary measures for tar elimination in biomass gasification processes", *Biomass and Bioenergy,* vol. 24, no. 2, pp. 125-140.

Difs, K., Wetterlund, E., Trygg, L. & Söderström, M. 2010, "Biomass gasification opportunities in a district heating system", *Biomass and Bioenergy,* vol. 34, no. 5, pp. 637-651.

Downie, A., Crosky, A. & Munroe, P. 2009, "Physical properties of biochar", *Biochar for environmental management: Science and technology*, pp. 13-32.

Emrich, W. 1985, "Handbook of charcoal making. The traditional and industrial methods".

Evans, R.J. & Milne, T.A. 1997, "Chemistry of tar formation and maturation in the thermochemical conversion of biomass" in *Developments in thermochemical biomass conversion* Springer, pp. 803-816.

Fremaux, S., Beheshti, S., Ghassemi, H., & Shahsavan-Markadeh, R. (2015). An experimental study on hydrogen-rich gas production via steam gasification of biomass in

a research-scale fluidized bed. Energy Conversion and Management, 91, 427-432. doi:http://dx.doi.org.prox.lib.ncsu.edu/10.1016/j.enconman.2014.12.048

Han, J. & Kim, H. 2008, "The reduction and control technology of tar during biomass gasification/pyrolysis: An overview", *Renewable and Sustainable Energy Reviews,* vol. 12, no. 2, pp. 397-416.

Hasan, J., Keshwani, D.R., Carter, S.F. & Treasure, T.H. 2010, "Themochemical Conversion of Biomass to Power and Fuels." in *Biomass to Renewable Energy Processes* CRC Press, Taylor & Francis Group, , pp. 437-489.

Hasler, P. & Nussbaumer, T. 1999, "Gas cleaning for IC engine applications from fixed bed biomass gasification", *Biomass and Bioenergy,* vol. 16, no. 6, pp. 385-395.

Huangfu, Y., Li, H., Chen, X., Xue, C., Chen, C. & Liu, G. 2014, "Effects of moisture content in fuel on thermal performance and emission of biomass semi-gasified cookstove", *Energy for Sustainable Development,* vol. 21, pp. 60-65.

Ippolito, J.A., Laird, D.A. & Busscher, W.J. 2012, "Environmental benefits of biochar", *Journal of environmental quality,* vol. 41, no. 4, pp. 967-972.

James R, A.M., Yuan, W., Boyette, M.D., Wang, D. & Kumar, A. 2014, "In-chamber thermocatalytic tar cracking and syngas reforming using char-supported NiO catalyst in an updraft biomass gasifier", *International Journal of Agricultural and Biological Engineering,* vol. 7, no. 6, pp. 91-97.

Kinoshita, C., Wang, Y. & Zhou, J. 1994, "Tar formation under different biomass gasification conditions", *Journal of Analytical and Applied Pyrolysis,* vol. 29, no. 2, pp. 169-181.

Knoef, H. 2005, "Practical aspects of biomass gasification." in *Handbook biomass gasification*, ed. H. Knoef, BTG biomass technology group, The Netherlands.

Kutahyah, C. & Eral, M. 2004, "Selective adsorption of uranium from aqueous solutions using activated carbon prepared from charcoal by chemical activation", *Separation and purification technology,* vol. 40, no. 2, pp. 109-114.

Laird, D., Fleming, P., Wang, B., Horton, R., & Karlen, D. (2010). Biochar impact on nutrient leaching from a midwestern agricultural soil. Geoderma, 158(3), 436-442.

Lv, P.M., Xiong, Z.H., Chang, J., Wu, C.Z., Chen, Y. & Zhu, J.X. 2004, "An experimental study on biomass air–steam gasification in a fluidized bed", *Bioresource technology,* vol. 95, no. 1, pp. 95-101.

Manya, J.J. 2012, "Pyrolysis for biochar purposes: a review to establish current knowledge gaps and research needs", *Environmental science & technology,* vol. 46, no. 15, pp. 7939-7954.

Menon, P. G. (1995). Ammonia: Catalysis and manufacture: By A. nielsen (editor), springer verlag GmbH, heidelberg, 1995, ISBN 3-540-58335-1, vii + 346 pp., DM 298.00. Applied Catalysis A: General, 133(1), 177-178. doi:http://dx.doi.org/10.1016/0926-860X(96)80016-0

McKendry, P. 2002, "Energy production from biomass (part 3): gasification technologies", *Bioresource technology,* vol. 83, no. 1, pp. 55-63.

Milne, T.A., Abatzoglou, N. & Evans, R.J. 1998, *Biomass gasifier" tars": their nature, formation, and conversion,* National Renewable Energy Laboratory Golden, CO.

Morris, M., Waldheim, L., Faaij, A. & Stahl, K. 2005, "Status of large-scale biomass gasification and prospects", *Handbook Biomass Gasification*.

Mukunda, H., Dasappa, S., Paul, P., Rajan, N., Yagnaraman, M., Ravi Kumar, D. & Deogaonkar, M. 2010, "Gasifier stoves–science, technology and field outreach", *Current science,* vol. 98, no. 5, pp. 627-638.

Narvaez, I., Orio, A., Aznar, M.P. & Corella, J. 1996, "Biomass gasification with air in an atmospheric bubbling fluidized bed. Effect of six operational variables on the quality of the produced raw gas", *Industrial & Engineering Chemistry Research,* vol. 35, no. 7, pp. 2110-2120.

Peterson, S.C. & Jackson, M.A. 2014, "Simplifying pyrolysis: Using gasification to produce corn stover and wheat straw biochar for sorptive and horticultural media", *Industrial Crops and Products,* vol. 53, pp. 228-235.

Qian, K., Kumar, A., Patil, K., Bellmer, D., Wang, D., Yuan, W. & Huhnke, R.L. 2013, "Effects of biomass feedstocks and gasification conditions on the physiochemical properties of char", *Energies,* vol. 6, no. 8, pp. 3972-3986.

Reed, T. & Larson, R. 1997, "A wood-gas stove for developing countries" in *Developments in Thermochemical Biomass Conversion* Springer, , pp. 985-993.

Reed, T.B. & Das, A. 1988, *Handbook of biomass downdraft gasifier engine systems,* Biomass Energy Foundation.

Richardson, Y., Blin, J. & Julbe, A. 2012, "A short overview on purification and conditioning of syngas produced by biomass gasification: catalytic strategies, process

intensification and new concepts", *Progress in Energy and Combustion Science,* vol. 38, no. 6, pp. 765-781.

Richardson, Y., Drobek, M., Julbe, A., Blin, J. & Pinta, F. 2015, "Chapter 8 - Biomass Gasification to Produce Syngas" in *Recent Advances in Thermo-Chemical Conversion of Biomass*, ed. Sukumaran,Ashok PandeyThallada BhaskarMichael StöckerRajeev K., Elsevier, Boston, pp. 213-250.

Rivas, Arthur Mc Carty James 2012, *The effect of biomass, operating conditions, and gasifier design on the performance of an updraft biomass gasifier*.

Saravanakumar, A., Haridasan, T., Reed, T.B. & Bai, R.K. 2007, "Experimental investigation and modelling study of long stick wood gasification in a top lit updraft fixed bed gasifier", *Fuel,* vol. 86, no. 17, pp. 2846-2856.

Snip, O.C., Woods, M., Korbee, R., Schouten, J.C. & van den Bleek, C.M. 1996, "Regenerative removal of SO2 and NOx for a 150 MWe power plant in an interconnected fluidized bed facility", *Chemical Engineering Science,* vol. 51, no. 10, pp. 2021-2029.

Stevens, D.J. 2001, "Hot gas conditioning: recent progress with larger-scale biomass gasification systems", *NREL Subcontractor Report (NREL/SR-510-29952)*.

Thengane, S.K., Hoadley, A., Bhattacharya, S., Mitra, S. & Bandyopadhyay, S. 2014, "Cost-benefit analysis of different hydrogen production technologies using AHP and Fuzzy AHP", *International Journal of Hydrogen Energy,* vol. 39, no. 28, pp. 15293-15306.

Tijmensen, M.J., Faaij, A.P., Hamelinck, C.N. & van Hardeveld, M.R. 2002, "Exploration of the possibilities for production of Fischer Tropsch liquids and power via biomass gasification", *Biomass and Bioenergy,* vol. 23, no. 2, pp. 129-152.

Tryner, J., Willson, B.D. & Marchese, A.J. 2014, "The effects of fuel type and stove design on emissions and efficiency of natural-draft semi-gasifier biomass cookstoves", *Energy for Sustainable Development,* vol. 23, pp. 99-109.

Uchimiya, M., Cantrell, K.B., Hunt, P.G., Novak, J.M. & Chang, S. 2012, "Retention of heavy metals in a Typic Kandiudult amended with different manure-based biochars", *Journal of environmental quality,* vol. 41, no. 4, pp. 1138-1149.

Vreugdenhil, B., Zwart, R. & Neeft, J.P.A. 2009, *Tar formation in pyrolysis and gasification,* ECN.

Warnecke, R. 2000, "Gasification of biomass: comparison of fixed bed and fluidized bed gasifier", *Biomass and Bioenergy,* vol. 18, no. 6, pp. 489-497.

Winsley, P. 2007, "Biochar and bioenergy production for climate change mitigation", *New Zealand Science Review,* vol. 64, no. 1, pp. 5-10.

Woolcock, P.J. & Brown, R.C. 2013, "A review of cleaning technologies for biomass-derived syngas", *Biomass and Bioenergy,* vol. 52, no. 0, pp. 54-84.

Yao, Y., Gao, B., Zhang, M., Inyang, M. & Zimmerman, A.R. 2012, "Effect of biochar amendment on sorption and leaching of nitrate, ammonium, and phosphate in a sandy soil", *Chemosphere,* vol. 89, no. 11, pp. 1467-1471.

CHAPTER 3 - Airflow and insulation effects on simultaneous syngas and biochar production in a top-lit updraft biomass gasifier

Abstract

The objective of this study was to understand the effect of airflow and insulation on syngas and biochar generations of rice hulls and woodchips in a top-lit updraft gasifier. Biochar yield was found to decrease with increasing airflow. The highest biochar yields of 39% and 27% were achieved at 8 lpm airflow for rice hulls and woodchips, respectively. Contrarily, the syngas mass balance increased with increasing airflow, ranged 88-89% for rice hulls and 93-94% for woodchips. The hydrogen composition in syngas also increased with higher airflow rates, peaked at 4.2-4.4% for rice hulls and 5.7-6.6% (v/v) for woodchips, which was not affected by insulation for both biomasses. The carbon monoxide content in syngas was not significantly affected by airflow or insulation in most cases, and ranged from approximately 12 to 15% (v/v). Average tar content in syngas decreased for both biomasses when the airflow increased but adding insulation resulted in significantly higher tar content in syngas. The lowest tar contents were approximately 1.16 and 11.88 g/m for rice hulls and woodchips, respectively, both occurred at 20 lpm airflow without insulation. The biomass type also had significant effects on the performance of the top-lit updraft gasifier. Biochar yields from rice hulls were greater than that from woodchips at all airflow rates. Tar contents in syngas from rice hulls were also much lower than woodchips. The H_2 contents in woodchips syngas were higher than that of rice hulls at the same airflow rate, but no differences were found in CO composition or the higher heating value of syngas from the two biomasses.

3.1. Introduction

Utilization of renewable biomass resources to generate bioenergy and bio-products has increased significantly in the last decades [1,2]. Among various technology choices, biomass gasification is relatively simple in process/reactor design and easy to implement [3]. It generally produces two potentially useful products: syngas and biochar. Syngas contains hydrogen and carbon monoxide that can be used to fuel internal combustion engines, turbines and boilers [4]; it can also be used to produce a wide variety of fuels and chemicals, such as gasoline, diesel and α-olefins via the Fischer-Tropsch process [5], ethanol by biological conversion or catalytic reactions, ammonia and methanol via catalytic hydrogenation [6,7]. Biochar is known for its carbon-rich nature that provides valuable benefits to the environment [8]. It can be used in a broad number of applications such as removal of pollutants in aqueous and gas media, and as soil conditioner to improve plant growth [9,10].

However, common methods for biochar production are reported to have high energy input and/or production of contaminants [11]. For instance, kilns and retorts in developing countries are known to release carbon monoxide, non-methane volatiles and particulate matters to the environment [12]. Modified pyrolysis units have been reported to reduce pollutant emissions and increase the yield of biochar [13]. For example high pressure pyrolysis reactors can produce biochar from 41 to 62% yields with minimal emissions; however, the use of high pressures (0.4 to 1 MPa) represents a major disadvantage [14]. Another example is the multistage pyrolysis reactors in which the progressive increase of the reaction temperature can reduce the energy input by 30% and achieved biochar yield of up to 27% [15]. However, these technologies require higher energy input compared with gasification systems. Common

gasification processes such as downdraft gasifiers and fluidized-bed gasifiers are focused on the production of syngas only [4]. Top-lit updraft (TLUD) gasification is an example of a potential technology for simultaneous production of biochar and syngas from biomass. Variations of TLUD gasifiers have been found to produce relatively high yields of biochar and parallel production of syngas [17,18]. The fact that syngas can be generated in top-lit updraft gasifiers not only helps reduce the pollution released to the environment when compared with traditional pyrolysis units [19,17], but can also help increase the overall energy efficiency of the process since the syngas can be used for other purposes [4]. However, previous studies were mostly focused on the utilization of TLUD gasifiers to fuel cookstoves in developing countries. There is not a full understanding of the process from the perspectives of how gasification-medium flow rate (e.g. air), biomass type and gasifier design affect simultaneous syngas and biochar production [20].

The objective of this project was to understand the TLUD gasification process through the quantification of biochar, syngas and tar, and their correlation with varying biomass type, airflow rate and reactor insulation. Two biomasses (rice hulls and woodchips) were studied at four airflow rates. For each condition, the TLUD gasifier was operated with and without insulation on its external surface.

3.2. Materials and methods

3.2.1 The gasification unit and tar and syngas sampling systems

The gasification unit was a 152-cm high and 10.1-cm diameter black iron tube (Fig. 3.1). Air was supplied to the reactor with an air compressor (1.5 kW – 8.62 Bar maximum operational pressure) equipped with an 18.92-liter (6-gallon) reservoir tank (WEN, Elgin, IL). The flow of air was controlled with a variable area flow meter (Cole-Parmer 150-mm, max. pressure 200 psi, Chicago, IL). The temperatures at the top, middle and bottom of the gasifier were recorded with a data logger (Measurement Computing, model: USB-5201, Norton, MA). Tar in the syngas was collected using a two-stage cold trapping method; the first stage contained two flasks cooled by ice in which heavy tar and water were collected. In the second stage, two flasks under dry ice (solid carbon dioxide) cooled the syngas and condensed the remaining tar in the gas mixture. When sampling tar, half of the intake airflow for gasification was used (e.g. when airflow rate was 8 lpm the tar sampling flow was 4 lpm) for 45 min. The tar collected was dried for 24 hours at 105ºC; the final weight of the dry material was defined as tar. Tar in biochar was determined by solvent extraction. One gram of biochar was placed in 25 ml of acetone and agitated for 4 hours. After that, the solid was washed with 25 ml of acetone again, then they were filtered with 110-mm diameter filter paper (Whatman™ Qualitative #1) to remove biochar. The biochar was dried at 105ºC for 1 hour to measure its dry weight. The weight difference between the initial biochar, the moisture content and the washed biochar was used to determine the percentage of weight loss reported as tar in biochar. Syngas samples were collected in a 0.5 liter Tedlar® sampling bags and analyzed in a GC

(SRI8610C, Torrance, CA) equipped with a TCD detector using helium as the carrier gas. Compositions of H_2, CO, CO_2, CH_4, O_2 and N_2 were determined.

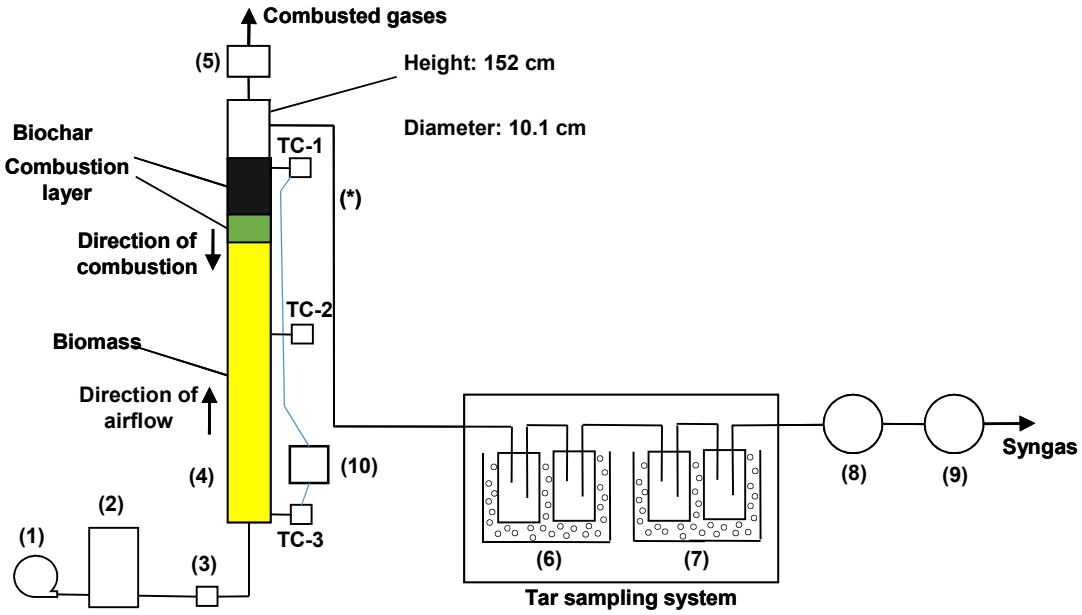

(1) Air compressor
(2) Reservoir tank
(3) Flow meter
(4) Top-lit updraft gasifier
(5) Flare
(6) Water ice – cold trapping
(7) Dry ice – cold trapping
(8) Gas filter
(9) gas sampling pump
(10) data logger
(*) tar and syngas sampling port
TC-# thermocouple, location from bottom
TC-1, 112.15 cm from the bottom
TC-2, 51 cm from the bottom
TC-3, 4.2 cm from the bottom

Fig. 3.1. Illustration of the top-lit updraft gasifier and syngas and tar sampling systems

3.2.2 Experimental procedures

Gasification was evaluated at 4 levels of airflow rate (8, 12, 16 and 20 lpm) and two insulation conditions (no insulation and insulating the reactor with 88.9 mm of Pinkplus Fiberglass® on the external wall). The equivalent superficial velocities for the airflow rates were 0.83, 1.25, 1.66 and 2.08 cm/s, respectively. Rice hulls and woodchips were selected as

the raw materials and their major properties are presented in Table 3.1. The two biomasses had noticeable differences in chemical composition. The carbon and volatile matter contents of woodchips were ~10% and ~16% higher, respectively, compared with rice hulls, whereas, the ash content in rice hulls was ~23% higher.

Table 3.1. Proximate and Ultimate analyses of the biomass

	Biomass	
	Rice hulls	Woodchips
C (%)	36.99	47.90
H (%)	5.14	1.70
N (%)	0.58	0.30
O [a] (%)	56.30	49.90
S (%)	1.0	0.20
Ash (%)	23.78	0.57
Volatile matter (%)	58.17	74.92
Fixed carbon [a] (%)	9.57	16.66
Moisture (%)	8.48	7.85
Bulk density (g/cm^3)	1.27	2.11
Particle size (mm)	$X \leq 2$	$3 < X \leq 10$

[a] calculated by difference

The operating procedure of the gasifier was as follows. Once the gasifier was loaded, the top layer of biomass in the gasifier was lit with a propane torch for 1 min; this initial heat supplied the needed energy for the combustion and pyrolysis reactions to start. Thereafter, air was injected from the bottom and the combustion layer started moving downward leaving biochar on the top and producing syngas. Once the peak reaction temperature was sensed by the bottom thermocouple, the reaction was complete and stopped. Then, biochar was collected and the yield of biochar was calculated based on the dry weight of biomass and the final dried biochar. Statistical analysis of the results was performed using SAS® software. The GLM

procedure was used for multiple comparisons of the flow rates and insulation cases. Tukey HSD method was used for significance analysis (α=0.1).

3.3. Results and discussion

3.3.1 The temperature profiles of the gasifier

Reaction temperature was found to correlate with airflow rate. Increase in airflow resulted in increased combustion zone temperature (CZT) for the two biomasses at the two insulation conditions, as shown in Fig. 3.2A and 3.2B. The CZT of rice hulls consistently increased from 700 to 862ºC without insulation (R^2=0.99), and from 714 to 868ºC (R^2=0.98) with insulation. Similarly, the CZT of woodchips increased from 648 to 815ºC (R^2=0.95) and from 661 to 840ºC (R^2=0.96) without and with insulations, respectively. This increase in the CZT comply with previous findings that the temperature of thermochemical reactions was strongly influenced by the amount of air provided to the combustion of the system; increase in air supply for gasification was found to increase the reaction temperature [24].

The addition of insulation seemed to increase the CZT. However, the statistical comparison of the CZT for individual biomasses at every airflow rate presented no significant differences in the CZT when insulation was added. In order to evaluate the effect of insulation on the reaction temperature, the average temperature of forty-minutes after the peak temperature was reached was calculated. This temperature was calculated for the top thermocouple of the reactor (TC-1). The average temperature could help understand how fast the temperature decreased within the gasifier at different airflows and insulation conditions. Fig. 3.2C and 3.2D present the average temperature. It can be seen that no insulation resulted in lower average

reaction temperatures which were not significantly different between the two biomasses at every airflow rate. However, the utilization of insulation exhibited linear increase with the airflow rate for both biomasses with R^2=0.98. This suggests that the insulation on the reactor considerably helped to reduce heat loss through the gasifier's wall; as a result, higher average temperatures of the biomass bed were formed after the combustion zone had crossed.

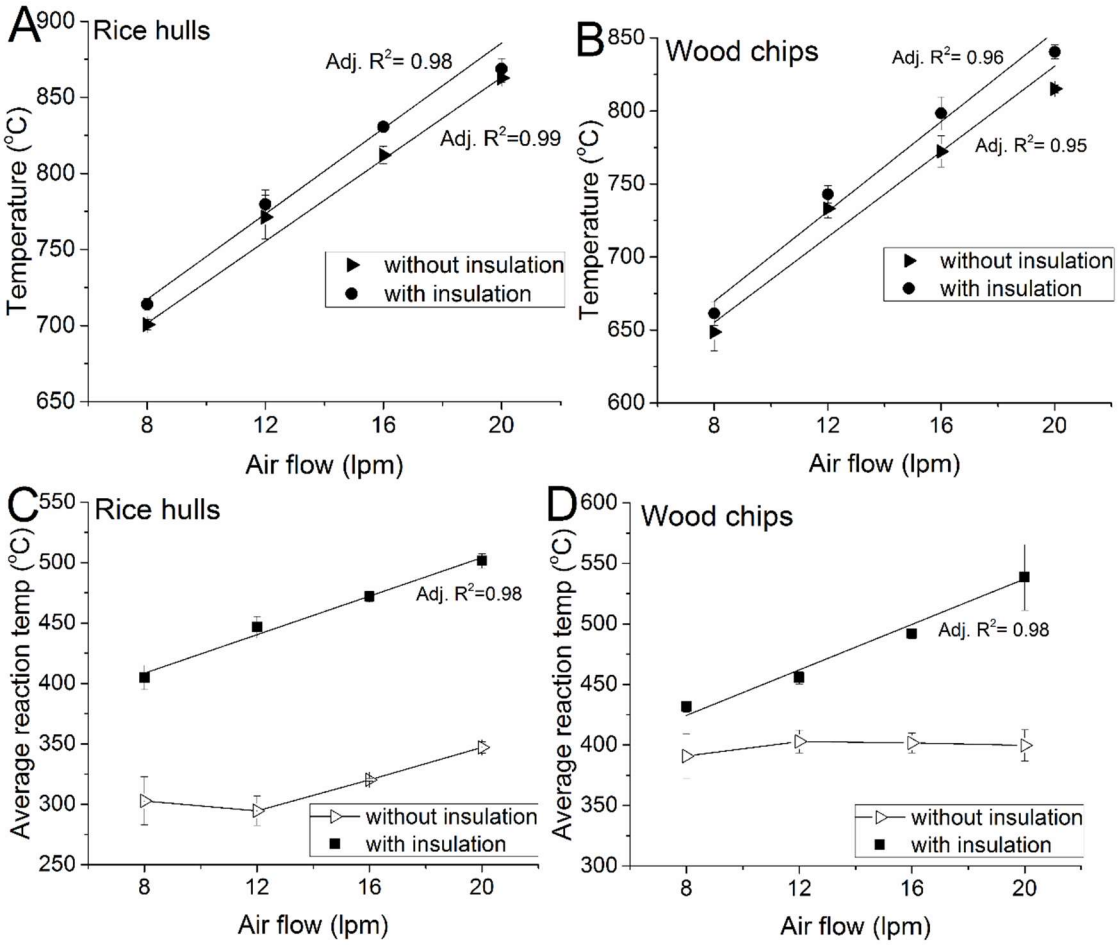

Fig 3.2. Combustion zone temperature of (A) rice hulls and (B) woodchips; Average combustion temperature of (C) rice hulls and (D) woodchips.

Fig. 3.3 shows the temperature profiles of the two biomasses and two insulation conditions using 12 lpm as an example. It can be seen that once the flame reached the first thermocouple (TC-1), the temperature rapidly increased from the ambient temperature to the peak temperature. This sudden increase of temperature as the combustion zone moves had been previously reported when a top-lit updraft cookstove was tested. The authors found that the temperature of the biomass abruptly increased from the ambient temperature to ~600°C when wheat straw was gasified [21]. Differences in the pace of cooling can also be observed when comparing the temperature profiles of insulation and no insulation. The insulated gasifier cooled slower, and the combustion zone reached the next thermocouple sooner.

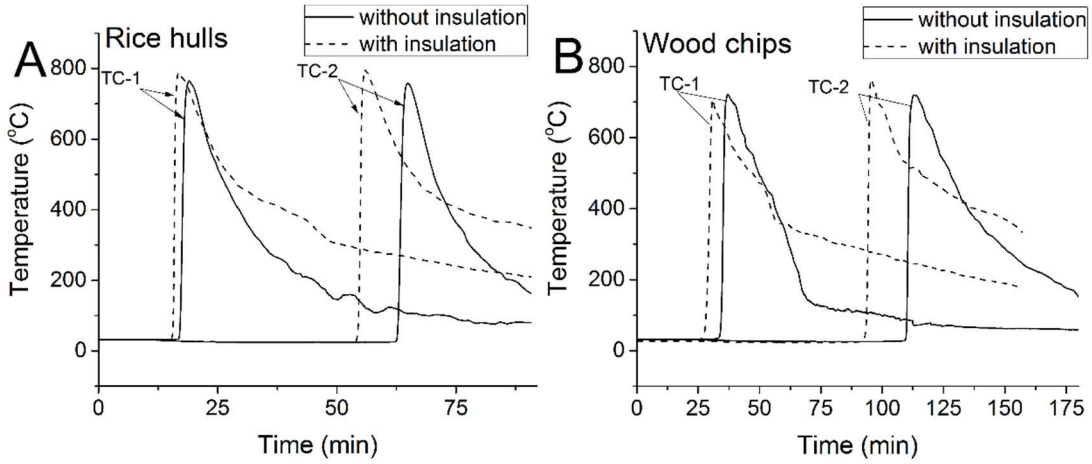

Fig. 3.3. The temperature profile of (A) rice hulls and (B) woodchips showing movement of flame (airflow of 12 lpm). TC-1 (thermocouple 1), TC-2 (thermocouple 2)

3.3.2 The burning rate of biomass

The burning rate was defined as the speed at which the flame traveled from the top to the bottom of the gasifier (mm/min). It was calculated using the time elapse that the flame (the highest temperature) reached the top (TC-1) and middle (TC-2) thermocouples as presented in

Fig. 3.3. In Fig. 3.4, the burning rates of rice hulls and woodchips are presented at the varying airflows and the two insulation cases. Increase in airflow rate from 8 to 20 lpm in the gasification of rice hulls resulted in increasing burning rates for no insulation and insulation as follows: 11.6 to 18.3 mm/min and 12.6 to 19.1 mm/min, respectively. Similarly, in the gasification of woodchips, it was noticed that the burning rate increased as more air for gasification was supplied. Without insulation, the burning rate varied from 6.3 to 10.2 mm/min and with insulation from 8.1 to 13.2 mm/min when increasing the airflow rate. Burning rate was found to linearly correlate with airflow rate (R^2 = 0.95 - 0.99). The increase in the burning rate at higher airflow rates was consistent with the increase in the CZT because more fuel (biomass) was needed to promote the generation of heat in combustion reactions. Despite the fact that the CZT was not significantly increased at different insulation conditions, the insulation increased the overall reaction temperature (Fig. 3.2). As a result, the burning rate further increased because more heat that was initially lost through the gasifier walls was now used to devolatilize the biomass in the gasifier chamber.

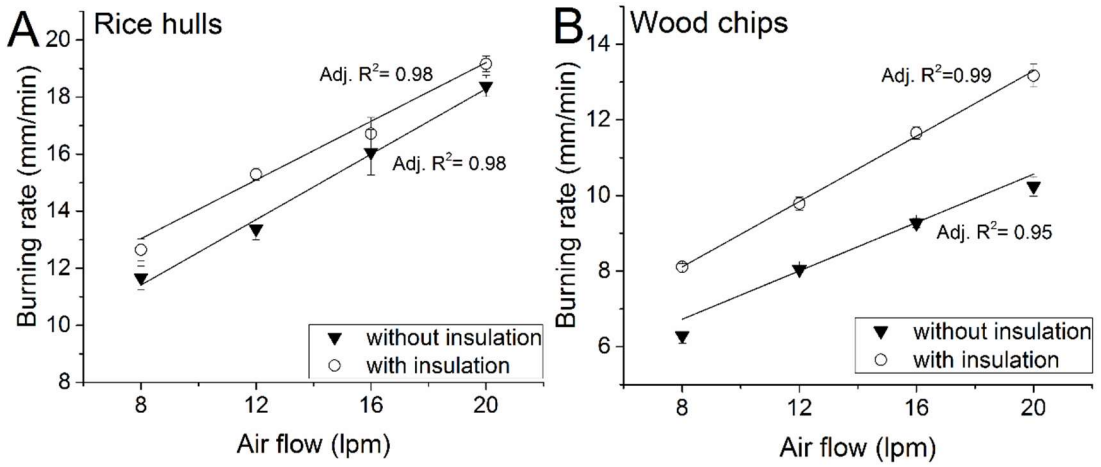

Fig. 3.4. The burning rate of (A) rice hulls and (B) woodchips at the two insulation conditions

3.3.3 The yield of biochar

The biochar yield of the two biomasses was found to decrease as the airflow rate increased (Fig. 3.5). The yield of biochar from rice hulls reduced from 38.0 % to 31.6% and from 39.3% to 31.3% for no insulation and with insulation, respectively, when airflow increased from 8 to 20 lpm. Lower biochar yields were observed in the gasification of woodchips when compared with rice hulls. Without insulation, the biochar yield ranged from 12.9 to 27.1% and with insulation from 12.3 to 18.8%. This decrease in biochar yield with increasing airflow can be correlated with the progressive increase of CZT (R^2=0.93). Most of the fuel for the combustion reactions in top-lit updraft gasifier is provided by the volatiles released during the pyrolysis of the immediate biomass below the combustion zone [23]; however, the increase in the airflow can also promote the combustion of the biochar layer that was formed above the combustion flame. A well-known representation of this process can be observed in a flaming match where the pyrolysis vapors from the internal reactions of the wood were released fueling the flame and producing biochar [24]. In another previous work, Demirbas [25] reported that the biochar yield decreased with increasing carbonization temperature, which was consistent with Fig. 3.5 and Fig. 3.2. From Fig. 3.5A, it can also be observed that there were no significant differences in the yield of biochar from rice hulls between insulation and no insulation. Moreover, the yield of biochar from woodchips showed different behaviors than rice hulls at lower airflow rates. The addition of insulation considerably reduced the yield of biochar at airflow rates of 8 and 12 lpm.

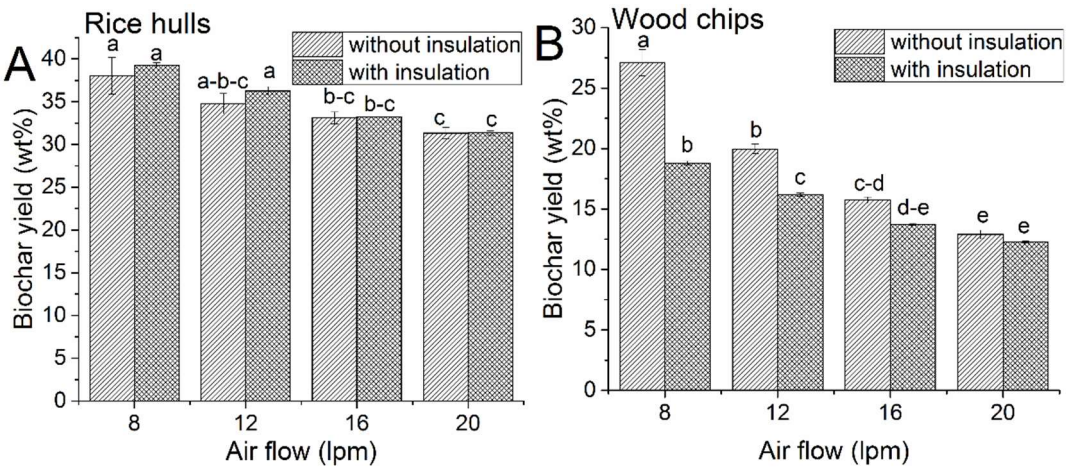

Fig. 3.5. The biochar yield (wt% db) of (A) rice hulls and (B) woodchips at the two insulation conditions. Different letters indicate significant differences by Tukey's HSD test (α=0.1)

Fig. 3.6 presents the percentages of tar in biochar from rice hulls and woodchips. Rice hulls biochar generated from the insulated reactor showed tar contents ranging from 0.63% to 0.84%. Without insulation the tar content in biochar was generally higher, reaching 2.29% at 12 lpm (Fig. 3.6a). Tar in biochar from woodchips has similar trends as presented in Fig. 3.6b. Large amounts of tar were found in the biochar when no insulation was used, which however decreased from 14.9% to 0% as the airflow increased from 8 to 20 lpm. With the use of insulation the highest tar content in woodchip biochar was only 0.07% at 8 lpm and no tar was found at higher airflow rates. Overall, the biochar produced when the gasifier was insulated contained less than 1% tar, in the same way, less tar was found at higher airflow rates regardless of the insulation condition. Biochar with low tar content can be directly used for certain applications such as activated carbon and soil conditioner [26,27] in which the tar content might represent a major concern. Consideration between the tar in the biochar and tar in the syngas needs to be taken into account when selecting a specific airflow rate and gasifier

configuration. Biochar with excessive tar might require further treatments after production; this can increase the operational cost of biochar production.

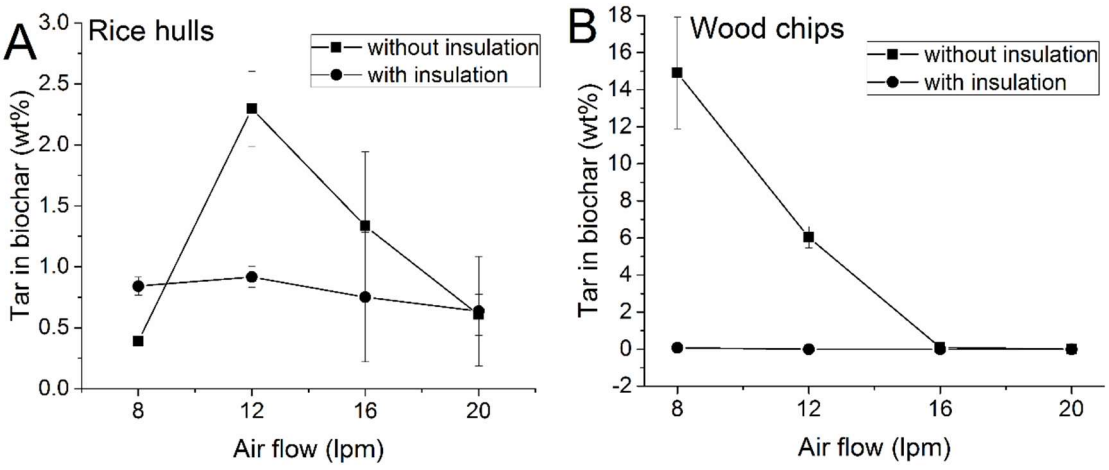

Fig. 3.6. Tar content in biochar (wt% db) from (A) rice hulls and (B) woodchips.

3.3.4 Syngas compositions

Fig. 3.7 shows the composition of hydrogen in syngas for rice hulls and woodchips at different airflow rates and insulation conditions. H_2 content generally increased when the airflow increased. For example, rice hulls syngas contained from 2.3% to 4.4% and from 2.8% to 4.2% H_2, for no insulation and with insulation, respectively. In a similar way, the hydrogen content of syngas from woodchips increased from 2.56% to 5.7% and 3.3% to 6.6% for no insulation and with insulation, respectively, when airflow increased from 8 to 20 lpm. Hydrogen content in syngas was found to be positively correlated with the CZT (R^2=0.85). However, insulation had no significant effects on the hydrogen content when independent airflow rates were compared. This increase in the hydrogen content as result of the increasing combustion temperature was believed to be due to the oxidation and cracking of tars [31]. Lv

reported a similar tendency in the hydrogen content that increased from 22 to 40% when the temperature increased from 700 to 900ºC [32].

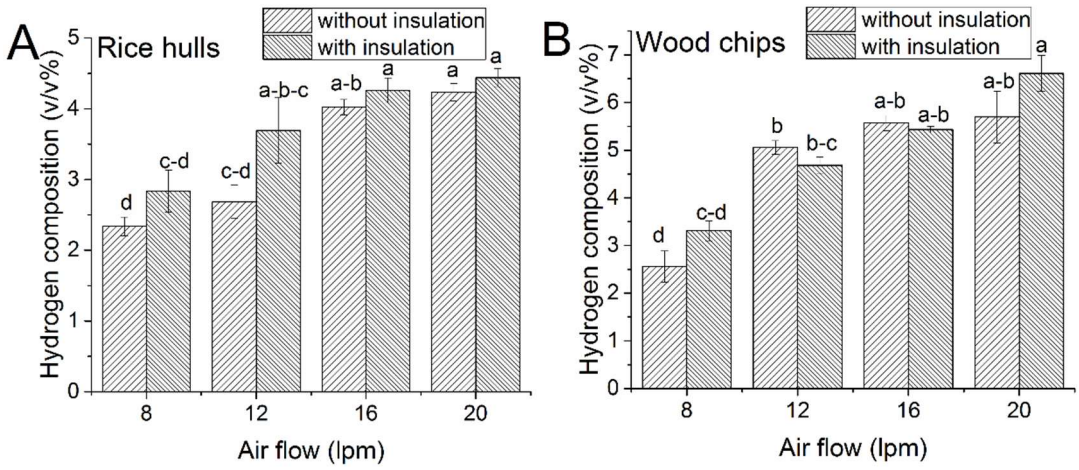

Fig. 3.7. Hydrogen composition in syngas (v/v %) from (A) rice hulls and (B) woodchips at the two insulation conditions. Different letters indicate significant differences by Tukey's HSD test (α=0.1)

Fig 3.8 presents the CO composition of rice hulls and woodchips at different levels of insulation. As the airflow rate increased from 8 to 20 lpm little difference was noticed in the CO composition of rice hulls that ranged from 13.4 to 15.8% (Fig. 3.8A). Similarly, the CO composition of syngas from woodchips varied from 11.4 to 14.9% when increasing the airflow rate (Fig. 3.8B). No significant differences in CO composition at different levels of airflow rates and insulation conditions were observed except for woodchips at 8 lpm without insulation, at which the CO composition was significantly lower. It can be found from Fig. 3.2 that woodchips at 8 lpm without insulation had very low combustion temperature (~650 ºC), which was close to pyrolysis rather than gasification, thus CO generation was low. Other conditions were closer to gasification with higher temperatures and stable CO generation [28].

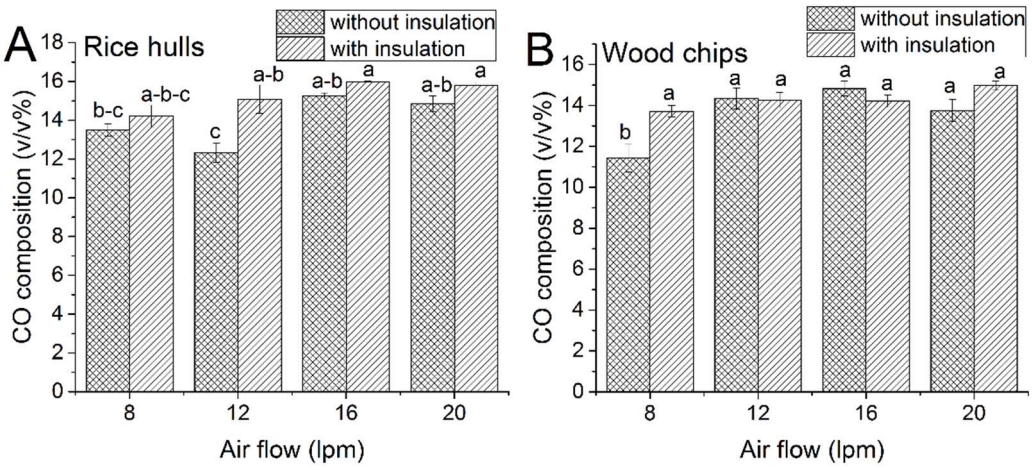

Fig. 3.8. Carbon monoxide composition (v/v %) in syngas from (A) rice hulls and (B) woodchips at the two insulation conditions. Different letters indicate significant differences by Tukey's HSD test (α=0.1)

3.3.5 Tar contents in biochar and syngas

Results of tar content in syngas are presented in Fig. 3.9. Airflow rate for rice hulls gasification without insulation had no significant effects on syngas tar contents. However, the utilization of insulation significantly increased the concentration of tar especially at lower airflow rates. When insulating the reactor, airflow of 8 lpm was found to produce the highest tar content of 16.6 g/m^3 for rice hulls, which was reduced to 2.76 g/m^3 at 20 lpm (Fig. 3.9A). Gasification of woodchips showed much higher tar contents, which decreased from 58.7 to 11.8 g/m^3 as the airflow rate increased from 8 to 20 lpm without insulation. Insulation also significantly increased tar contents. The highest tar content for woodchips was 86.2 g/m^3 at 8 lpm (insulated), Fig. 3.9B. The decrease in tar content as increasing the airflow suggested that raising the combustion temperature can reduce the subsequent production of tar in syngas. Previous gasification studies reported that the generation of tar was discouraged by the increase in the reaction temperature [29,30,25]. Similarly, increasing the airflow can also increase the equivalence ratio (ER) at which the biomass reacts. It has been proven that at low ER (close to

0) pyrolysis reactions predominate, increasing the production of condensable aromatic hydrocarbons including tars; however, at higher ER (close to 1) complete combustion is approached promoting the production of gases [4] without tars.

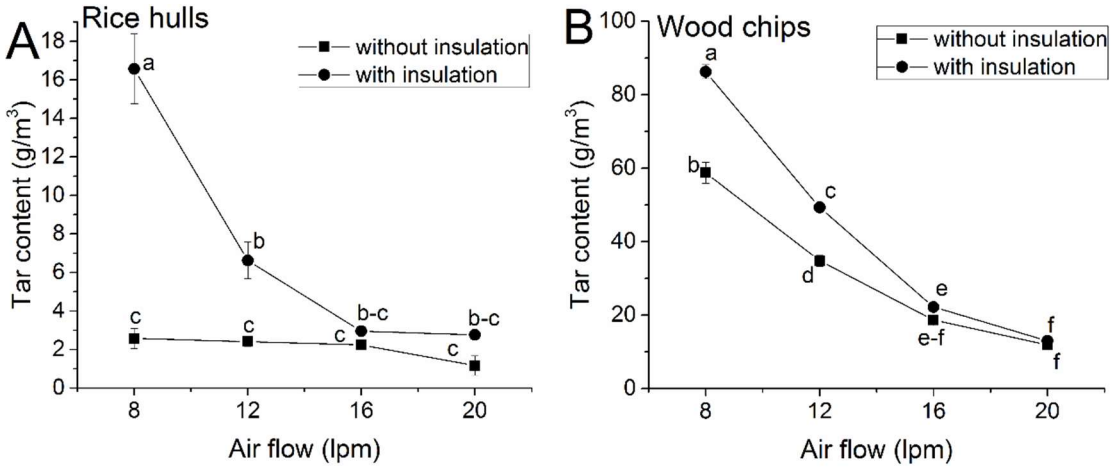

Fig. 3.9. Tar content in syngas from (A) rice hulls and (B) woodchips at the two insulation conditions. Different letters indicate significant differences by Tukey's HSD test (α=0.1)

3.3.6 Effect of biomass type

Table 3.2 summarizes the statistical analyses with ANOVA multiple comparison procedure between rice hulls and woodchips. The results showed that the combustion temperature had the same tendency for both biomasses, but it was significantly higher for rice hulls at the same airflow rate from 8 to 16 lpm. However, at 20 lpm the combustion temperatures of the two biomasses were not significantly different. In contrast, no differences were noticed in the average reaction temperature between the two biomasses. The burning rate of rice hulls was higher than that of woodchips at all levels of airflow rate. This could be explained by comparing the particle size and bulk density of the two biomasses. Rice hulls had particles with sizes lower that 2 mm. In contrast, woodchips had particle sizes between 3 and

10 mm. Likewise, rice hulls presented a lower bulk density of 1.27 g/cm^3 compared with woodchips of 2.11 g/cm^3. The thin configuration of the particles contributed to faster devolatilization of the biomass thus it increased the burning rate [22].

Rice hulls had higher biochar yields than woodchips at all airflow rates. High yield of biochar from rice hulls that had high ash content is an indication of the large amount of inorganic components in the unreacted biomass [33]. This is because gasification reactions are driven mainly by the heat produced due to the oxidation of organic matters in the biomass that decrease as the biomass losses weight during carbonization [34]. The comparison of the tar generated showed that woodchips had larger amounts of tar when compared with rice hulls. This difference in the tar content of the two biomasses can be also associated with the bulk density of the biomass. Since woodchips had approximately two times the bulk density of rice hulls, it was expected that more mass of woodchips would be concentrated in the reaction area. Similarly, James et al. [35] compared the tar content produced by woody biomass and a low bulk density biomass (sorghum biomass) in an updraft biomass gasifier when varying the ER from 0.21 to 0.29. The results showed that the overall production of tar from sorghum biomass was 3 g/m^3 and from woodchips 8 g/m^3 at similar gasification conditions. This suggested that the excessive release of volatile components produced by biomass with higher bulk density can be attributed to the fact that there is more biomass per unit volume. Therefore, more condensable products are generated when compared with low bulk density biomasses.

The hydrogen contents in syngas of woodchips were significantly higher than rice hulls at the same airflow rate from 12 to 20 lpm, however, no differences were found in CO composition or the higher heating value of syngas from the two biomasses at all airflow rates.

Table 3.2. Effect of biomass type on gasification performance. Different letters among analyses indicate significant differences in the order of a>b>c>d>e.

	Rice hulls				Woodchips			
Airflow (lpm)	8	12	16	20	8	12	16	20
Combustion temperature (°C)	c	b	a	a	d	c	b	a
Average react. Temp. (°C)	b	ab	ab	ab	ab	ab	ab	a
Burning rate (mm/min)	bc	b	a	a	e	de	cd	c
Biochar yield (wt%)	a	ab	b	b	c	d	de	e
Tar content in syngas (g/m^3)	cd	d	d	d	a	b	c	cd
Syngas HHV (MJ/m^3)	abc	bc	ab	ab	c	ab	a	a
H_2 in syngas (v/v %)	e	de	c	cd	e	bc	ab	a
CO in syngas (v/v %)	NS	NS	NS	NS	NS	NS	NS	NS

NS – not significant

3.3.7 The mass balance of the gasification process

Fig. 3.10A and 3.10B present the mass fraction of rice hull gasification products per the total input including biomass and air. It can be seen that increase in the airflow rate reduced the amount of biochar produced, but it encouraged the production of gases. Tar in syngas was negligible. This relative increase in the gas phase and decrease in the solid phase (biochar) can be explained by the increase in CZT as a result of increasing airflow for reactions. Demirbas [25] reported that increase in the reaction temperature reduced the amount of biochar and tar during biomass carbonization. This phenomenon encourages the production of gases when biomass is reacted at higher temperatures. The effect of insulation can also be observed in Fig. 3.10A and 3.10B. At low airflow rates (e.g., 8 and 12 lpm), the addition of insulation promoted increase of 7-8% in the gas phase. At high airflow rates (e.g., 16 and 20 lpm), the differences were small and not significant.

Gasification of woodchips (Fig. 3.10C and 3.10D) presented similar tendency as rice hulls. As the airflow rate increased the biochar fraction was minimized and the gas phases

increased. Gases from gasification increased from 80% to 94% when the reactor was not insulated, and from 82 to 93% when insulated. The addition of insulation stimulated the generation of tars in the syngas at low airflow rates. For both biomasses, the moisture content of biochar was reduced when the airflow rate increased without insulation. No moisture was found in the biochar when insulation was added, probably because of higher average temperatures in the reactor.

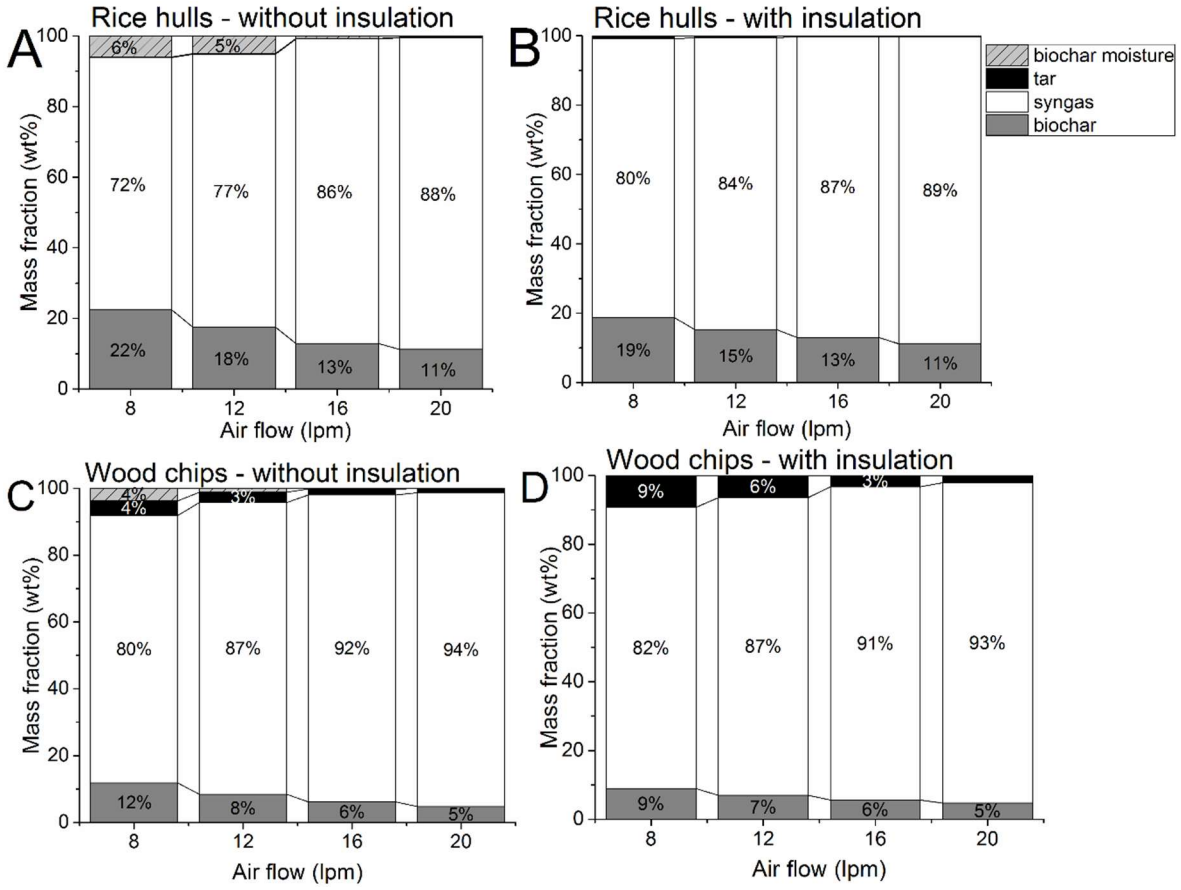

Fig. 3.10. The mass balance of rice hulls gasification (A) without insulation and (B) with insulation; the mass balance of woodchips gasification (C) without insulation and (D) with insulation.

Common gasification systems designed to maximize the production of syngas have mass fraction distributions of approximately 10% biochar, 85% gases and 5% liquids [16]. It can be observed that these conditions were approached as the airflow rate increased in the top-lit updraft gasifier. This fact can help to select the appropriate operational parameters in this reactor when the production of either syngas or biochar is the priority.

3.4. Conclusions

Airflow rate significantly influenced the combustion zone temperature, which increased as the airflow rate increased regardless of the insulation condition. The syngas composition was enhanced by the increase in airflow rate. The hydrogen composition increased with increasing airflow, but no differences were noticed with the use of insulation. Little difference in CO composition was observed when increasing the airflow.

The addition of insulation on the external wall of the reactor did not significantly affect the combustion zone temperature, however it increased the average temperature in the reactor because of the minimization of heat loss through the reactor wall. This increase in the average reactor temperature led to rising biomass burning rate and reduced biochar yield. The addition of insulation also helped to reduce tars in the biochar but tars in syngas increased significantly.

The biomass type also played a significant role in the performance of top-lit updraft gasification. Rice hulls had a higher burning rate at all levels of airflow because of its lower density when compared with woodchips. Woodchips produced much larger amounts of tar in syngas when compared with rice hulls. In addition, the yield of biochar from rice hulls was greater than woodchips probably because rice hulls had higher ash content (23%). At last,

biomass type showed some effects on the H_2 content in the syngas (woodchips > rice hulls), but no differences were found in CO composition or the higher heating value of syngas from the two biomasses at all airflow rates.

3.5. Acknowledgements

This material was based upon the work supported by the U.S. Department of Agriculture and Sun Grant (Award No. 2010-38502-21836 and Subaward No. AB-5-67630. KSU11) and the startup fund of North Carolina State University. The lead author was also partially supported by the scholarship program of IFARHU-SENACYT from the Government of Panama. We would also like to thank Mr. Justin Macialek, research assistant at NCSU, for his help building the top-lit updraft gasifier.

3.6. References

[1] Casler MD, Mitchell R, Richardson J, Zalesny RS. Biofuels, bioenergy, and bioproducts from sustainable agricultural and forest crops. BioEnergy Research 2009;2:77-78.

[2] McCord J, Owens V, Rials T, Stokes B. Summary Report on the 2012 Sun Grant National Conference: Science for Biomass Feedstock Production and Utilization. BioEnergy Research 2014;7:765-768.

[3] Hasan J, Keshwani DR, Carter SF, Treasure TH. Thermochemical Conversion of Biomass to Power and Fuels. Biomass to Renewable Energy Processes: CRC Press, Taylor & Francis Group; 2010, p. 437-489.

[4] Knoef H, Ahrenfeldt J. Handbook biomass gasification. : BTG biomass technology group The Netherlands; 2005.

[5] Dry ME. The Fischer–Tropsch process: 1950–2000. Catalysis Today 2002;71:227-241.

[6] Jadhav SG, Vaidya PD, Bhanage BM, Joshi JB. Catalytic carbon dioxide hydrogenation to methanol: A review of recent studies. Chem Eng Res Design 2014;92:2557-2567.

[7] Griffin DW, Schultz MA. Fuel and chemical products from biomass syngas: a comparison of gas fermentation to thermochemical conversion routes. Environmental Progress & Sustainable Energy 2012;31:219-224.

[8] Lorenz K, Lal R. Biochar application to soil for climate change mitigation by soil organic carbon sequestration. J Plant Nutr Soil Sci 2014;177:651-670.

[9] Hyland C, Sarmah AK. Advances and Innovations in Biochar Production and Utilization for Improving Environmental Quality. Bioenergy Research: Advances and Applications 2014:435-446.

[10] Joseph S, Peacocke C, Lehmann J, Munroe P. Developing a Biochar classification and test methods. In: Lehmann J, Joseph S, editors. Biochar for environmental managenement: science and tecnology. 1st ed. London: Earthscan; 2009. p. 107-126.

[11] Garcia-Perez M, Lewis T, Kruger C. Methods for Producing Biochar and Advanced Biofuels in Washington State, Part 1: Literature Review of Pyrolysis Reactors. First Project Report: Department of Biological Systems Engineering and the Center for Sustaining Agriculture and Natural Resources 2010. Ecology publication number 11-07-017. Available at: https://fortress.wa.gov/ecy/publications/publications/1107017.pdf (accessed 14 March 2015).

[12] Sparrevik M, Adam C, Martinsen V, Jubaedah, Cornelissen G. Emissions of gases and particles from charcoal/biochar production in rural areas using medium-sized traditional and improved “retort” kilns. Biomass Bioenergy 2015;72:65-73.

[13] Brown R. Biochar production technology. In: Lehmann J, Joseph S, editors. Biochar for environmental management: Science and technology. 1st ed. London: Earthscan; 2009:127-146.

[14] Antal MJ, Croiset E, Dai X, DeAlmeida C, Mok WS, Norberg N, et al. High-yield biomass charcoal. Energy Fuels 1996;10:652-658.

[15] Oyedun AO, Lam KL, Hui CW. Charcoal production via multistage pyrolysis. Chin J Chem Eng 2012;20:455-460.

[16] Brick S, Lyutse S. Biochar: Assessing the promise and risks to guide US policy. Natural Resources Defense Council Issue Paper 2010.
Availableat: http://www.nrdc.org/energy/files/biochar_paper.pdf (accessed: January 31, 2015).

[17] Birzer C, Medwell P, Wilkey J, West T, Higgins M, MacFarlane G, et al. An analysis of combustion from a top-lit up-draft (TLUD) cookstove. Journal of Humanitarian Engineering 2013;2:1-7.

[18] Tryner J, Willson BD, Marchese AJ. The effects of fuel type and stove design on emissions and efficiency of natural-draft semi-gasifier biomass cookstoves. Energy for Sustainable Development 2014;23:99-109.

[19] Kammen DM, Lew DJ. Review of technologies for the production and use of charcoal. Renewable and Appropriate Energy Laboratory Report 2005;1. Available at: http://rael.berkeley.edu/old_drupal/sites/default/files/old-site-files/2005/Kammen-Lew-Charcoal-2005.pdf (accessed: October 7, 2015)

[20] Lehmann J, Joseph S. Biochar for environmental management: science and technology. 1st ed. London: Earthscan; 2009.

[21] Peterson SC, Jackson MA. Simplifying pyrolysis: Using gasification to produce corn stover and wheat straw biochar for sorptive and horticultural media. Industrial Crops and Products 2014;53:228-235.

[22] Hernández JJ, Aranda-Almansa G, Bula A. Gasification of biomass wastes in an entrained flow gasifier: Effect of the particle size and the residence time. Fuel Process Technol 2010;91:681-692.

[23] Saravanakumar A, Haridasan T, Reed TB, Bai RK. Experimental investigation and modelling study of long stick wood gasification in a top lit updraft fixed bed gasifier. Fuel 2007;86:2846-2856.

[24] Reed T, Reed TB, Das A, Das A. Handbook of biomass downdraft gasifier engine systems. Golden, CO: Solar Energy Research Institute; 1988.

[25] Demirbaş A. Carbonization ranking of selected biomass for charcoal, liquid and gaseous products. Energy Conversion and Management 2001;42:1229-1238.

[26] Manyà JJ. Pyrolysis for biochar purposes: a review to establish current knowledge gaps and research needs. Environ Sci Technol 2012;46:7939-7954.

[27] Downie A, Crosky A, Munroe P. Physical properties of biochar. In: Lehmann J, Joseph S, editors. Biochar for environmental management: Science and technology. 1st ed. London: Earthscan; 2009:13-32.

[28] Turn, S., Kinoshita, C., Zhang, Z., Ishimura, D., & Zhou, J. An experimental investigation of hydrogen production from biomass gasification. International Journal of Hydrogen Energy, 1998;23:641-648.

[29] Milne TA, Abatzoglou N, Evans RJ. Biomass gasifier" tars": their nature, formation, and conversion. 1998. Available at: http://www.ps-survival.com/PS/Gasifiers/Biomass_Gasifier_Tars_Their_Nature_Formation_And_Conversion_1998.pdf (accessed: October 7, 2015).

[30] Hanping C, Bin L, Haiping Y, Guolai Y, Shihong Z. Experimental investigation of biomass gasification in a fluidized bed reactor. Energy Fuels 2008;22:3493-3498.

[31] Galindo AL., Lora, E. S., Andrade, R. V., Giraldo, S. Y., Jaén, R. L., & Cobas, V. M. Biomass gasification in a downdraft gasifier with a two-stage air supply: Effect of operating conditions on gas quality. Biomass and Bioenergy 2014;61:236-244.

[32] Lv, PM., Xiong, Z. H., Chang, J., Wu, C. Z., Chen, Y., & Zhu, J. X. An experimental study on biomass air–steam gasification in a fluidized bed. Bioresource Technology 2004;95:95-101.

[33] Antal, MJ., & Grønli, M. The art, science, and technology of charcoal production. Industrial & Engineering Chemistry Research 2003;42:1619-1640.

[34] Bryden, K., & Ragland, K. Combustion of a single wood log under furnace conditions. In Bridgwater AV, Boocock DGB, editors. Developments in thermochemical biomass conversion, London: Chapman and Hall; 1997;1331-1345.

[35] James, A., W. Yuan, M. Boyette, and D. Wang. The effect of air flow rate and biomass type on the performance of an updraft biomass gasifier, BioResources 2015;10:3615-3624.

CHAPTER 4 – Characterization of Biochar from Rice hulls and Wood chips produced in a Top-Lit Updraft Biomass Gasifier

Abstract

The objective of this study was to characterize biochar produced from rice hulls and wood chips in a top-lit updraft gasifier. Biochar from four airflows (8, 12, 16 or 20 lpm) and two insulation conditions (not insulated or insulated with 88.9 mm of Fiberglass® on the external wall of the gasifier) were evaluated. Measurement of elemental compositions, high heating value, BET surface area and proximate analyses of the biochar were carried out. It was found that the airflow rate and reactor insulation significantly influenced the chemical composition of the biochar depending on the biomass type. For instance, the carbon content of biochar from rice hulls decreased from 40.9 to 27.2% and the high heating value decreased from 14.8 to 10.2 MJ/kg as the airflow increased from 8 to 20 lpm when the reactor was insulated. In contrast, the carbon content of biochar from wood chips increased from 82% to 86% and the high heating value stayed stable at 32 to 33.2 MJ/kg at the same conditions. Despite these variations, the BET surface area of biochar from both biomasses increased with increasing airflow and additional insulation, for example, rice hulls biochar had a maximum BET surface area of 183 m^2/g at 20 lpm airflow with insulation. The BET surface of biochar from wood chips peaked at 405 m^2/g at the same conditions.

4.1 Introduction

Biochar is usually defined as one of the products of biomass carbonization at temperatures lower than 700ºC in the absence of oxygen (Lehmann and Joseph, 2010). This

carbon-rich material can be widely used in applications such as soil conditioning to improve nutrients retention, adsorption of contaminants in liquid and gas media, and for high-value chemical manufacture (Manya, 2012; Antal and Gronli, 2003). Since biochar production is often performed using pyrolysis processes, extensive literature is available in these production methods (Kammen and Lew, 2005; Trossero, 2008). The properties of the biomass and the reaction parameters have been correlated with the physical and chemical properties of the biochar (Antal et al., 1996; Sun et al., 2014; Demirbas, 2004). This has helped to identify optimum production conditions for biochar in a variety of pyrolysis units. However, despite the advances of biochar production over the last decades, biochar production technologies are found to have low energy efficiencies (Antal et al., 1990; Antal and Gronli, 2003) because of the heat needed for reactions. In pyrolysis units, such heat is provided by external heating elements (Kwapinski et al., 2010) or the combustion of pyrolysis vapors generated during reactions (Garcia-Perez, 2010).

Gasification of biomass has been considered as an alternative to pyrolysis-based biochar production, but the low yields is a major challenge since gasifiers are designed to maximize the yield of gas products (Bridgwater, 2012; Brick and Lyutse, 2010). Several studies have demonstrated the possibility to implement gasification systems for biochar production (Shackley et al., 2012; Brown, 2009). Qian et al. (2013) produced biochar in a fluidized bed reactor with switchgrass, sorghum biomass and red cedar. The reaction temperature ranged from 700 to 800ºC at different equivalent ratios. The results showed that the quality of the biochar was affected by the gasification operational parameters and the biomass type. However, it was also reported that not all the biochar was recovered because of the inability of

the cyclone to retrieve the product. Likewise, most fixed bed reactors might also present challenges for the production of biochar because of the temperature instability within the gasification bed that can generate hot spots of exothermal reactions that lead to large variations in the products of gasification (Warnecke, 2000). As result, current gasification technologies require modifications in order to be implemented for biochar production.

Top-lit updraft (TLUD) gasification has been presented as a gasification technology for biochar production (Peterson and Jackson, 2014; Huangfu et al., 2014). Relatively high yield of biochar, parallel production of syngas and the generation of exothermal heat for gasification and pyrolysis reactions are some examples of the advantages of implementing TLUD gasification for biochar production (Birzer et al., 2013; Tryner et al., 2014). Thus far, small-scale TLUD gasifiers have been proven as an effective alternative to common woodstoves in developing countries (Mukunda et al., 2010). For such application, it has been found to reduce the amount of smoke and other contaminants emitted from the cookstove (Birzer et al., 2013; Reed and Larson, 1996). This is because of the combustion of volatiles in the reactor to produce biochar and syngas, and then the combustion of syngas to produce heat for cooking. The biochar produced in these small TLUD gasifiers might be useful for other applications (Brewer, 2012). However, little is known about the biochar quality since no previous studies of biochar characterization as a function of the available air for gasification and reactor design has been reported to date. Limited information is available to identify other potential applications for the biochar from this process (Brown, 2009). The objective of this research was then to study the key properties of biochar from top-lit updraft gasification and correlate such properties with the airflow rate and the utilization of insulation on the gasifier. This can help to identify

variations in chemical and physical properties of the biochar due to changes in the temperature distribution within the gasifier.

4.2 Materials and methods

The experiments were carried in a top-lit updraft gasifier with 10.1-cm internal diameter and 152-cm height. This gasifier was equipped with three thermocouples located at the top, middle and bottom; and a data logger (Onset® Model UX120-014M, USA) recorded the temperatures, as shown in Fig. 4.1. Two insulation conditions were used to produce biochar: no insulation or insulating the reactor with 88.9-mm of Fiberglass® insulation. Additionally, airflow rates of 8, 12, 16 and 20 lpm were used for biochar production which were supplied by an air compressor (1.5 kW – 8.62 bar max. pressure) equipped with a 22.7-liter reservoir tank (WEN, Elgin, IL). The equivalent superficial velocities for the airflow rates were 0.83, 1.25, 1.66 and 2.08 cm/s, respectively. Rice hulls from Carolina Greenhouses (Kinston, NC) and pine wood chips from a local grinding company (Newton County, NC) were used as the feedstocks. The particle size of the rice hulls was measured using different screen sizes; it was found that the average particles were smaller than 2 mm. Pine wood chips with particle size smaller than 10 mm. Particles smaller than 3 mm were removed using a 3-mm screen. The final particle size of the wood chips ranged between 3 and 10 mm. The main properties of these two biomasses are presented in Table 4.1. Elemental composition of biomass and biochar were measured in a CHNS/O elemental analyzer (Elmer Perkin 2400, CT, USA). Volatile matter content was determined based on ASTM D3175-11 standard (ASTM,

2011). Ash content was determined following ASTM E1755 – 01 (ASTM, 2015). The fixed carbon was calculated based on the percentage difference of volatile matter, ash and moisture.

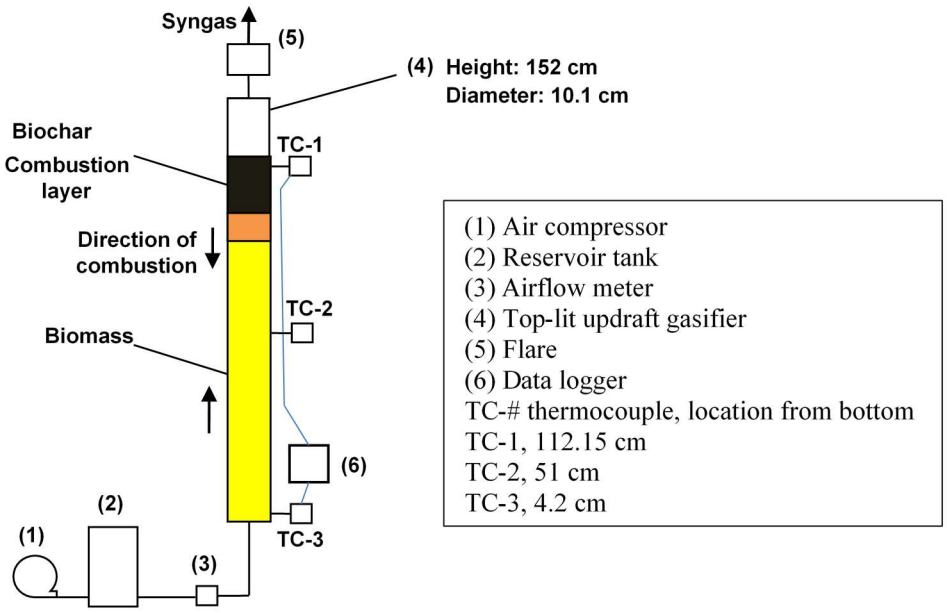

Fig. 4.1. A schematic diagram of the top-lit updraft gasifier setup

In addition, the high heating value was determined for the two biomasses and all the biochar samples. This analysis was carried out in a bomb calorimeter (IKA-Calorimeter C 200, IKA-Werke GmbH and Co. KG, Staufen, Germany) with benzoic acid as the standard. BET surface area of the samples was measured with a surface area analyzer (Autosorb-1C, Quantachrome, Bouton Beach, FL) operated under isothermal nitrogen sorption; all samples were degassed for 12 hours at 250ºC under vacuum before BET analysis. The recorded chemical properties of the biochar was statistically analyzed to identify differences in the effect of the airflow, insulation condition and biomass type. A GLM procedure in SAS® software

corrected with Tukey HSD (honestly significant difference) was used with a confidence level of 90%.

Table 4.1. Elemental composition of rice hulls and wood chips

	Biomass	
	Rice hulls	Wood chips
C (%)	36.99	47.90
H (%)	5.14	1.70
N (%)	0.58	0.30
O[a] (%)	56.30	49.90
S (%)	1.0	0.20
Ash (%)	23.78	0.57
Volatile matter (%)	58.17	74.92
Fixed carbon a (%)	9.57	16.66
Moisture (%)	8.48	7.85
HHV (MJ/kg)	14.42	19.53
Particle size (mm)	$X \leq 2$	$3 < X \leq 10$

[a] calculated by difference

4.3. Results and discussion

4.3.1 The reaction temperatures

The increase in combustion temperature in the TLUD gasifier positively correlated with airflow as presented in Fig. 4.2. This tendency was observed for both rice hulls (from 700 to 868ºC) and wood chips (from 648 to 840ºC), which had different chemical properties (Table 4.1). However, no significant difference in the combustion temperature was noticed when two insulation conditions were evaluated at all airflow rates. Because the insulation helped to reduce heat loss through the gasifier's wall, the increase in the overall temperature in the gasifier with insulation was observed. The biggest temperature increase was nearly 154ºC for rice hulls and 138ºC for wood chips. The reaction temperature across carbonization units has

been found to play a significant role in the final chemical composition and quality of biochar. This is because of the decomposition of different compounds of biomass at different temperatures (Demirbas et al., 2001) which can lead to the formation of different pore arrangements, surface areas and chemical properties of biochar (Antal and Gronli, 2003).

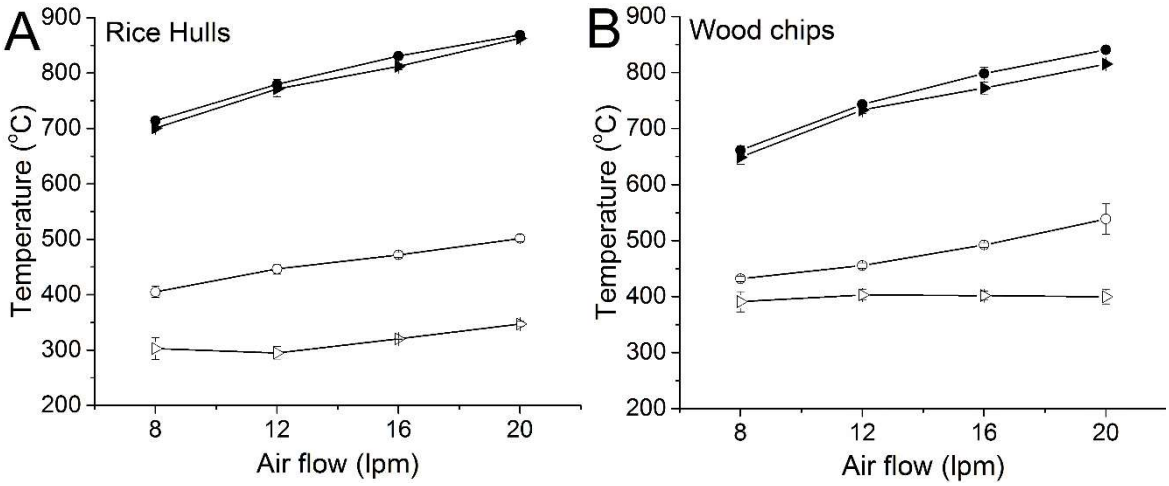

Fig. 4.2. Airflow rate and insulation effects on the combustion zone temperature and average temperature of TLUD gasification of (A) rice hulls and (B) wood chips. ► without insulation, ● with insulation, □ average temperature without insulation, ○ average temperature with insulation.

4.3.2 The elemental composition of biochar

Fig. 4.3A shows the elemental carbon content in biochar produced from rice hulls. The carbon content decreased from 40% to 27~28% as the airflow increased from 8 to 20 lpm, which might be attributed to the increased combustion temperature. Insulation had no significant effects on elemental C content of the biochar. The comparison of the carbon content of the biochar and the initial carbon composition of rice hulls (36.99%) reveals that higher carbon content was achieved after the carbonization process at lower airflows (8 and 12 lpm). In contrast, the yielded carbon produced at higher airflow rates (16 and 20 lpm) was significantly lower than that of the initial biomass. Gasification systems are fueled by the

carbon based materials present in the biomass; thus the carbon content of the biomass might be reduced depending on the carbonization mechanism during reactions. Reduction of carbon content has been associated with carbonization due to oxidation of the molecular components of biomass matter (Baldock and Smernik, 2002) which can present a more significant impact due to the low organic composition of rice hulls.

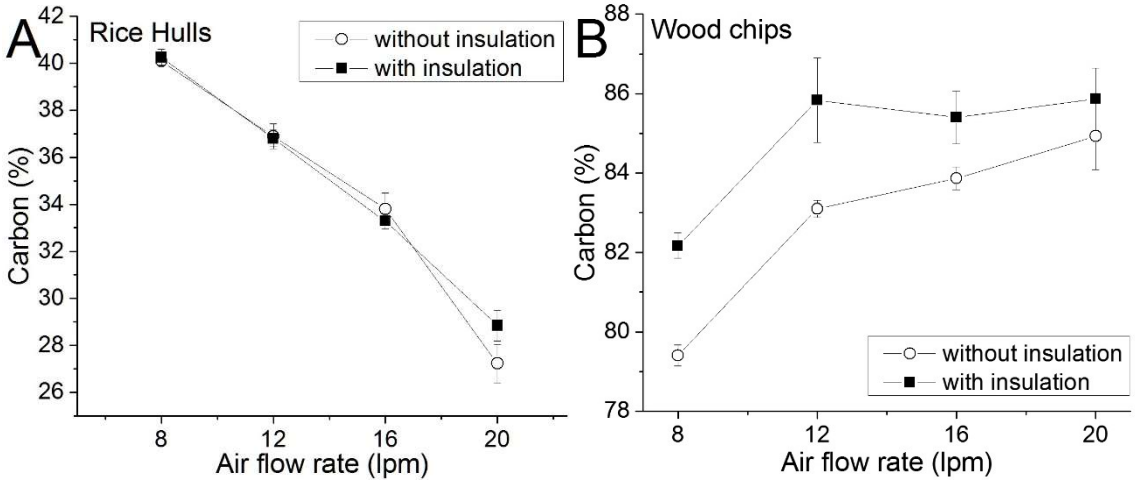

Fig. 4.3. Elemental carbon composition in biochar from (A) rice hulls and (B) wood chips

Divergent to rice hulls gasification, the carbon content of biochar from wood chips increased from 79% to 85% without insulation, and from 82% to 86% with insulation, with increasing airflow rates (Fig. 4.3B). In both insulation conditions and under all airflows, the carbon contents of wood chips biochar were significantly higher than that in the source biomass (47.9%). Nevertheless, this was due to the fact that oxygen, hydrogen and nitrogen were detached from the biochar at temperatures above 600ºC at which the carbon concentration in the biochar was increased (Amonette and Joseph, 2009). In addition, the increase in carbon

content was also enhanced by the increase in the airflow rate and the addition of insulation, as a result of a higher overall temperature within the gasifier. It is apparent that the tendency of the carbon content from these two biomasses was opposite regardless of the insulation condition. This phenomenon can be explained by the ash content of these two raw materials. Antal and Gronli (2003) stated that the carbonization of biomass with low ash content can increase the carbon content in biochar because of the reduction of weight due to the devolatilization. However, this was opposite for biomass with high ash content which can present decrease in carbon content as it is carbonized. Rice hulls in this study contained 23% ash which was significantly higher than the 0.57% ash in wood chips (Table 4.1). High amounts of ash represented a partially unchanged amount of ash within the produced biochar during reactions. As result, less carbon based reactants were available which reduced the carbon content of the biochar due to carbon conversion in the gasification and combustion reactions (Qian et al., 2013). A similar tendency was observed in the results from a previous study (Peterson and Jackson, 2014) in which corn stover (28% ash) and wheat straw (12% ash) were pyrolyzed at temperatures from 400 to 700^{o}C. The results showed that the carbon content of the biochar from wheat straw increased from 73 to 81% while for corn stover it decreased from 60 to 58%.

The nitrogen content in the biochar from rice hulls was also found to decrease without insulation (from 0.82 to 0.48%) and with insulation (from 0.57 to 0.36%) as the airflow increased. Moreover, no insulation resulted in higher overall nitrogen content in the biochar than with insulation, as presented in Fig. 4.4A. This decrease in the nitrogen content with increasing airflow rate indicated that nitrogen from rice hulls was removed because of the

thermochemical degradation of biomass. Nitrogen in biomass materials is represented as amino acids and proteins that are easily converted in thermochemical processes to nitrogen based chemicals such as ammonia, nitrogen oxides and molecular nitrogen due to gas solid reactions at high temperatures (Hu et al., 2008). However, this observation was not true for wood chip biochar, which presented no significant differences in nitrogen content at all levels of airflow and insulation (Fig. 4.4B).

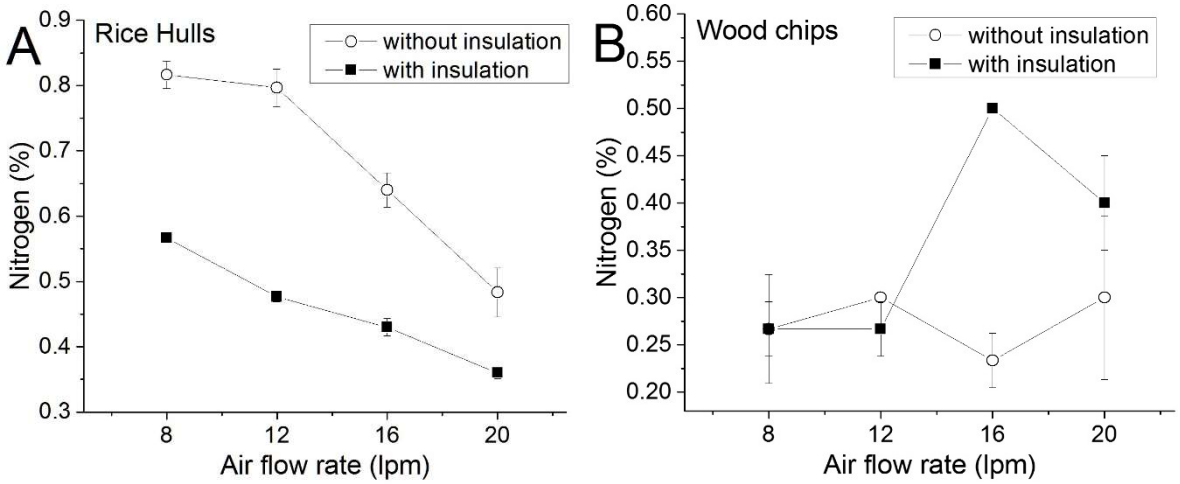

Fig. 4.4. Elemental nitrogen composition in biochar from (A) rice hulls and (B) wood chips

Fig. 4.5 displays the hydrogen content of biochar from rice hulls and wood chips. The hydrogen content of biochar from rice hulls decreased as the airflow rate increased regardless of the insulation. However, significantly higher hydrogen content in the biochar was found at lower airflows (8 and 12 lpm) when the reactor was not insulated, implying that a lower overall temperature within the gasifier can generate higher hydrogen content. This reduction in the hydrogen content can be attribute to dehydration, dehydrogenation and cracking of hydrogen binding chains within the biochar that can be induced by increasing the reaction temperature

(Kim et al., 2012; Baldock and Smernik, 2002). A similar pattern was found in the hydrogen content of biochar from wood chips with no insulation. Likewise, decrease in hydrogen content with increasing reaction temperatures was previously reported by Demirbas (2004), who studied the pyrolysis of corncob, olive husk and tea wastes and found that when increasing the temperature from 175 to 975ºC, the hydrogen content of biochar decreased from approximately 5.5 to 1%.

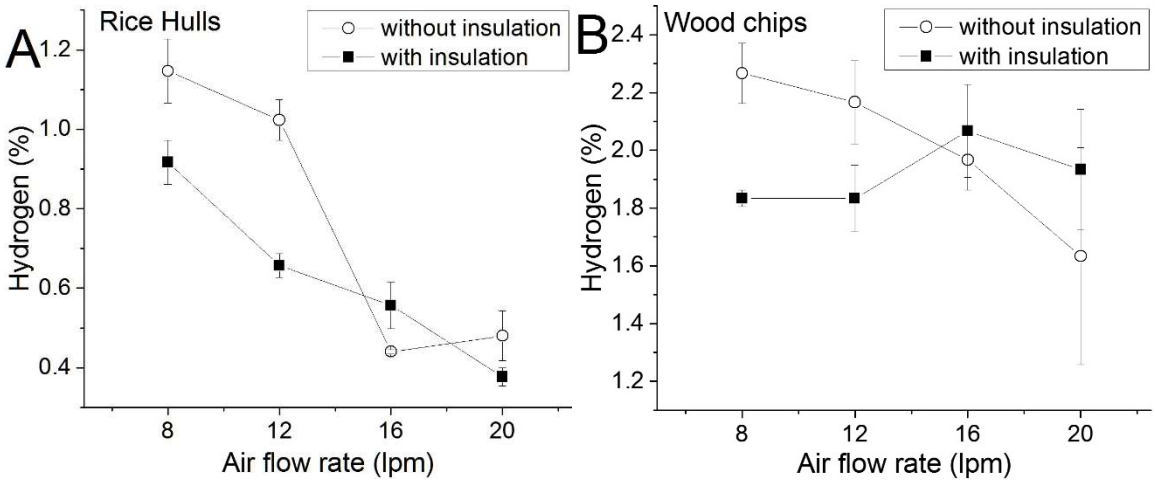

Fig. 4.5. Elemental hydrogen composition in biochar from (A) rice hulls and (B) wood chips

The oxygen content of biochar from rice hulls significantly increased from 57 to 71% as the airflow rate increased, but there was no significant difference when comparing the oxygen content of the two insulation conditions (Fig. 4.6A). Comparing Fig. 4.3A and Fig 4.6A, it can be noticed that the trend of the carbon content was contrary to that presented by the oxygen content. As a result, the increase in the oxygen content suggested a strong influence of oxidation reactions on the formation of carbon during the carbonization process rather than aromatic carbon formation (Baldock and Smernik, 2002).However, the oxygen content in

biochar from wood chips exhibited noticeable decrease from 17.8 to 12.8% as the airflow rate increased from 8 to 20 lpm (Fig. 4.6B). Biochar produced at 8 lpm was found to be significantly different in O content from those generated at higher airflow rates (>12 lpm) regardless of the insulation condition. It is also interesting to see that rice hull biochar had much higher O contents than woodchip biochar. This suggested that contrary to the gasification of rice hulls, the gasification of wood chips presented a predominant level of aromatization that promoted the carbonization of aromatic components within the molecular structure of the biochar. The former contained oxygen in the biomass was 49%, while the latter contained only from11.5% to 17.80%. As a result, it can be stated that biochar from biomass of high ash content can contain higher oxygen content as the airflow increases due to the predomination of oxidation reactions during biochar formation. In contrast, low ash content in the biomass can promote reduction in oxygen content in biochar when the airflow increases due to dominating aromatization on the produced biochar.

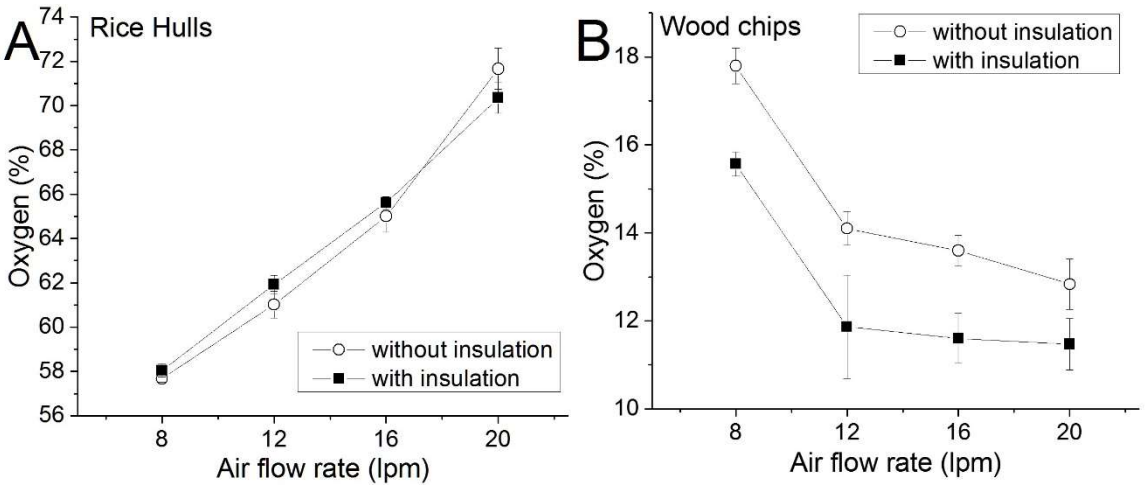

Fig. 4.6. Elemental oxygen composition in biochar from (A) rice hulls and (B) wood chips

4.3.3. Proximate analysis

The average fixed carbon in rice hull biochar decreased from 34 to 23% as the airflow rate increased (Fig. 4.7A and 4.7B). However, no statistically significant difference was found when the airflow and insulation were varied. In contrast, the fixed carbon of biochar from wood chips was observed to significantly increase with increasing airflow (Fig. 4.7C and 4.7D). The lowest fixed carbon content (63.6%) was at 8 lpm without insulation and the highest (91.0%) at 20 lpm with insulation. This increase in the fixed carbon can be attributed to the overall increase in the reaction temperature and the low ash content of the unreacted biomass; similar to the tendency presented by the elemental carbon content of this biomass.

The gasification of rice hulls exhibited increase in the ash content from 52.6 to 60.4% as the airflow increased with no insulation. Similarly, the ash content in the biochar further increased from 54.2 to 66.8% when the insulation was applied. This phenomenon might be due to the fact that most ash components are minerals (Joseph et al., 2009) that might remain unreacted during gasification reactions. However, carbon based components such as tar and fixed carbon react when the temperature raises; this generates gases that are transported with gas phase (Jameel, et al., 2009). Therefore, the ash content in rice hulls (23%) might be considered a fixed amount which appeared to increase when compared with the decreasing carbon content. Due to its low ash content, carbon content in the biochar from wood chips was not considerably impacted. Moreover, ash content increased as increasing the airflow. Despite this increase, the highest ash content derived from wood chips was 2.59% at 20 lpm (no insulation) which represented ~1.5% more ash when compared with the initial biomass (Fig. 4.7C).

The volatile matter content of biochar from rice hulls varied between 5.5 and 9.6% which was significantly lower than that in the unreacted rice hulls (Fig. 4.7A & 4.7B). However, no significant difference was found in the volatile matter of biochar from rice hulls when comparing every level of airflow or insulation. In a similar way, as increasing the airflow rate, the volatile matter of biochar from wood chips decreased from 31.8 to 6.6% without insulation and from 12 to 5.3% with insulation (Fig. 4.7C & 4.7D). The combustion zone in top-lit updraft gasifiers is partially fueled by the volatiles released from the biomass below this zone, in a process often known as flaming pyrolysis (Saravanakumar et al., 2007; Hangfu et al., 2014). This devolatilization phenomenon can be observed by comparing the initial volatile in the biomasses with those in the biochar; rice hulls initially contained 58% volatiles and wood chips 74%. As the airflow increased more of the volatiles were removed because of the increasing reaction temperatures in the gasifier (Fig. 4.2).

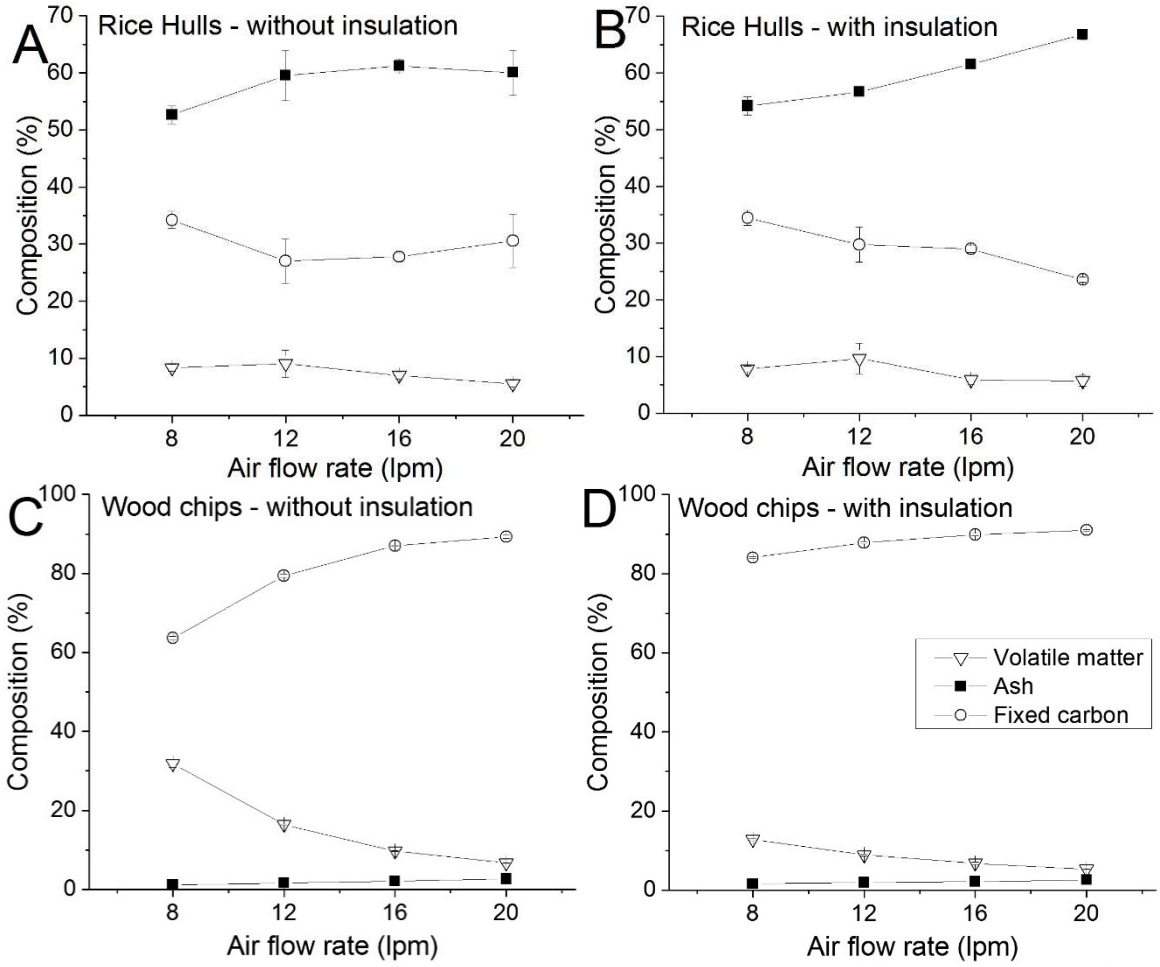

Fig 4.7. Proximate analysis of rice hulls (A) without insulation and (B) with insulation, and wood chips (C) without insulation and (D) with insulation.

4.3.4. High heating value and specific surface area

Results of the high heating value of the biochar are presented in Fig. 4.8. It is observed that the high heating value of biochar from rice hulls decreased from 14.9 to 9.5 MJ/kg without insulation and from 14.8 to 10.2 MJ/kg with insulation as the airflow increased (Fig 4.8A). Although the biochars produced at every airflow rate were significantly different, no significant differences were noticed when independent insulation conditions were evaluated at different airflows. In contrast, the high heating value of biochar from wood chips increased

from 29 to 33 MJ/kg with no insulation when raising the airflow (Fig. 4.8B). However, no significant differences were presented in the high heating value of the biochar, which varied from 32 to 33.2 MJ/kg when the insulation was added.

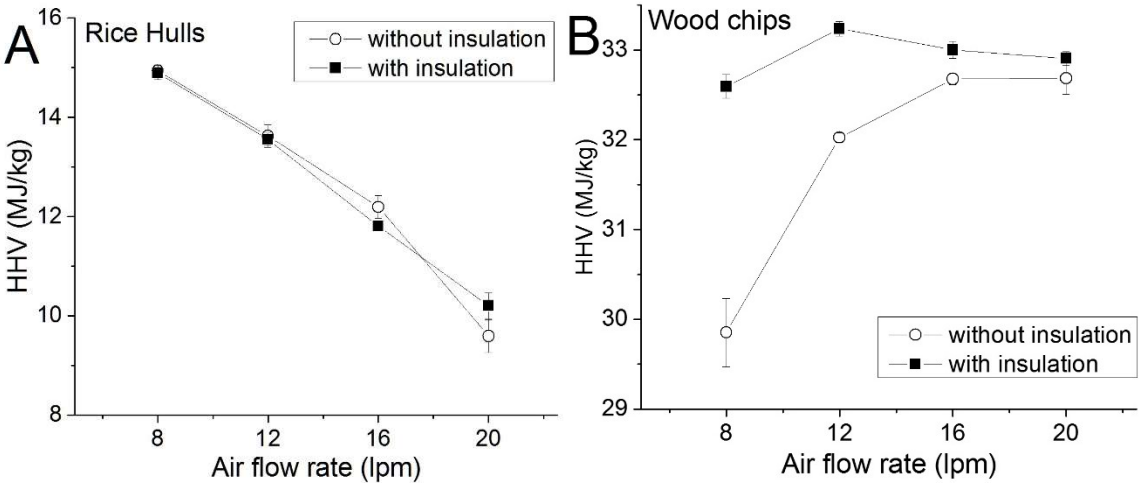

Fig 4.8. High heating value of biochar from (A) rice hulls and (B) wood chips

When comparing the heating values of the biomass with the heating value of the biochar; it can be noticed that besides the heating value at 8 lpm, rice hulls biochar presented lower heating value than the initial biomass (14.4 MJ/kg). Nonetheless, all biochars produced from wood chips yielded heating values higher than that of the biomass (19.5 MJ/kg). This tendency can be attribute to the ash content of the biomasses. Brewer (2012) converted corn stover, switchgrass and hard wood into biochar using pyrolysis and gasification methods. The results showed that biomasses with large ash content produced biochar with a lower heating potential when compared with biomass of low ash content which produced biochar with a high heating potential. This suggests that the high heating value of biochar is not only a factor of

the selected operational parameters during conversion, but also influenced by the chemical properties of the biomass.

Results of the BET surface area are presented in Fig. 4.9. The biochar produced from rice hulls presented increase in the surface areas from 1.66 to 30.4 m^2/g without insulation and from 9.4 to 183 m^2/g with insulation as the airflow increased from 8 to 20 lpm (Fig. 4.9A). Without insulation, the BET surface area of biochar from wood chips increased from 1.46 to 332 m^2/g, and with insulation from 56 to 405 m^2/g. This increase in BET surface areas of both biomasses was correlated with the combustion temperature of the gasification reaction. When the airflow varied from 8 to 20 lpm without insulation, the combustion temperature increased from 700 to 862ºC which presented a linear correlation with an adjusted R^2 of 0.80. With the addition of insulation, the temperature increased from 714 to 868ºC with an adjusted R^2 of 0.99. Likewise, the BET surface area of biochar from wood chips was found to be correlated with the combustion temperature that increased from 648 to 815ºC with an adjusted R^2 of 0.65 without insulation, and with insulation increased from 661 to 840ºC with an adj. R^2 of 0.99. It can also be observed that the increase in the overall reaction temperature as a result of the addition of the insulation represented a positive effect on the BET surface area. Similar increase in the BET surface area was reported by Peterson (2014) when conducting experiments in a pyrolysis unit raising the temperature from 400 to 700ºC. The results showed that the surface area of biochar from corn stover increased from 18 to 451 m^2/g. Likewise, Lua et al., (2004) studied the effect of the temperature in the pyrolysis of pistachio-nut shells. It was observed that as increasing the reaction temperature from 250 to 1000ºC, the BET surface area of the biochar increased from 333 to 601 m^2/g which was attributed to evacuation of

micro-pores within the biochar structure. This indicated that the proportional increase in the combustion temperature because of the increase in airflow and addition of insulation can promote increase in the BET surface area of the biochar produced by top-lit gasification regardless of the biomass type. Biochar from wood chips depicted much higher surface areas when compared with rice hulls. Biochar derived from woody biomass have been found to produce larger surface areas when compared with biochar from agricultural crops and grasses (Downie et al., 2009). This tendency has been previously associated to the lower ash content of woody biomass that correspond to a larger carbon based composition (Sun et al., 2014; Qian et al., 2013).

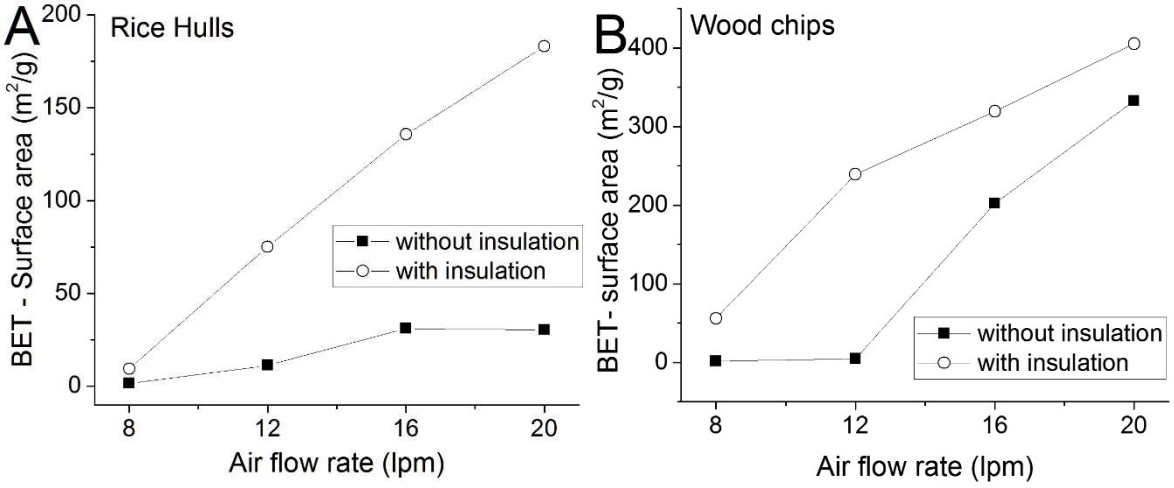

Fig. 4.9. BET surface area of biochar produced from (A) rice hulls and (B) wood chips.

4.4. Conclusions

The properties of biochar produced in a top-lit updraft gasifier were strongly affected by the increase in airflow. However, different effects were observed for different biomasses. Rice hulls biochar showed significant decrease in their carbon, hydrogen, nitrogen, and fixed

carbon contents and high heating value as the airflow increased, but the oxygen content increased with increasing airflow. This was related to the high ash content of rice hulls and the oxidation nature of the gasification process. In contrast, wood chip biochar showed increases in the carbon and fixed carbon contents and high heating value as the airflow increased. Moreover, the addition of insulation maximized the increase in biochar carbon content for biomass with low ash content (wood chips) because of the increasing aromaticity as the overall reaction temperature increased. However, adding insulation did not significantly affect the carbonization of biomass with high ash content (rice hulls). The volatile matters in biochar were significantly lower than that presented in the unreacted biomasses. This was because of the utilization of volatiles in the combustion reactions in the gasifier. In addition, the BET surface areas of biochar were found to increase with increasing airflow and additional insulation regardless of the biomass type. Biochar from wood chips presented much higher BET surface area than that of rice hulls. Furthermore, the addition of insulation resulted in further increases in BET surface area because of the increasing overall reaction temperature within the gasifier.

4.5. Acknowledgements

This material was based upon the work supported by the U.S. Department of Agriculture and Sun Grant (Award No. 2010-38502-21836 and Subaward No. AB-5-67630. KSU11) and the startup fund of North Carolina State University. The lead author was also partially supported by the scholarship program of IFARHU-SENACYT from the Government

of Panama. We would also like to thank Mr. Justin Macialek, research assistant at NCSU, for his help building the top-lit updraft gasifier.

4.6 References

Antal, M. J., Mok, W. S., Varhegyi, G. and Szekely, T. (1990). Review of methods for improving the yield of charcoal from biomass. Energy & Fuels, 4(3): 221-225. DOI: 10.1021/ef00021a001

Antal, M. J. and Grønli, M. (2003). The art, science, and technology of charcoal production. Industrial & Engineering Chemistry Research, 42(8): 1619-1640. DOI: 10.1021/ie0207919

Antal, M. J., Croiset, E., Dai, X., DeAlmeida, C., Mok, W. S., Norberg, N., Richard, J. and Al Majthoub, M. (1996). High-yield biomass charcoal. Energy & Fuels, 10(3): 652-658. DOI: 10.1021/ef9501859

Amonette, J. E., and Joseph, S. (2009). Characteristics of biochar: Microchemical properties. Biochar for Environmental Management: Science and Technology, 33

ASTM D3175-11 standard. (2011). Standard Test Method for Volatile Matter in the Analysis Sample of Coal and Coke, ASTM Coal and Coke. DOI: 10.1520/D3175-11

ASTM E1755 – 01 standard. (2015). Standard Test Method for Ash in Biomass, ASTM Bioenergy and Industrial Chemicals from Biomass. DOI: 10.1520/E1755-01R15

Baldock, J. A., and Smernik, R. J. (2002). Chemical composition and bioavailability of thermally altered pinus resinosa (red pine) wood. Organic Geochemistry, 33(9), 1093-1109. DOI:http://dx.doi.org/10.1016/S0146-6380(02)00062-1

Birzer, C., Medwell, P., MacFarlane, G., Read, M., Wilkey, J., Higgins, M. and West, T. (2014). A Biochar-producing, Dung-burning Cookstove for Humanitarian Purposes. Procedia Engineering, 78, 243-249. DOI:10.1016/j.proeng.2014.07.063

Birzer, C., Medwell, P., Wilkey, J., West, T., Higgins, M., MacFarlane, G. and Read, M. (2013). An analysis of combustion from a top-lit up-draft (TLUD) cookstove. Journal of Humanitarian Engineering 2(1), 1-8.

Brewer, C. E. (2012). Biochar characterization and engineering. Ames, Iowa; Iowa State University, Chemical Engineering.

Brick, S. and Lyutse, S. (2010). Biochar: Assessing the promise and risks to guide US policy. Natural Resources Defense Council. Retrieved from http://www.nrdc.org/energy/files/biochar_paper.pdf (accessed 3 November 2012).

Bridgwater, A. V. (2012). Review of fast pyrolysis of biomass and product upgrading. Biomass and Bioenergy, 38(0): 68-94. DOI:10.1016/j.biombioe.2011.01.048

Brown, R. (2009). Biochar production technology. In Biochar for environmental management: Science and technology (pp. 127-146). UK: Earthscan.

Demirbas, A. (2004). Effects of temperature and particle size on bio-char yield from pyrolysis of agricultural residues. Journal of Analytical and Applied Pyrolysis, 72(2): 243-248. DOI:10.1016/j.jaap.2004.07.003

Demirbas, A. (2001). Carbonization ranking of selected biomass for charcoal, liquid and gaseous products. Energy Conversion and Management, 42(10): 1229-1238. DOI: 10.1016/S0196-8904(00)00110-2

Downie, A., Crosky, A. and Munroe, P. (2009). Physical properties of biochar. In Biochar for environmental management: Science and technology (pp. 13-32). UK: Earthscan.

Garcia-Perez, M., Lewis, T. and Kruger, C. (2010). Methods for Producing Biochar and Advanced Biofuels in Washington State, Part 1: Literature Review of Pyrolysis Reactors. First Project Report 11-07-017. Department of Biological Systems Engineering and the Center for Sustaining Agriculture and Natural Resources. Retrieved from https://fortress.wa.gov/ecy/publications/documents/1107017.pdf

Hasan, J., D. R. Keshwani, S. F. Carter and T. H. Treasure. (2010). Themochemical Conversion of Biomass to Power and Fuels. In Biomass to Renewable Energy Processes, (pp. 437-489). Boca Raton, FL. CRC Press, Taylor & Francis Group.

Hu, S., Xiang, J., Sun, L., Xu, M., Qiu, J., & Fu, P. (2008). Characterization of char from rapid pyrolysis of rice husk. Fuel Processing Technology, 89(11), 1096-1105. DOI:http://dx.doi.org/10.1016/j.fuproc.2008.05.001

Huangfu, Y., Li, H., Chen, X., Xue, C., Chen, C. and Liu, G. (2014). Effects of moisture content in fuel on thermal performance and emission of biomass semi-gasified cookstove. Energy for Sustainable Development, 21, 60-65. DOI: 10.1016/j.esd.2014.05.007

Joseph, S., C. Peacocke, J. Lehmann and P. Munroe. 2009. Developing a Biochar classification and test methods. In Biochar for environmental managenement: science and technology (pp. 107-126. UK: Earthscan.

Kammen, D. M. and Lew, D. J. (2005). Review of Technologies for the Production and Use of Charcoal. Renewable and Appropriate Energy Laboratory. Report 1. Berkley, CA: National Renewable Laboratory. Retrieved from http://rael.berkeley.edu/old_drupal/sites/default/files/old-site-files/2005/Kammen-Lew-Charcoal-2005.pdf

Kim, K. H., Kim, J., Cho, T., & Choi, J. W. (2012). Influence of pyrolysis temperature on physicochemical properties of biochar obtained from the fast pyrolysis of pitch pine (pinus rigida). Bioresource Technology, 118, 158-162. DOI:http://dx.doi.org/10.1016/j.biortech.2012.04.094

Kwapinski, W., Byrne, C. M., Kryachko, E., Wolfram, P., Adley, C., Leahy, J., Novotny, E. H. and Hayes, M. (2010). Biochar from biomass and waste. Waste and Biomass Valorization, 1(2), 177-189. DOI: 10.1007/s12649-010-9024-8

Lehmann, J. and S. Joseph. (2009). Biochar for environmental management: an introduction. In Biochar for environmental management: Science and technology (pp. 1-12). UK: Earthscan.

Lua, A. C., Yang, T. and Guo, J. (2004). Effects of pyrolysis conditions on the properties of activated carbons prepared from pistachio-nut shells. Journal of Analytical and Applied Pyrolysis, 72(2), 279-287. DOI: 10.1016/j.jaap.2004.08.001

Manyà, J. J. (2012). Pyrolysis for biochar purposes: a review to establish current knowledge gaps and research needs. Environmental science & technology, 46(15), 7939-7954. DOI: 10.1021/es301029g

Mukunda, H., Dasappa, S., Paul, P., Rajan, N., Yagnaraman, M., Ravi Kumar, D. and Deogaonkar, M. (2010). Gasifier stoves–science, technology and field outreach. Current science, 98(5) 627-638.

Peterson, S. C. and Jackson, M. A. (2014). Simplifying pyrolysis: Using gasification to produce corn stover and wheat straw biochar for sorptive and horticultural media. Industrial Crops and Products, 53, 228-235. DOI: 10.1016/j.indcrop.2013.12.028

Qian, K., Kumar, A., Patil, K., Bellmer, D., Wang, D., Yuan, W. and Huhnke, R. L. (2013). Effects of biomass feedstocks and gasification conditions on the physiochemical properties of char. Energies, 6(8), 3972-3986. DOI: 10.3390/en6083972

Reed, T. and Ronal, L. (1996). A wood-gas stove for developing countries. Banff, Canada: Developments in Thermochemical Biomass Conversion Conference.

Saravanakumar, A., Haridasan, T., Reed, T. B. and Bai, R. K. (2007). Experimental investigation and modelling study of long stick wood gasification in a top lit updraft fixed bed gasifier. Fuel 86(17), 2846-2856. DOI: 10.1016/j.fuel.2007.03.028

Shackley, S., Carter, S., Knowles, T., Middelink, E., Haefele, S., Sohi, S., Cross, A. and Haszeldine, S. (2012). Sustainable gasification–biochar systems? A case-study of rice-husk gasification in Cambodia, Part I: Context, chemical properties, environmental and health and safety issues. Energy Policy 42, 49-58. DOI: 10.1016/j.enpol.2011.11.026

Sun, Y., Gao, B., Yao, Y., Fang, J., Zhang, M., Zhou, Y., Chen, H. and Yang, L. (2014). Effects of feedstock type, production method, and pyrolysis temperature on biochar and hydrochar properties. Chemical Engineering Journal, 240, 574-578. DOI: 10.1016/j.cej.2013.10.081

Trossero, M., J. Domac and R. Siemons. (2008). Industrial charcoal production. TCP/CRO/3101(A) Development of a sustainable charcoal industry. Zagreb, Croatia. FAO project. Retrieved from: http://pvbiochar.org/forum/index.php?action=dlattach;topic=1335.0;attach=234

Tryner, J., Willson, B. D. and Marchese, A. J. (2014). The effects of fuel type and stove design on emissions and efficiency of natural-draft semi-gasifier biomass cookstoves. Energy for Sustainable Development, 23, 99-109. DOI: 10.1016/j.esd.2014.07.009

Warnecke, R. (2000). Gasification of biomass: comparison of fixed bed and fluidized bed gasifier. Biomass and Bioenergy, 18(6), 489-497. DOI: 10.1016/S0961-9534(00)00009-X

CHAPTER 5 - The Effect of Biomass Physical Properties on Top-Lit Updraft Gasification of Woodchips

Abstract

The performance of a top-lit updraft gasifier and the properties of the produced biochar were studied. Four levels of particle size, moisture content and biomass compactness were evaluated in terms of the biochar yield, biomass burning rate, syngas composition and tar content, and the physiochemical properties of biochar. The highest biochar yield increase (from 12.2% to 21.8%) was achieved by varying the particle size from 7 to 30 mm, however larger particle size triggered tar generation that reached its maximum of 93.5 g/m^3 at 30 mm; in contrast, the hydrogen content reached its minimum of 2.89% at this condition. As a result of the reduced fixed carbon content of biochar, the BET surface area increased from 405 to 6.2 m^2/g when the particle size increased from 7 to 30 mm. The increase in moisture content from 10 to 22% reduced biochar yield from 12 to 9.9%. It also reduced the tar content from 12.9 to 6.2 g/m^3 which was found to be the lowest range of tar content in this work. Similarly, the carbon monoxide composition decreased to its minimum of 11.16% at moisture content of 22%. Likewise, the increase in moisture content reduced the fixed carbon (from 91 to 88%) and the BET surface area (from 405 to 352 m^2/g). Finally, the biomass compactness increased biochar yield up to 17% when the packing mass was 3 kg. However, the addition of compactness also increased the tar content in syngas, and reduced the BET surface area (from 405 to 191 m^2/g), but little effect was noticed in syngas composition. These results indicated that the physical properties of the biomass feedstock played an important role in the gasification process and in the quality of the produced biochar.

5.1. Introduction

The use of lignocellulosic biomass to produce energy and high-value products have increased in the last decades (Isikgor and Becer, 2015; Salehi and Taherzadeh, 2015). Agricultural residues, energy crops and biomass-based municipal wastes are some examples of preferred raw materials for biofuel and biomaterial generation (No Soo-Young, 2014). This is because of the minimization of the carbon released to the atmosphere during production and utilization (Ullah et al., 2015). Compared to petroleum based products, biomass based fuels generate insignificant quantities of net carbon since these biomass based materials were formed as a result of carbon dioxide used by plants during the growing process (Wyman, 1994). Similarly, biomaterials are reported to be more environmentally friendly than their petroleum based equivalents (Schrader et al., 2014). Biochar and syngas are some examples of well-known products from biomass conversion processes. Biochar is the result of the thermal devolatilization or pyrolysis of biomass in an oxygen-free atmosphere at temperatures higher than 300^{o}C (Emrich, 1985). This carbon rich material can have high absorption capacity, thus can be used to purify liquid and gas media (Ahmad et al, 2007; Sadasivam and Reddy, 2015). In addition, biochar can be used to improve soil quality because of the improved retention of nutrients and its surface area that serves as support for microbes in the soil (Winsley, 2007). In a similar way, the thermochemical conversion of biomass as a result of incomplete combustion produces syngas which is a gas mixture of hydrogen and carbon monoxide (Cao, 2006). This gas fuel can be used to produce heat in boilers, electricity in turbines, hydrocarbons via Fischer-Tropsch processes and ethanol through biological conversion (Dry, 2002; Knoef, 2005; Latif et al., 2014). Extensive work has been published on the individual production of

biochar or syngas (Kirubakaran et al., 2009; Antal and Gronli, 2003). However, attempts to simultaneously produce biochar in biomass gasifier systems has led to difficulties in collection of this carbonaceous product among other problems (Cheah et al., 2014). For instance, Qian et al., (2013) tested a fluidized bed gasifier for the production and characterization of biochar. However, the yield of biochar was not reported due to incapacity to retrieve the produced biochar after reaction, as consequence of the use of a system designed to generate gas products.

The top-lit updraft gasifier also known as inverter downdraft gasifier has the capabilities to produce syngas and biochar simultaneously (Nsamba et al., 2015). However, little is understood about the performance of this gasifier. Most of the available work was focused on the application of this reactor for cooking purposes in developing countries since it generates low pollution emissions with relatively high efficiency (Reed and Larson, 1996; Birzer et al., 2014; Mukunda et al., 2010; Tryner et al., 2014). Brown (2009) recognized the potential of the top-lit updraft configuration for the production of biochar and remarked the lack of research on this process. The fact that this reactor can produce biochar and syngas in a single chamber can represent increase in the overall efficiency of this process. However, it is important to determine how the physical properties of the biomass can affect the performance of gasification and the quality of the biochar (Brizner et al., 2013). Huangfu et al. (2014) carried out experiments in a top-lit updraft stove to investigate the effect of the biomass moisture content. However, information about the syngas composition, tar content and properties of the biochar were not reported. In a similar way, Tinaut et al. (2008) investigated the effect of the particle size on the performance of a top-lit updraft gasifier. However, the work was focused on the rate of biomass consumption as well as the heat transfer distribution throughout the

gasification bed. Therefore, it did not contribute to understanding the effect of the particle size on the products of gasification.

The objective of this study was to understand the effect of the physical properties of the biomass on the performance of a top-lit updraft biomass gasifier and the quality of the biochar. Woodchips with varying particle sizes, moisture contents and biomass compactness were studied. Combustion temperature, burning rate, biochar yield, syngas composition and the physiochemical properties of the biochar produced were evaluated. This approach could help to identify potential variations of product distribution and gasification mechanisms due to changes in the physical properties of the raw material.

5.2. Materials and methods

The investigation of the effect of particle size, moisture content and biomass compactness was performed in a 10.1-cm internal diameter steel gasifier column with 152-cm height. A layer of 8.89-cm Fiberglass® insulation was used to reduce heat transfer through the wall of the reactor. Initially, this gasifier was filled with woodchips. Then, the top layer of the biomass was lit with a propane torch for one minute, in order to provide the initial exothermic heat for reaction. Air was provided by an air compressor (1.5 kW – 8.62 Bar max. operational pressure, WEN, Elgin, IL) equipped with a reservoir tank (18.90-liter) to maintain a uniform flow. The airflow rate was controlled using a variable area flow meter (Cole-Parmer 150-mm, max. pressure 200 psi, Chicago, IL). As air was injected, the combustion front moved from top to bottom. The temperatures within the gasifier were measured with thermocouples at the top, middle and bottom; and were recorded with a data acquisition system (HOBO® onset®,

UX120-014M, Bourne, MA), as shown in Fig. 5.1. Once the flame front reached the bottom, the airflow rate was suppressed; as a result, the oxidation reactions were stopped. The cooled biochar was collected and the yield was calculated based on the final weight of the biochar and the weight of the biomass, as presented in equation 1.

$$Biochar\ Yield\ (\%) = \frac{DWC - MC}{DWB + MB} \text{x } 100 \quad (1)$$

where DWC is the dry weight of biochar (g), DWB is dry weight of biomass (g), MC is the moisture in biochar (g) and MB is the moisture in biomass (g).

Woodchips from a local grinding company (Newton County, NC) were selected as the raw material due to their availability, Table 5.1 presents a summary of the main properties of the biomass. The particle sizes of the biomass were controlled progressively using screens of 3, 10, 25 and 35-mm. Throughout this work, the average particle size (e.g. 2, 7, 17, and 30) was used to represent each range of particles. The moisture and the biomass compactness were kept at 10% and 0, respectively. Similarly, four moisture contents were tested, 10, 14, 18 and 22%, while the particle size and the biomass compactness were maintained at 7-mm and 0, respectively. The required moisture content was achieved by calculating the amount of water needed to increase the moisture content of the biomass by equation 2. Then, the biomass was placed in a container and water was sprayed using a 946-ml (32oz) all-purpose sprayer bottle. The initial moisture of the biomass was determined by drying the biomass at 105°C for 24 hours.

$$water\ added\ (g) = \frac{DM * DWB}{100 - D} - MB(g) \quad (2)$$

where DM is the desirable moisture content (%), DWB is the dry weight of biomass (g) and MB is the moisture in biomass (g).

Table 5.1. Properties of wood chips

C (%)	47.90
H (%)	1.70
N (%)	0.30
O[a] (%)	49.90
S (%)	0.20
Ash (%)	0.57
Volatile matter (%)	72.63
Fixed carbon a (%)	16.66
Moisture (%)	10.14
HHV (MJ/kg)	19.53
Bulk density (g/cm^3) / particle size	0.207 / 2 mm
	0.211 / 7 mm
	0.196 / 17 mm
	0.192 / 30 mm

[a] calculated by difference

In addition, the four biomass compactness levels were no compacting (0), 1, 2 and 3 kg packing masses. The increasing density was tested with the particle size of 7-mm and 10% moisture content. The biomass compactness within the gasifier chamber was controlled by gradually adding 100 g of biomass and compacting it with the respective mass weight until the reactor was full.

During reaction, tar samples were collected from the gasifier using the cold-trapping method presented in Fig. 5.1. The first stage of this tar sampling system was composed of two flasks submerged in ice (0ºC) in which water and heavy tars were condensed. The second stage was composed of two additional flasks submerged in dry ice (approximately -79ºC) at which

most of the remaining tars was condensed. A vacuum pump (Cole-Parmer, L-79200-30, Monroe, LA) was used to flow the syngas within the tar sampling system, and a gas flow meter (Omega, PMR1-014697, Stanford, CT) controlled the sampling rate at 10 lpm. The tar samples were dried in an oven at 105^{o}C for 24 hours and the final weight of the samples was reported as tar. The syngas was also sampled from the gasifier using 0.5-liter Teldar® sampling bags, and it was analyzed in a Gas Chromatograph (SRI8610C, SRI, Torrance, CA) with a thermo-conductivity detector (TCD) using helium as the carrier gas.

Elemental analysis, proximate analysis, higher heating value and BET surface area were evaluated for the produced biochar. The elemental analysis was determined in a CHNS/O elemental analyzer (Elmer Perkin 2400, CT, USA). A part of the proximate analysis, the volatile matter content was determined based on ASTM D3175-11 standard (ASTM, 2011) and the ash content was measured following ASTM E1755 – 01 (ASTM, 2015). The fixed carbon was calculated based on the percentage difference of volatile matter, ash and moisture. The higher heating value was performed in a bomb calorimeter (IKA-Calorimeter C 200, IKA-Werke GmbH and Co. KG, Staufen, Germany) using benzoic acid as the standard. For BET surface area analysis, the samples were degassed for 12 hours at 250^{o}C under vacuum. A surface area analyzer (Autosorb-1C, Quantachrome, Boyton Beach, FL) using isothermal nitrogen sorption was used to determine the BET surface area of the samples. Every experiment was replicated three times and the recorded data was analyzed using SAS ® software. Multiple comparison analyses were performed to investigate variations in the output factor as a result of the physical properties of the biomass. In addition, multiple linear regressions of the gasification parameters and the biomass physical properties were carried out.

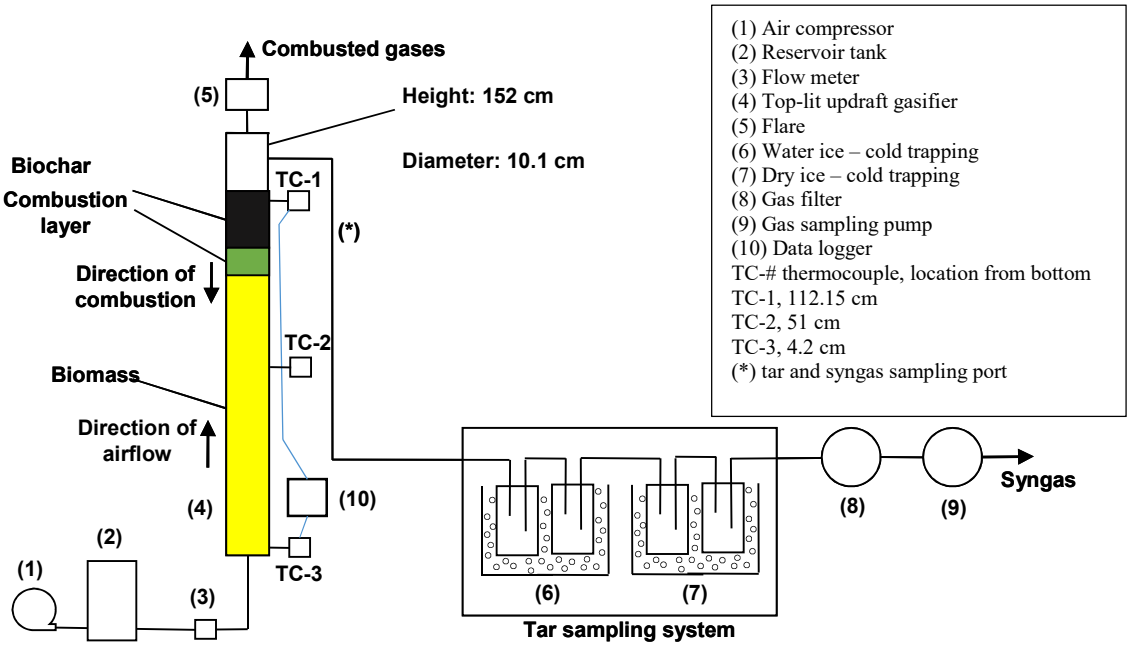

Fig. 5.1. The top-lit updraft biomass gasification system setup.

The selection of the airflow rate was completed using a performance criteria factor. This value was the result of the evaluation of airflow rates ranging from 8 to 24 lpm and the two insulation conditions. It was calculated using the biochar mass fraction, biomass to syngas conversion efficiency, surface area ratio and tar content effect. Equation 3 shows the calculation of the performance criteria. The optimum airflow rate was selected based on the maximization of the BET surface area and minimization of the tar content in the biochar while maintaining an acceptable biochar yield. As a result, 20 lpm (equivalent superficial velocity: 2.08 cm/s) and the addition of insulation were selected as the optimum conditions for biochar production. This was because of the fact that further increase in the airflow rate decreased the biochar yield below 10% with no considerable increase of the performance factor, Fig. 5.2.

$$PC\ facto \quad \frac{DWC}{DWB}\frac{HHV_S V_S}{HHV_{bms} - HH_b}\frac{BET_b}{BET_{comp.}}\frac{WTar}{DWC} \quad (3)$$

Where DWC is the dry weight of biochar (g), DWC dry weight of biomass (g), HHVs higher heating value of syngas (MJ/m^3), HHV_{bms} Higher heating value of biomass (MJ/kg), HHV_b Higher heating value of biochar (MJ/kg), Vs Volume of syngas (m^3), BET_b BET surface area of biochar (m^2/g), $BET_{comp.}$ – BET surface area for comparison (600 m^2/g) and WTar Weight of tar in biochar (g).

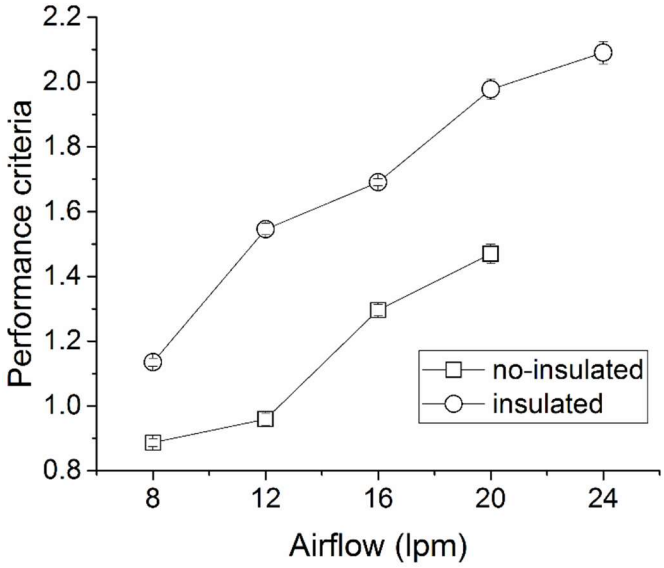

Fig. 5.2. Performance criteria for the selection of optimal gasification condition

5.3. Results and discussion

5.3.1. The effect of biomass particle size

The size of biomass particles significantly influenced the gasification performance. It can be seen from Fig. 5.3A that as the particle size increased from an average size of 2 to 7 mm, the yield of biochar significantly decreased from 19% to 12%. Consistent with this

reduction, Fig. 5.3B shows that the combustion temperature was elevated from 657 to 840ºC. However, as the size of the particles further increased from an average size of 7 to 17 mm, the yield of biochar started to increase from 12 to 19.8%. Moreover, this was not significantly different from the biochar yield (21.8%) achieved with a larger particle of average size of 30 mm. In contrast to the increasing yield of biochar the reaction temperature was reduced from 840 to 614ºC (Fig. 5.3B). It was evident that the yield of biochar was negatively affected by the combustion temperature. Previous studies found that there was a high correlation between the reaction temperature and biochar yield (Demirbas 2001; Sun et al., 2014). Demirbas (2004) performed pyrolysis experiments with olive husk, corncob and tea waste varying the reaction temperature from 450 to 1250 K. They found that the yield of biochar decreased for all biomasses as the temperature increased. For instance, the yield of corncob was reduced from 30 to 5%. In addition to the characteristic tendency of the combustion temperature, it is important to note that the effect of biomass particle size on biochar yield can also be associated with the bulk density of the biomass. Biomass with an average particle size of 2 mm presented a bulk density of 0.207 g/cm^3, which increased to 0.211 g/cm^3 when the particle size was increased to an average of 7 mm. However, larger particle sizes presented decreasing bulk densities as shown in Table 5.1. As the bulk density decreased less biomass was concentrated, as a result less fuel was generated during the devolatilization reactions. Therefore, the combustion temperatures decreased.

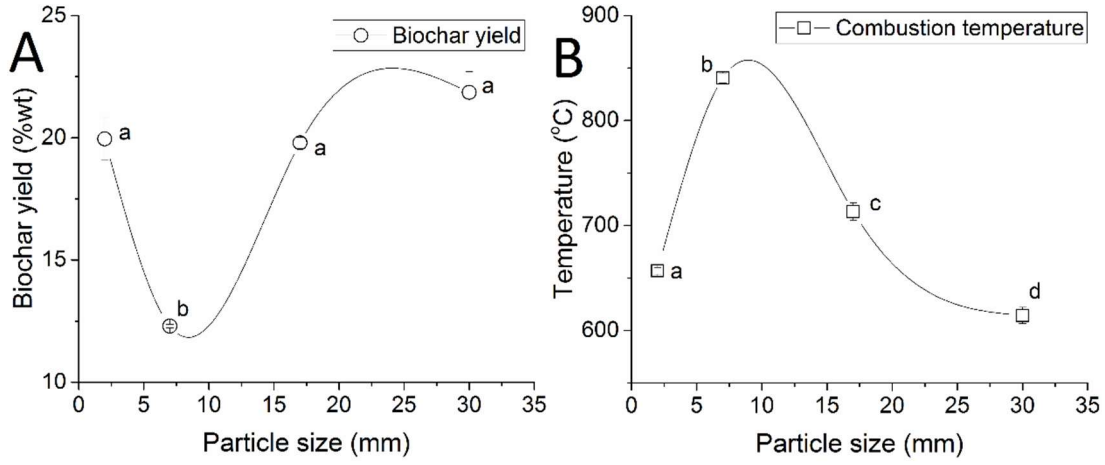

Fig. 5.3. (A) Biochar yield and (B) combustion temperature of wood chips at different particles sizes. Airflow 20 lpm, moisture content 20%, biomass compactness 0.

It is interesting to see that despite the increase in the combustion temperature presented in Fig. 5.3B, the burning rate (Fig. 5.4A) displayed a significant reduction from 16.6 to 13.2 mm/min as the particle size increased from 2 to 7 mm. However, the burning rate had an opposite tendency when the particle size was further enlarged (from 7 to 30 mm) increasing from 13.2 to 20.3 mm/min, regardless of the decrease in temperature presented when the particle size increased. This suggested that the burning rate was not only a factor of the reaction temperature, but it can also be a factor of the particle size because of the variations in biomass bulk density. If the burning rate is compared with the biomass bulk density, a lower bulk density of biomass resulted in a higher burning rate; in contrast, denser biomass reduced the burning rate.

The tar content in the syngas also showed a consistent tendency with the variation of the combustion temperature. As the particle size increased from 2 to 7 mm the tar content significantly decreased from 79.4 to 13 g/m^3 (Fig. 5.4B), as a result of the increasing

combustion temperature. However, as the combustion temperature reduced at larger particle sizes, the tar content in the syngas was elevated from 13 to 93 g/m^3. Increasing the reaction temperature of gasification systems have been proven to inhibit the production of tars because of the effect of tar cracking and reforming reactions (Vreugdenhil and Zwart, 2009; Kinoshita et al, 1994). For instance, Li et al. (2004) carried out experiments with sawdust in a fluidized bed gasifier increasing the reaction temperature from 700 to 815°C. The tar content decreased from 15.2 to 0.5 g/m^3.

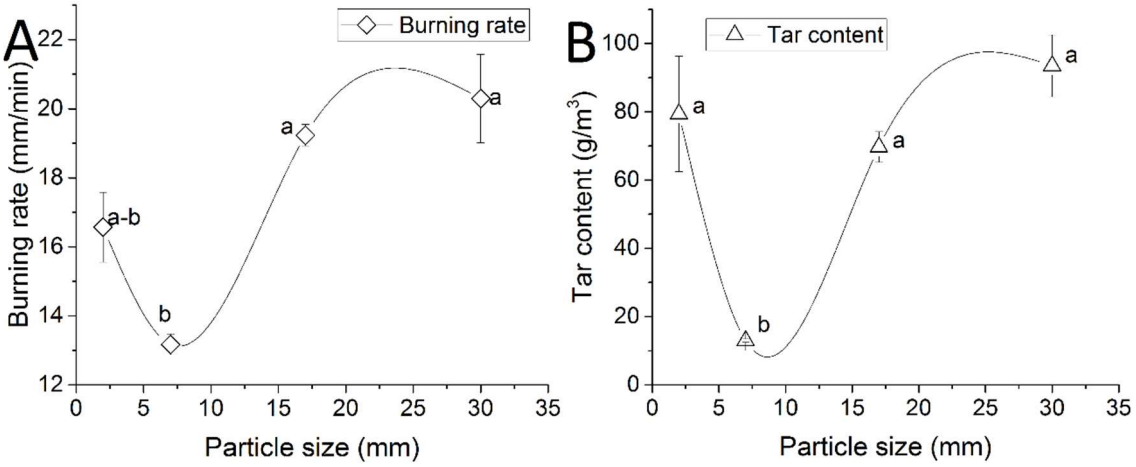

Fig. 5.4. (A) Gasification burning rate and (B) tar content in syngas at varying particle sizes (Airflow rate 20 lpm, moisture content 20%, and biomass compactness 0).

Fig. 5.5 shows the effect of particle size on the syngas composition. As the particle size increased from an average of 2 to 7 mm, the hydrogen content of the syngas increased from 4.26 to 6.61%. However, little variation was observed in the carbon monoxide composition. Further increasing the particle size from 7 to 30 mm significantly reduced the hydrogen composition from 6.6 to 2.9% and the carbon monoxide composition from 15 to 11.8%.

Consequently, the higher heating value declined from 3.67 to 2.7 MJ/m^3. Similar results were reported by Hernandez et al. (2010) who investigated the effect of particle size in an entrained flow gasifier at 1050°C. When the particle size varied from 0.5 to 8 mm, the H_2 and CO contents in the syngas reduced from 9 to 3% and from 14 to 5%, respectively. This change in the gas composition was attributed to the reduced surface area for gasification reaction due to the increasing particle size that discouraged mass and heat transfer throughout the biomass particles. Moreover, the reduction in H_2 content can also be attributed to the reaction temperature. Lv et al. (2004) studied the effect of particle size and reaction temperature in a biomass fluidized bed gasifier using air/steam mixtures. The results showed that as increasing the temperature from 700 to 900°C, the H_2 content increased from 20 to 40%. However, little difference was noticed in the H_2 content when the particle size was varied from 0.25 to 0.75 mm at 800°C. As a result, the tar reforming (e.g. C_xH_y (tar) + mH_2O → m CO + $(m+p/2)H_2$) and cracking reactions (e.g. C_xH_y (tar) → CO + C + H_2 + C_wH_v) were minimized at larger particle sizes (Guo et al., 2014).

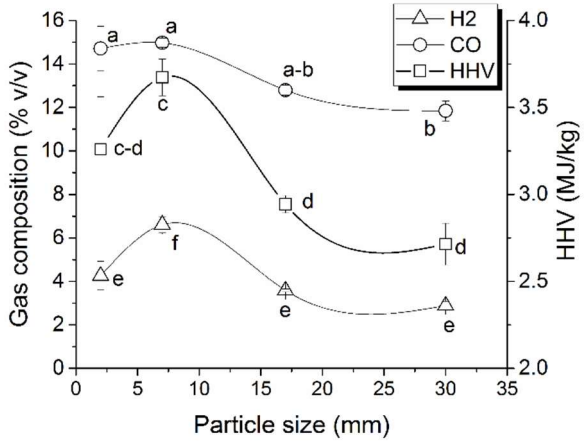

Fig. 5.5. CO and H_2 compositions and the higher heating value of syngas generated at varying particle sizes (Airflow rate 20 lpm, moisture content 20%, and biomass compactness 0).

5.3.2. The effect of biomass moisture content

The increase in the moisture content of the biomass was found to be linearly correlated with biochar yield (R^2=0.96). As increasing the moisture content from 10% to 22%, the yield of biochar significantly dropped from 12% to 9.9% (Fig. 5.6A). However, in spite of the apparent increase in the combustion temperature, no significant difference in the combustion temperature was found as the moisture content increased from 10 to 22% (Fig. 5.6B). As stated in the particle size analysis, the reaction temperature can be a strong indicator of minimization of biochar yield. Therefore, the reduction of the biochar yield due to addition of moisture content cannot be attributed to the combustion temperature.

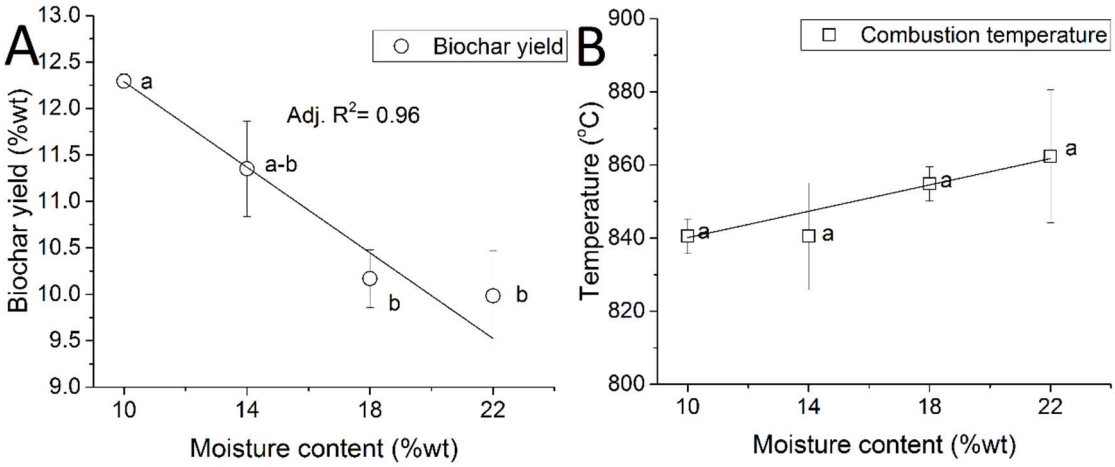

Fig. 5.6. (A) Biochar yield and (B) combustion zone temperature of wood chips at different moisture contents. Airflow 20 lpm, avg. particle size 7 mm, biomass compactness 0.

As presented in Fig. 5.7A, the burning rate was impacted by the addition of moisture to the biomass. The burning rate reduced from 13 to 10 mm/min as the moisture content increased from 10 to 22%. Biomass with higher moisture content burned at a slower pace due

to the additional heat required to evaporate the water in the biomass before its thermochemical conversion (McKendry, 2002). This suggested that the decrease in the biochar yield, as a result of increasing moisture content can be attributed to the decrease in the burning rate that stimulated the oxidation of more organic components within the produced biochar. Similar tendency of biochar yield has been previously reported by Huangfu et al. (2014) who carried out moisture content experiments in a natural draft top-lit updraft gasifier. The gasification of wood pellets with increasing moisture content (from 6 to 22%) was found to reduce the burning rate from 30 to 20 g/min, thus yield of biochar decreased from 26 to 20%.

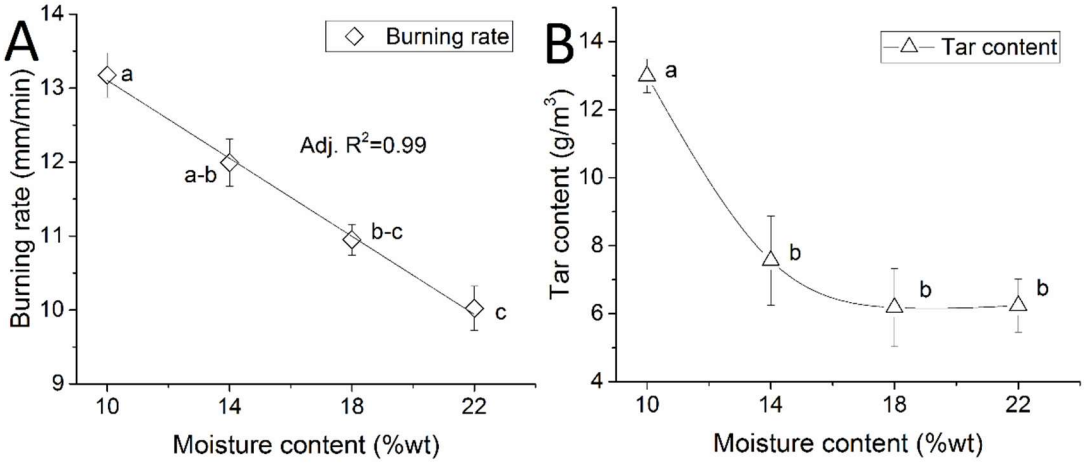

Fig. 5.7. (A) Burning rate and (B) tar content in syngas using biomass with varying moisture contents (Airflow rate 20 lpm, avg. particle size 7 mm, biomass compactness 0).

Moreover, the reduction in burning rate also reduced tars in syngas during the carbonization of biomass. The tar content reduced from 13 to 6.24 g/m^3 (Fig. 5.7B) which was identified as the lowest range of tar content achieved in the gasification of woodchips in this top-lit updraft gasifier. This indicated that a slower burning rate represented a more efficient

burning of biomass to balance the excessive moisture and maintain the combustion temperature. Therefore, tar cracking and reforming reactions were encouraged by the increasing moisture in the gas phase. A similar reduction in tar content was reported by Ponzio et al, (2006) in the evaluation of a high temperature air/steam gasification configuration (HTAG). It was reported that the gasification of paper at different air/steam mixtures, including 5, 53 and 82% water showed decreases in tar content from 2.3 to 1.4 mg per sample. The reduction in the tar content was attributed to the steam reforming reactions. The top-lit updraft gasifier configuration could also be further catalyzed by the produced biochar. Previous works (Wang et al., 2011; Shen et al., 2014) have investigated the catalytic effects of carbon in tar cracking reactions. For instance, James et al. (2014) performed tar cracking experiments in an in-situ thermo-catalytic reactor at approximately 900ºC using charcoal as the catalyst. It was found that charcoal alone removed up to 60% of the tars in the syngas. Therefore, the top-lit updraft configuration might also help to break down tar molecules since biochar with high carbon content was presented along the carbonization and reduction zones.

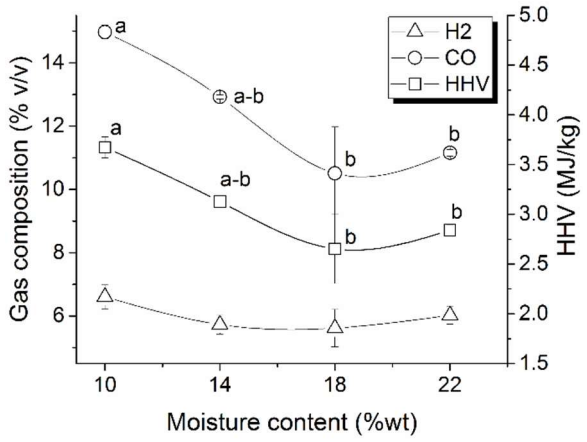

Fig. 5.8. Syngas composition and higher heating value at different moisture contents. Airflow 20 lpm, avg. particle size 7 mm, biomass compactness 0.

Fig. 5.8 presents the effect of moisture content on the syngas composition. The hydrogen composition was found to have no significant changes when the moisture content increased. In contrast, the carbon monoxide composition significantly reduced from 15.2 to 11.1% when the moisture increased from 10 to 18%, and slightly increased to 11.1% with further increase of moisture content to 22%. Likewise, the higher heating value of the syngas decreased from 6.67 to 2.65 MJ/m^3 when increasing the moisture content from 10 to 18%, and increased to 2.84 MJ/m^3 at 22% moisture content. Due to the configuration of the top-lit updraft gasifier, in which the combustion zone moves towards the bottom carbonizing the biomass; it can be assumed that the additional moisture added to the biomass is continuously supplied as steam. This is because the heat from the combustion zone uniformly dries the biomass as the combustion zone advances. This assumption can help to understand the effect of the moisture content using the steam to biomass ratio (S/B) which for this study can be represented as 0.11, 0.16, 0.22 and 0.28 for moisture content of 10, 14, 18 and 22, respectively. The S/B ratio is calculated as the mass of steam per dry mass of biomass used during gasification. Franco et al. (2003) investigated the effect of the S/B (from 0.5 to 0.8) on a fluidized bed gasifier at a temperature of 800ºC. The CO content in the syngas decreased from approximately 45 to 38% as increasing the S/B ratio. In a similar way, the higher heating value decreased from approximately 1.9 to 1.6 kJ/L, and the S/B ratio content increased the hydrogen content. This tendency of low hydrogen content and decreasing CO composition with increasing biomass moisture content from 10 to 22% suggested that there was not sufficient steam supplied to the

steam reforming reactions (e.g. C_xH_y (tar) + mH_2O → m CO + $(m+p/2)H_2$) and water-gas reactions (e.g. $C+H_2O$ → $CO + H_2$). Similar tendency was also found by Gil et al. (1999).

5.3.3. The effect of biomass compactness

Increasing the biomass compactness in the top-lit updraft biomass gasifier improved the yield of biochar from 12.2 to 17% when the compactness increased from 0 to 3 kg of mass (Fig. 5.9A). However, the combustion temperature did not statistically vary as the biomass compactness increased (Fig. 5.9B).

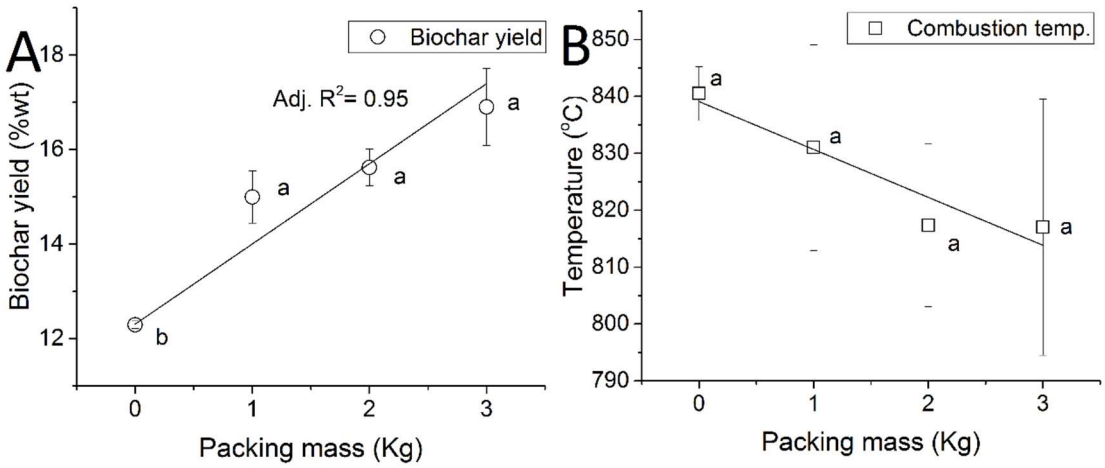

Fig. 5.9. (A) Biochar yield and (B) combustion zone temperature using biomass with different biomass compactness. Airflow 20 lpm, 10% moisture content, avg. particle size 7 mm.

Increasing the biomass compactness means a higher mass of biomass per unit area which indicates that more biomass was carbonized when compared with no compacting it. Subsequently, if the reaction temperature remained unchanged, the burning rate was expected to decrease. As shown in Fig. 5.10A, the average burning rate of biomass decreased from 13 to 10.2 mm/min as increasing the biomass compactness from 0 to 2 kg, but it slightly increased

to 11 mm/min when further increasing the biomass density. Moreover, the variation when all compacting masses were implemented was not statistically different. The fact that the combustion temperature did not present significant differences (Fig. 5.9B) when increasing the compactness suggested a more efficient carbonization of biomass.

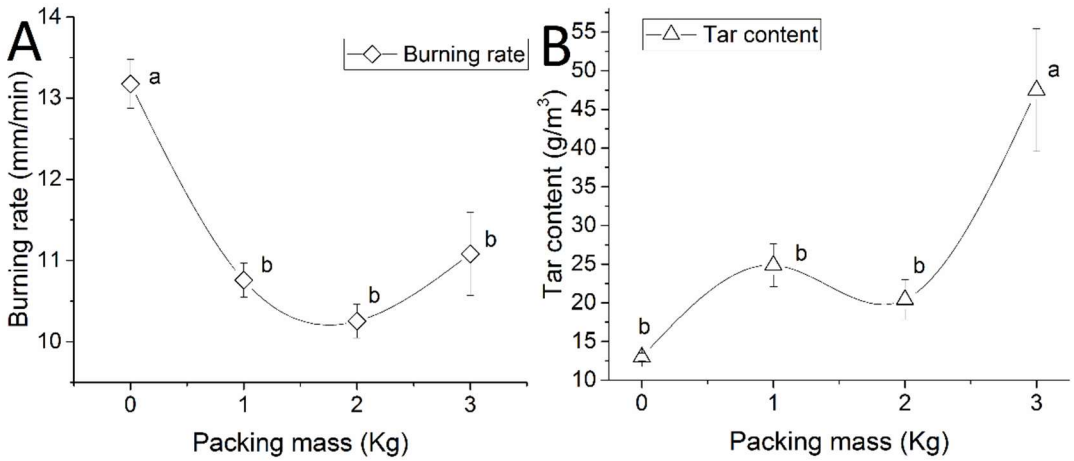

Fig. 5.10. (A) Burning rate and (B) tar content in syngas using biomass at different biomass compactness. Airflow 20 lpm, 10% moisture content, avg. particle size 7 mm.

In contrast, the biomass compactness had a negative effect on the tar content. It raised from 13 to 47 g/m^3 as the compactness increased from 0 to 3 kg (Fig. 5.10B). This confirmed that the compaction significantly increased the number of biomass particles within the gasifier. Thus more volatiles emanated from the biomass when compared with lower levels of compactness. However, despite this increased amount of volatiles the combustion temperature did not increase because of the limited availability of air for reaction. Contrary to the particle size and moisture content, the biomass compactness did not have statistically significant effects on the syngas compositions or syngas higher heating value (Fig. 5.11).

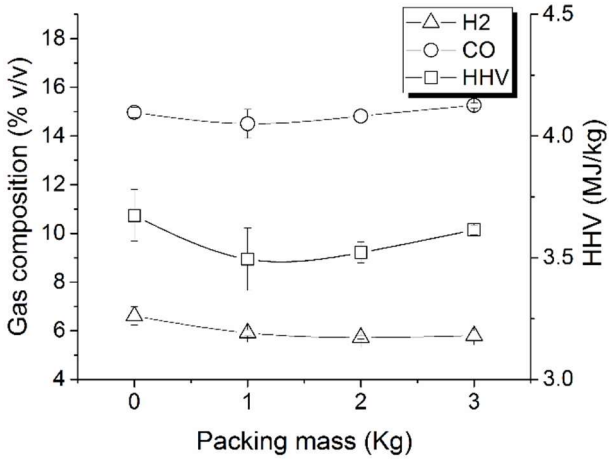

Fig. 5.11. Syngas composition and higher heating value at different biomass compactness. Airflow 20 lpm, 10% moisture content, avg. particle size 7 mm.

Table 5.2 summarizes the physiochemical properties of the biochar generated with different particle sizes. Biochar produced with biomass with an average particle size of 7 mm had a lower volatile content (5.30%) than with smaller (16.69%) and greater (15.63%) particles sizes. Therefore, the volatile content was associated with the reaction temperature (R^2=0.91) that with 7 mm presented the highest value for this test (840ºC). This confirmed that increase in the reaction temperature helped, not only to reduce the amount of volatiles within the biochar, but it also maximized the fixed carbon content to 91% that was also correlated with the temperature (R^2=0.87). As a result, the BET surface area of the biochar increased to its maximum of 405 m^2/g. In addition, the increase in the carbon content due to the increase in the reaction temperature also help to slightly increase the HHV of the biochar. Similar findings were reported by Sun et al. (2014) that studied the properties of biochar produced with different feedstocks in a pyrolysis reactor using temperatures from 400 to 600ºC. The results showed

that as increasing the reaction temperature, the carbon content of biochar increased from 53.3 to 81.8%. Proportionally, the BET surface area of the biochar increased from 1.3 to 401 m^2/g.

Table 5.2. Average* physiochemical properties of biochar produced with different particle sizes. Different letters in the superscripts indicates significant difference among groups.

Avg. Particle Size (mm)	Moisture (wt%)	Compacting mass (kg)	Volatile (%)	Ash (%)	Fixed Carbon (%)	C (%)	H (%)	N (%)	S (%)	O ** (%)	HHV MJ/kg	BET Surface area (m^2/g)
2	10	0	16.69^{a}	2.20^{a}	79.55^{c}	84.02^{b}	2.49^{a-b}	0.46^{a}	0.38^{b}	12.66^{a}	31.65^{c}	N/A
7	10	0	5.30^{c}	2.53^{a}	91.00^{a}	85.87^{a-b}	1.93^{b}	0.40^{a-b}	0.33^{b}	11.47^{a}	32.91^{a-b}	405.3
17	10	0	10.28^{b}	1.72^{a}	86.08^{b}	88.12^{a}	2.80^{a-b}	0.38^{a-b}	0.48^{a-b}	8.23^{b}	33.38^{a}	50.9
30	10	0	15.63^{a}	1.42^{a}	81.48^{c}	85.23^{a-b}	3.86^{a}	0.33^{b}	0.63^{a}	9.95^{a-b}	32.65^{b}	6.2
*average of three replications. **calculated by difference. N/A – not available due to high tar content in the biochar.												

The physiochemical properties of biochar produced with different moisture contents are presented in Table 5.3. When the moisture content varied from 10 to 14%, the fixed carbon content decreased from 91 to 88%. Further increasing the moisture content cause little variation of the fixed carbon content. Therefore, the addition of moisture to the biomass caused increase in the combustion of carbon due to the energy needed to evaporate the moisture. The changes in the fixed carbon were correlated with the volatile content (R^2=0.79) that decreased as the fixed carbon increased. This indicates that the increase in the carbon content promoted a more complete carbonization due to the low moisture content. As a result, the increase in moisture content and subsequent reduction of the fixed carbon reduced the BET surface area from 405 to 352 m^2/g.

Table 5.3. Average* physiochemical properties of biochar produced with different moisture contents. Different letters in the superscripts indicates significant difference among groups.

Avg. Particle Size (mm)	Moisture (wt%)	Compacting mass (kg)	Volatile (%)	Ash (%)	Fixed Carbon (%)	C (%)	H (%)	N (%)	S (%)	O ** (%)	HHV MJ/kg	BET Surface area (m^2/g)
7	10	0	5.30^{c}	2.53^{a}	91.00^{a}	85.87^{b}	1.93^{a}	0.40^{a}	0.33^{a}	11.47^{a}	32.91^{a}	405.3
7	14	0	7.57^{a}	2.67^{a}	88.89^{c}	89.84^{a}	1.50^{a}	0.33^{a}	0.24^{a-b}	8.09^{b}	32.61^{a}	380.3
7	18	0	6.44^{b}	2.73^{a}	89.81^{b}	90.12^{a}	1.50^{a}	0.37^{a}	0.19^{b}	7.82^{b}	32.66^{a}	384.0
7	22	0	6.11^{b-c}	3.02^{a}	89.36^{b-c}	89.21^{a}	1.38^{a}	0.32^{a}	0.18^{b}	8.90^{b}	32.39^{a}	352.8

*average of three replications. **calculated by difference. N/A – not available due to high tar content in the biochar.

The increase of the biomass compactness from 0 to 3 kg reduced the fixed carbon of the biochar from 91 to 85%, Table 5.4. This reduction of the fixed carbon can be associated with the reaction temperature that was positively correlated with the fixed carbon (R^2=0.76) and negatively correlated with the volatile content (R^2=0.71). Thus the reduction of the temperature negatively impacted the BET surface area that decreased from 405 to 191 m^2/g as the biomass compactness increased. Lua et al. (2004) conducted experiments to test the effect of pyrolysis in the properties of biochar and activated carbon. The results showed that at pyrolysis temperatures higher than 500ºC, the BET surface was reduced because of the lack of structure within the biochar despite the increase in the fixed carbon. In contrast, biomass gasification showed increasing BET surface area as the reaction temperature increased because of the more stable structure when the fixed carbon increased.

Table 5.4. Average* physiochemical properties of biochar produced with different biomass compactness. Different letters in the superscripts indicates significant difference among groups.

Avg. Particle Size (mm)	Moisture (wt%)	Compacting mass (kg)	Volatile (%)	Ash (%)	Fixed Carbon (%)	C (%)	H (%)	N (%)	S (%)	O ** (%)	HHV MJ/kg	BET Surface area (m^2/g)
7	10	0	5.30^{b}	2.53^{a}	91.00^{a}	85.87^{b}	1.93^{a-b}	0.40^{a}	0.33^{a}	11.47^{a}	32.91^{a}	405.3
7	10	1	7.89^{a-b}	2.21^{b}	88.49^{a-b}	90.03^{a}	1.84^{b}	0.33^{a}	0.27^{a}	7.54^{b}	32.81^{a}	266.7
7	10	2	8.19^{a-b}	2.53^{a}	88.05^{a-b}	89.56^{a}	1.85^{b}	0.32^{a}	0.27^{a}	8.01^{b}	32.86^{a}	281.9
7	10	3	11.49^{a}	2.15^{b}	85.32^{b}	88.66^{a}	2.44^{a}	0.31^{a}	0.33^{a}	8.26^{b}	32.59^{a}	191.8

*average of three replications. **calculated by difference. N/A – not available due to high tar content in the biochar.

5.3.4 Multiple linear regression analysis

Statistical multiple linear regression of the biochar yield, tar content and burning rate were carried out. Backward selection analysis was performed for each output of the process using SAS® regression (reg) command. It was assumed that the error was random and the variables were identically random normal distributed with mean 0 and variance σ^2 (Rao, 2007). In case of major violations of the assumptions, the dependent variable (response) was corrected. As result, tar content was adjusted to Ln(tar), natural logarithm of tar. The effect of the airflow rate, insulation condition, particle size, moisture content and biomass compactness were evaluated. Airflow rate and insulation condition data from chapter 1 were integrated to the model. The use of orthogonal coefficients was implemented to help determine the tendency of the means for consecutive number of experiments. This is usually performed using equally spaced intervals and the same number of replicates (Broota, 1989) such as the airflow rate, moisture content and biomass compactness. However, the particle size was unequally distributed with averages particle size values of 2, 7, 17 and 30 mm. As a result, the procedure suggested by Grandage (1958) was used to determine the coefficient of the particle size, See Appendix – A.

For the biochar yield, the linear and quadratic contribution of the airflow significantly contribute to the model; as well as the linear influence of the moisture content and the particle

size, equation (4). The model presented R^2=0.64, and the selected independent variables were found to have p-values<0.0095. The insulation condition and the biomass compactness were observed no to contribute to the model. The multiple linear regression of the burning rate showed that only the linear effects of all the studied factors explained part of the burning rate response. The airflow rate, insulation condition, moisture content, particle size and biomass compactness presented p-values<0.0001. Consequently, the model explained 83% (R^2=0.83) of the variability of the burning rate, equation (5). This suggests that the burning rate can be easily affected by multiple factors as presented in previous sections. As a result, care must be taken when selecting the operational conditions and properties of the biomass in order to have the best possible outcome. Similarly, the logarithmic response of the tar content exhibited significant variation due to the linear influence of the airflow, insulation, moisture content and particle size. Moreover, the quadratic terms of the moisture content and the particle size also explained the tar content in the top-lit updraft gasification system. However, the biomass compactness did not show significant influence on the tar content, equation (6). This model was found to describe 70.6% (R^2=0.706) of the natural logarithm of the tar response. Appendix – B shows the consideration of the model and the SAS® software code.

Biochar yield (%) = 16.42 -1.29 AFL* + 1.38 AFQ* – 1.07 WTL* + 0.264 PSL (4)

BR (mm/min) = 5.88 + 0.95 AFL* + 2.88 INS. – 0.76 WTL* + 0.27 PSL – 0.74 PKL* (5)

Tar content (g/m^3) = 2.72 – 0.20 AFL* + 0.57 INS. – 0.23 WTL* + 0.32 WTQ* + 0.048 PSL + 0.004 PSQ (6)

*Coefficient of orthogonal polynomials for 4 levels equally distributed: Linear (-3, -1, 1, 3) and quadratic (1, -1, -1, 1)

5.4. Conclusions

The particle size, moisture content and biomass compactness of woodchips were found to influence the gasification process and the quality of the products of top-lit updraft

gasification. The variation of the particles size presented two different tendencies that were related to the bulk density of the biomass. The size of the particles can affect the performance of the gasifier because of the variation of the reaction temperature. For instance, as increasing the particle size from 7 to 30 mm the combustion temperature reduced more than 200^{o}C. As a result, tar content increased and the BET surface area was reduced to its minimum of 6.2 m^2/g. In contrast, this increase in the particle size increased the yield of biochar. The addition of moisture to the biomass represented reduction in the burning rate that promote the utilization of carbon from the biochar and reduced the biochar yield. Similarly, it also reduced the carbon monoxide and the surface area. However, the major contribution of the moisture content was to help reduce the tar content due to reforming and cracking reactions that were catalyzed by the excess of water and the abundant carbon in the reactor. In addition, the yield of biochar increased when the biomass compactness increased, but it produced more condensable aromatic hydrocarbons. As a result, the surface area of the biochar decreased and the tar content increased. This was because of the increase amount of biomass within the gasifier chamber at higher levels of biomass compactness. The physiochemical properties of the biochar produced from biomass with different physical properties showed that the temperature of reaction plays an important role in the determination of the volatile and carbon content of the biochar. Biochar with high fixed carbon presented higher BET surface area because of the additional supported structure provided by the fixed carbon in the biochar.

5.5. Nomenclature

PC factor – Performance criteria factor

HHV_s – Higher heating value of syngas MJ/m^3

HHV_b – Higher heating value of biochar MJ/kg

HHV_{bms} – Higher heating value of biomass MJ/kg

V_s – Volume of syngas (m^3)

BET_b – BET surface area of biochar m^2/g

$BET_{comp.}$ – BET surface area for comparison - 600 m^2/g

AFL – airflow rate linear

AFQ – airflow rate quadratic

WTL – moisture content rate linear

WTQ – moisture content quadratic

PSL – particle size linear

PSQ – particle size quadratic

PKL – biomass packing linear

INS – insulation

DM – Desirable moisture content (%)

DWC – Dry weight of biochar (g)

DWB – Dry weight of biomass (g)

WTar - Weight of tar in biochar (g)

MC – Moisture in biochar (g)

MB – Moisture in biomass (g)

5.6. Acknowledgements

This material was based upon the work supported by the U.S. Department of Agriculture and Sun Grant (Award No. 2010-38502-21836 and Subaward No. AB-5-67630. KSU11) and the startup fund of North Carolina State University. The lead author was also partially supported by the scholarship program of IFARHU-SENACYT from the Government

of Panama. We thank Mr. Justin Macialek, research assistant at NCSU, for his help building the top-lit updraft gasifier, and Dr. Arellano from NC State University Statistics Department for her helpful advices on multiple linear regression analyses.

5.7. References

Ahmad, A., Loh, M., & Aziz, J. (2007). Preparation and characterization of activated carbon from oil palm wood and its evaluation on methylene blue adsorption. *Dyes and Pigments, 75*(2), 263-272.

Birzer, C., Medwell, P., MacFarlane, G., Read, M., Wilkey, J., Higgins, M., & West, T. (2014). A biochar-producing, dung-burning cookstove for humanitarian purposes. *Procedia Engineering, 78*, 243-249. doi:10.1016/j.proeng.2014.07.063

Birzer, C., Medwell, P., Wilkey, J., West, T., Higgins, M., MacFarlane, G., & Read, M. (2013). An analysis of combustion from a top-lit up-draft (TLUD) cookstove. *Journal of Humanitarian Engineering, 2*(1) Retrieved from http://www.ewb.org.au/jhe/index.php/jhe/article/viewFile/11/11 Last accessed: August 2015

Broota, K. D. (. (1989). *Experimental design in behavioural research*. New York: Wiley. Retrieved from http://www2.lib.ncsu.edu/catalog/record/UNCb2320334

Brown, R. (2009). Biochar production technology. *Biochar for Environmental Management: Science and Technology,* , 127-146.

Cao, Y., Wang, Y., Riley, J. T., & Pan, W. (2006). A novel biomass air gasification process for producing tar-free higher heating value fuel gas. *Fuel Processing Technology, 87*(4), 343-353.

Cheah, S., Malone, S. C., & Feik, C. J. (2014). Speciation of sulfur in biochar produced from pyrolysis and gasification of oak and corn stover. *Environmental Science & Technology, 48*(15), 8474-8480. doi:10.1021/es500073r

Demirbas, A. (2004). Effects of temperature and particle size on bio-char yield from pyrolysis of agricultural residues. *Journal of Analytical and Applied Pyrolysis, 72*(2), 243-248. doi:10.1016/j.jaap.2004.07.003

Demirbas, A. (2001). Carbonization ranking of selected biomass for charcoal, liquid and gaseous products. *Energy Conversion and Management, 42*(10), 1229-1238. doi:10.1016/S0196-8904(00)00110-2

Dry, M. E. (2002). The Fischer–Tropsch process: 1950–2000. *Catalysis Today, 71*(3–4), 227-241. doi:http://dx.doi.org/10.1016/S0920-5861(01)00453-9

Emrich, W. (1985). Handbook of charcoal making. Reidel Publishing Co. Dordrecht, Holland.

Franco, C., Pinto, F., Gulyurtlu, I., & Cabrita, I. (2003). The study of reactions influencing the biomass steam gasification process☆. *Fuel, 82*(7), 835-842. doi:http://dx.doi.org/10.1016/S0016-2361(02)00313-7

Grandage, A. (1958). 130. query: Orthogonal coefficients for unequal intervals. *Biometrics, 14*(2), 287-289.

Hernández, J. J., Aranda-Almansa, G., & Bula, A. (2010). Gasification of biomass wastes in an entrained flow gasifier: Effect of the particle size and the residence time. *Fuel Processing Technology, 91*(6), 681-692. doi:http://dx.doi.org/10.1016/j.fuproc.2010.01.018

Huangfu, Y., Li, H., Chen, X., Xue, C., Chen, C., & Liu, G. (2014). Effects of moisture content in fuel on thermal performance and emission of biomass semi-gasified cookstove. *Energy for Sustainable Development, 21*, 60-65. doi:10.1016/j.esd.2014.05.007

Isikgor, F., & Becer, C. R. (2015). Lignocellulosic biomass: A sustainable platform for production of bio-based chemicals and polymers. *Polymer Chemistry,* doi:10.1039/C5PY00263J

Kinoshita, C. M., Wang, Y., & Zhou, J. (1994). Tar formation under different biomass gasification conditions. *Journal of Analytical and Applied Pyrolysis, 29*(2), 169-181. doi:http://dx.doi.org/10.1016/0165-2370(94)00796-9

Knoef, H. (2005). In contributors: Jesper Ahrenfeldt ... et al.], editor Harrie Knoef, Ahrenfeldt J. and Knoef H. (Eds.), *Handbook biomass gasification*. Netherlands: BTG Biomass Technology Group. Retrieved from http://www2.lib.ncsu.edu/catalog/record/NCSU1969911 Last Accessed: August 2015.

Latif, H., Zeidan, A. A., Nielsen, A. T., & Zengler, K. (2014). Trash to treasure: Production of biofuels and commodity chemicals via syngas fermenting microorganisms. *Current Opinion in Biotechnology,27*, 79-87. doi:http://dx.doi.org/10.1016/j.copbio.2013.12.001

Lua, A. C., Yang, T., & Guo, J. (2004). Effects of pyrolysis conditions on the properties of activated carbons prepared from pistachio-nut shells. Journal of Analytical and Applied Pyrolysis, 72(2), 279-287. doi:http://dx.doi.org/10.1016/j.jaap.2004.08.001

McKendry, P. (2002). Energy production from biomass (part 3): Gasification technologies. *Bioresource Technology, 83*(1), 55-63. doi:http://dx.doi.org/10.1016/S0960-8524(01)00120-1

Mukunda, H., Dasappa, S., Paul, P., Rajan, N., Yagnaraman, M., Ravi Kumar, D., & Deogaonkar, M. (2010). Gasifier stoves–science, technology and field outreach. *Current Science, 98*(5), 627-638.

No, Soo-Young. (2014). Application of bio-oils from lignocellulosic biomass to transportation, heat and power generation—A review. *Renewable and Sustainable Energy Reviews, 40*, 1108-1125. doi:http://dx.doi.org/10.1016/j.rser.2014.07.127

Nsamba, H. K., Hale, S. E., Cornelissen, G., & Bachmann, R. T. (2015). Designing and performance evaluation of biochar production in a top-lit updraft up-scaled gasifier. *Journal of Sustainable Bioenergy Systems, 5*(02), 41. doi:10.4236/jsbs.2015.52004

Qian, K., Kumar, A., Patil, K., Bellmer, D., Wang, D., Yuan, W., & Huhnke, R. L. (2013). Effects of biomass feedstocks and gasification conditions on the physiochemical properties of char. *Energies, 6*(8), 3972-3986. doi:10.3390/en6083972

Rao, P. V. (2007). *Statistical research methods in the life sciences*. Belmont, CA]: Thomson Wadsworth. Retrieved from http://www2.lib.ncsu.edu/catalog/record/NCSU2220612

Reed, T. B., & Larson, R. (1996). A wood-gas stove for developing countries. *Energy for Sustainable Development, 3*(2), 34-37. doi:http://dx.doi.org/10.1016/S0973-0826(08)60589-X

Sadasivam, B. Y., & Reddy, K. R. (2015). Adsorption and transport of methane in landfill cover soil amended with waste-wood biochars. *Journal of Environmental Management, 158*, 11-23. doi:http://dx.doi.org/10.1016/j.jenvman.2015.04.032

Salehi Jouzani, G., & Taherzadeh, M. J. (2015). Advances in consolidated bioprocessing systems for bioethanol and butanol production from biomass: A comprehensive review. *Biofuel Research Journal,2*(1), 152-195. doi:10.18331/BRJ2015.2.1.4

Schrader, J., McCabe, K., Graves, W., & Grewell, D. (2014). Function and biodegradation in soil of bioplastic horticultural containers made of PLA-BioResTM composites. *Iowa State Research Farm Progress Reports,* Retrieved from: http://lib.dr.iastate.edu/cgi/viewcontent.cgi?article=3160&context=farms_reports Last accessed: August 2015.

Shen, Y., Zhao, P., Shao, Q., Ma, D., Takahashi, F., & Yoshikawa, K. (2014). In-situ catalytic conversion of tar using rice husk char-supported nickel-iron catalysts for biomass pyrolysis/gasification. *Applied Catalysis B: Environmental, 152–153*, 140-151. doi:http://dx.doi.org/10.1016/j.apcatb.2014.01.032

Sun, Y., Gao, B., Yao, Y., Fang, J., Zhang, M., Zhou, Y., . . . Yang, L. (2014). Effects of feedstock type, production method, and pyrolysis temperature on biochar and hydrochar properties. *Chemical Engineering Journal, 240*, 574-578. doi:http://dx.doi.org/10.1016/j.cej.2013.10.081

Tinaut, F. V., Melgar, A., Pérez, J. F., & Horrillo, A. (2008). Effect of biomass particle size and air superficial velocity on the gasification process in a downdraft fixed bed gasifier. an experimental and modelling study. *Fuel Processing Technology, 89*(11), 1076-1089. doi:http://dx.doi.org/10.1016/j.fuproc.2008.04.010

Tryner, J., Willson, B. D., & Marchese, A. J. (2014). The effects of fuel type and stove design on emissions and efficiency of natural-draft semi-gasifier biomass cookstoves. *Energy for Sustainable Development, 23*, 99-109. doi:10.1016/j.esd.2014.07.009

Ullah, K., Kumar Sharma, V., Dhingra, S., Braccio, G., Ahmad, M., & Sofia, S. (2015). Assessing the lignocellulosic biomass resources potential in developing countries: A critical review. *Renewable and Sustainable Energy Reviews, 51*, 682-698. doi:http://dx.doi.org/10.1016/j.rser.2015.06.044

Vreugdenhil, B., Zwart, R., & Neeft, J. P. A. (2009). Tar formation in pyrolysis and gasification, Energy research Center of the Netherlands (ECN). Retrieved from: ftp://130.112.2.101/pub/www/library/report/2008/e08087.pdf Last accessed: August 2015

Wang, D., Yuan, W., & Ji, W. (2011). Char and char-supported nickel catalysts for secondary syngas cleanup and conditioning. *Applied Energy, 88*(5), 1656-1663. doi:http://dx.doi.org/10.1016/j.apenergy.2010.11.041

Winsley, P. (2007). Biochar and bioenergy production for climate change mitigation. *New Zealand Science Review, 64*(1), 5-10.

Wyman, C. E. (1994). Ethanol from lignocellulosic biomass: Technology, economics, and opportunities. *Bioresource Technology, 50*(1), 3-15. doi:http://dx.doi.org/10.1016/0960-8524(94)90214-3

CHAPTER 6 - The effect of operational parameters and biomass physical properties on the surface chemistry of biochar produced in a top-lit updraft biomass gasifier

Abstract

The objective of this study was to investigate the effect of airflow rate and biomass particle size, moisture content and compactness on the pH, acid and basic functional groups, and anion exchange capacity (AEC) and cation exchange capacity (CEC) of biochar. Wood chips were used as the feedstock. The airflow rate from 8 to 20 lpm was found to produce basic biochars (Ph>7.0) that contained basic functional groups. The biochar showed increasing CEC when increasing the airflow rate, but no acid functional groups were presented. The variation of moisture content, particle size and biomass compactness showed significant effects on the surface chemistry of biochar. The addition of moisture from 10 to 14% caused decrease in the pH from 12 to 7.43 but small or large particle sizes resulted in low pH. For instance, 30 mm particles generated biochar with pH of 2.3. As a result, the carboxylic functional group increased at low pH. Similarly, the biomass compactness exhibited a negative correlation with the pH that reduced with increasing compactness level. Thus the carboxylic acid functional groups of biochar increased from 0 to 0.016 mmol g^{-1}, and the basic functional group decreased from 0.115 to 0.073 mmol g-1 when biomass compactness increased from 0 to 3 kg.

6.1. Introduction

Biochar can be produced from a wide variety of organic wastes (Zhu et al., 2015). This carbon rich substance can be used for a number of applications such as carbon sequestration, soil conditioning and filtration of pollutants from aqueous and gas media (Ahmad et al., 2014;

Cheng et al., 2008; Kim et al. 2013). Initiatives to investigate new ways to produce biochar have been implemented in different parts of the globe (Brewer et al., 2009; Zhu et al., 2015; Kim et al., 2012; Qian et al., 2013). However, to date, slow pyrolysis is still the most known method for biochar production that is characterized for the thermal conversion of biomass in an oxygen-free atmosphere (Brick and Lyutse, 2010; Jameel et al., 2010). This process can take place at temperatures between 350 and 700^{o}C (Zhu et al., 2015). The operational parameters and the biomass type play an important role in the surface chemistry of biochar. Extensive work has been done in the evaluation of pyrolysis systems for production of biochar with specific properties (Mukherjee et al., 2011; Cheng et al., 2006; Moreno-Castilla 2000; Zhu et al., 2015). For example, Bagreev et al. (2001) characterized biochar from sewage sludge. It was reported that chemical modification induced by the variation of temperature caused modification to the chemical composition of the biochar that was initially identified by increase in pH (Nguyen et al., 2009). Similarly, Mukherjee et al. (2014) observed that the properties of biochar can drastically vary when comparing freshly produced biochar with aged biochar.

Biomass gasification has been demonstrated as an alternative to pyrolysis for the production of biochar (Brown, 2009). However, common gasification processes produce little biochar compared to the amount of gases generated (Qian et al., 2013). Consequently, there is insufficient literature on the characterization of the surface chemistry of this biochar. Top-lit updraft gasification is believed to have potential for biochar production because of its relatively high yield of biochar (up to 39%) with low energy input (Huangfu et al., 2014; Nsamba et al., 2014). Despite of all this, there is not sufficient literature focused on the surface chemistry of

biochar and the effect of the operational parameters and physical properties of the biomass. The characterization of biochars from top-lit updraft gasification can be a major indicator of the possible applications for the produced biochar (Ahmad et al., 2014).

The objective of this work was to investigate the effect of airflow rate and biomass moisture content, particle size and biomass compactness on the pH, anion exchange capacity *(*AEC), cation exchange capacity (CEC), and basic and acid functional groups of biochar produced in a top-lit updraft gasifier. Surface functional groups, pH and surface charge were some of the properties used to characterize the biochar and determine similitudes and correlations at different experimental parameters.

6.2. Materials and methods

Biochar from pine wood chips and rice hulls produced in a top-lit updraft gasifier were used. The biochar was generated at different airflow rates (8, 12, 16 and 20 lpm) and two insulation conditions, as described in chapter 1. The equivalent superficial velocities for the airflow rates were 0.83, 1.25, 1.66 and 2.08 cm/s, respectively. Biochar produced under different biomass physical properties was also evaluated. Wood chips with different average particle sizes (from 2 to 30 mm), moisture content (from 10 to 22%) and biomass compactness (from 0 to 3 kg) were used, as presented in chapter 3. The pH of the biochar samples was determined by mixing 0.4 g of biochar in 20 mL of de-ionized water for 8 hours (Bagreev et al., 2001;Das et al., 2013). The resulting solution was filtered with Whatman® filter paper (Qualitative #1) to remove large particles of biochar. Then, the final solution was filtered with Target2® nylon filters (0.2 μm). The pH of the solution was measured using a bench pH meter

(Model: UltraBasic U-10, Denver Instruments, Bohemia NY). Boehm titration method (Boehm, 1966) was implemented to determine the surface functional groups of the biochar. Four solutions ($NaHCO_3$, Na_2CO_3, NaOH and HCl) with 0.05 M were prepared. Fifty ml of each solution was mixed individually with 1 g of biochar for 24 hr. The final solutions were filtered using the same filtration method as the pH analysis. Finally, the solutions were titrated with the HCl (bases) and NaOH (acid) using methyl orange and phenolphthalein indicators, respectively. The AEC of the biochar samples was determined according to Lawrinenko (2014). 1 g of biochar was mixed with 40 ml of de-ionized water and 2 mL of KBr (1 M) for 48 h. Then, the biochar residue was filtered with Whatman® filter paper (Qualitative #1) and rinsed to achieve 5µS conductivity (Model: HI 9813-6, Hanna Instruments, Ann Arbor, MI). Next, 2 mL of $CaCl_2$ (2.5M) was added to the biochar slurry which was mixed for 48 h. The concentrated biochar was diluted with 200 mL of di-ionized water; 10 mL of this solution was then filtered with Target2® nylon filters (0.2 µm) and further diluted with 100 mL of di-ionized water. Bromide was detected from the final solution using an Ion Chromatograph (Dionex 500, Thermo Fischer Sci, Sunnyvale CA). The CEC was measured based on Kloss et al. (2012) and Dumroese et al. (2011). Initially, 2 g of biochar and 40 mL of de-iodized water were mixed overnight. Then, the samples were filtered with Whatman® filter paper (Qualitative #1). The washed biochar was placed in a flask with 20 mL of $BaCl_2$ (0.2 M) and mixed for 2 hours. The final solution was filtered with Target2® nylon filters (0.2 µm). The concentrations of Na, K, Mg, Ca, Al, Fe and Mn were measured via Inductively-coupled Plasma-Optical Emission Spectrometer (Perkin Elmar 8000, Waltham, MA). AEC and CEC calculations were performed following the methods described by Coleman et al., (1959). Statistical multiple comparison

analysis was performed to compared the effect of different levels of treatments. A SAS® GLM procedure with p-value<0.1 was implemented.

6.3. Results and discussion

6.3.1. Effects of gasification operational parameters on surface chemistry

Biochars produced at different airflow rates were found to be mainly basic (pH>7.0). As a result, no acidic functional groups were detected on the surface by Boehm titration characterization. Table 6.1 presents the results of the pH and the basic functional groups of the biochar when the airflow rate was increased in the top-lit updraft gasifier. In general, lower airflow rates resulted in biochar with lower pH. However, no statistical difference of the pH was presented when analyzing all the biochar samples. The basic functional group concentration increased with the airflow rate. It significantly increased from 0.0175 to 0.115 mmol g^{-1}. The increase in the basic functional group of the biochar was correlated with the peak reaction temperature of gasification that increased from 661 to 840°C (R^2=0.78). As increasing the airflow, the O/C atomic ratio of biochar was significantly reduced from 0.14 to 0.1 that indicated carbonization due to aromatization (Shafizadeh and Sekiguchi, 1982). Similarly, Zhu et al. (2015) performed microwave pyrolysis experiments with corn stover increasing the reaction temperature from 550 to 650°C. The increase of the temperature caused reduction in the O/C ratio of the biochar from 0.06 to 0.04. This suggested a more aromatic biochar due to the increase in carbon content and reduction of O (Kim et al., 2013). As a result, the basic functional group of biochar increased. The characterization of the biochar surface functional groups usually presents a combination of carboxylic, lactone and phenolic acidic

functional groups (Das et al., 2013; Bagreev et al., 2001). However, in the analysis of biochar produced at different airflow rates via top-lit updraft gasification, no acidic functionalities were detected. This is attributed to the fact that the carbonization of biomass in an oxygen-rich atmosphere can lead to the absence of acidic components on the surface of biochar. Boehm (1966) reported that the oxidation of black carbon at 420°C did not present formation of acidic functional groups as a result of the rapid carbonization of organic materials in the presence of oxygen.

Table 6.1. Chemical properties of biochar from wood chips. Moisture content 10%(w/w), avg. particle size 7 mm, biomass compactness 0 kg. Different superscripts represent significant differences in the order of a>b>c>d.

Airflow (lpm)	Peak temperature (°C)	pH of biochar	Basic functional group mmol g^{-1}	AEC cmol kg^{-1}	CEC cmol kg^{-1}	Atomic ratio	
						H/C	O/C
8	661.33^{d}	10.39^{a}	0.0175^{c}	1.38^{a}	3.43^{b}	0.27^{a}	0.14^{a}
12	743.00^{c}	11.99^{a}	0.02^{c}	1.03^{b}	3.03^{b}	0.26^{a}	0.10^{b}
16	798.33^{b}	10.49^{a}	0.0625^{b}	1.01^{b}	3.90^{b}	0.29^{a}	0.10^{b}
20	840.50^{a}	12.04^{a}	0.115^{a}	1.59^{a}	6.33^{a}	0.27^{a}	0.10^{b}

The results of the surface charge of the biochar are also presented in Table 6.1. The CEC of biochar from wood chips increased from 3.43 to 6.33 cmole kg^{-1} when the airflow rate increased from 8 to 20 lpm. This increase in the CEC of the biochar can be associated with the combustion temperature (R^2=0.55) that increased as increasing the airflow rate. Nguyen et al. (2009) carried out experiments to study the effect of carbon decomposition with oak wood biochar produced with slow pyrolysis. The carbonization temperature caused variation in the CEC of the biochar. The CEC of biochar from oak wood decreased from 13.1 to 8.9 cmole kg^{-1}, as the temperature increased from 350 to 600°C. In contrast, the O/C ratio of oak wood

decreased from 0.26 to 0.10. The increase in CEC in biochar from top-lit updraft gasification can be also attributed to the degree of oxidation due to partial oxidation of the biomass. For instance, Lehmann (2007) stated that biochar can achieve increase in CEC due to long term natural oxidation. Biochar extracts from the Amazonian have been exposed to oxidation for centuries; as a result, they present high CEC that can range from 0.79 to 21.3 cmol kg^{-1} (Liang et al., 2006). The use of biomass gasification for biochar production can represent a more extreme oxidation of biochar that is due to thermochemical reactions. On the contrary, natural oxidation is the result of exposure to biotic and abiotic interactions (Cheng et al., 2006). In addition, the AEC of the biochar was found to decrease from 1.38 to 1.01 cmol kg^{-1} when the airflow increased from 8 to 16 lpm. Whereas it significantly increased from 1.01 to 1.59 cmol kg^{-1} when the airflow was further increased from 16 to 20 lpm. The CEC was correlated with the AEC (R^2=0.58) that increased as the CEC increased. Similar association of the AEC and CEC was reported by Mukherjee et al. (2014) that produced oak wood biochar to test physiochemical effects of aging on biochar. The results indicated that increasing the pyrolysis temperature from 250 to 650ºC caused decrease in the AEC from 4.9 to 4.5 cmol kg^{-1}. Similarly, it reduced the CEC from 39.9 to 10.2 cmol kg^{-1}.

6.3.2. Effect of moisture content

The pH of the biochar was significantly reduced from 12.0 to 7.43 when the moisture content of the biomass varied from 10 to 14%, Fig. 6.1A. However, further addition of moisture did not encourage the reduction of pH in the biochar since it showed no significant difference at moisture contents higher than 14%. As result, the variation of the moisture content did not show acid functional groups in the biochar. Moreover, the moisture content increased the basic

functional group that significantly increased from 0.115 to 0.15 mmol g^{-1} (Table 6.2). Thus the basic functional group exhibited correlation with the reaction temperature (R^2=0.66) and with the pH (R^2=0.81). This effect can be associated to the fact that the O/C atomic ratio was also significantly reduced from 0.1 to 0.068 when the moisture content increased from 10 to 14%. In addition, the O/C ratio was correlated with the pH (R^2=0.87) that increased at higher O/C ratios. Similarly, the H/C ratio was positively correlated with the pH (R^2=0.97). All this indicated that the addition of moisture to the biomass promoted the reduction of the oxidation effect that resulted in lower pH levels, and it caused increase in the basic functional group of biochar.

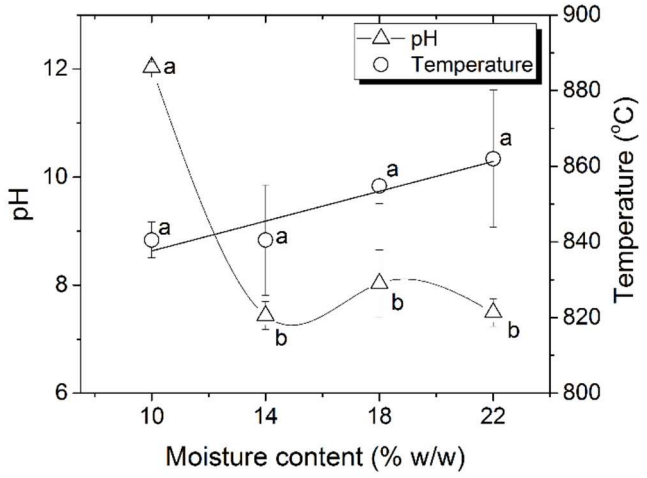

Fig. 6.1. (A) pH of biochar produced with biomass with different moisture contents (particle size 7 mm, biomass compactness 0 kg), and (B) pH and reaction temperature. Different superscripts represent significant difference.

Table 6.2. Atomic ratios of biochar from wood chips produced at different moisture contents – Different superscripts represent significant differences in the order of a>b>c>d.

Moisture content (%)	Basic functional group (mmol g^{-1})	Atomic ratios	
		H/C	O/C
10	0.115^{c}	0.271^{a}	0.100^{a}
14	0.135^{b}	0.200^{a}	0.068^{b}
18	0.137^{a-b}	0.200^{a}	0.065^{b}
22	0.15^{a}	0.186^{a}	0.075^{b}

6.3.3. Effect of particle size

In Fig. 6.2A, it is observed that biochar from particles with 2 mm size presented pH of 1.1, and it increased to 12.0 when increasing the average particle size to 7 mm. However, further increasing the particle size from 7 to 30 mm led to reduce the pH from 12.0 to 2.3. Likewise, the temperature was associated with the pH (R^2=0.91) since it increased with the reaction temperature (Fig. 6.2B). Therefore, the variation of the particle size and temperature no only contributed to change the pH of the biochar, but they also affected its surface chemistry because of the extreme pH levels, as presented in Table 6.3. The carboxylic acidic functional group of biochar decreased from 0.012 to 0 mmol g^{-1} when the particle size increased from 2 to 7 mm; whereas further increasing the particle size from 7 to 30 mm promoted increase of carboxylic functional groups from 0 to 0.012 mmol g^{-1}. Opposite to this, the basic functional group was maximum at particle size of 7 mm, and decreased to 0.012 mmol g^{-1} at small and large particle sizes. Acidic biochars exhibited carboxylic and basic functionalities which were correlated with the reaction temperature with R^2 of 0.88 and 0.73, respectively. This was different from the airflow and moisture content experiments that only had the basic functional group. In addition, the pH was found to be correlated with the carboxylic and basic functional groups with R^2 of 0.96 and 0.63, respectively.

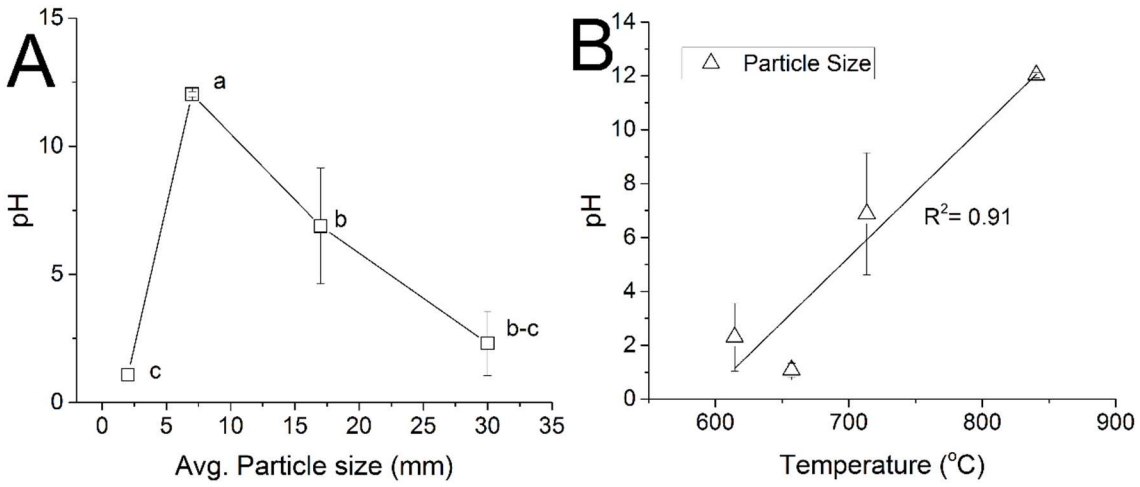

Fig. 6.2. (A) pH of biochar produced with wood chips with different particle sizes (moisture content 10%, biomass compactness 0 kg), and (B) pH and reaction temperature.

Variations in the carbonization temperature have been observed to play an important role in the surface chemistry of the biochar, and this changes can be initially identified by measuring pH of the carbonized materials (Bagreev et al. 2001). This effect of the reaction temperature has been widely reported in the literature (Bagreev et al., 2001P; Mukherjee et al., 2011). The increase in the peak temperature from 657 to 840°C when the particle size increase from 2 to 7 mm showed increase in the carbonization of the biomass. This can be observed in the reduction of the H/C atomic ratio from 0.35 to 0.27 that suggested decrease in polar functional groups (e.g. carboxylic) (Zhu et al., 2015). In an opposite way, the increase of the particle size from 7 to 30 mm caused reduction of the peak temperature from 840 to 614°C. Consequently, the carboxylic functional groups increased, and the H/C ratio was increased from 0.27 to 0.54 and it was correlated with the reaction temperature (R^2=0.72). Similar behavior was reported by Kim et al. (2013) that prepared biochar for aqueous metal removal

experiments. The results showed that as decreasing the reaction temperature from 600 to 300ºC the pH of the biochar reduced from 10 to 8.2. As a result, the H/C ratio of the biochar increased from 0.3 to 0.96. Overall, it was observed that large biomass particles promoted a higher level of aromatization since the O/C ratio decreased from 0.11 to 0.09. This can be attributed to the increased density of individual particles since the oxidation reactions are limited to the outer surface of the biochar (Bryden and Ragland, 1997).

Table 6.3. Chemical properties of biochar from wood chips produced with different particle sizes. Different superscripts represent significant differences in the order of a>b>c>d.

Avg. Particle size (mm)	Functional groups		Atomic ratios	
	Carboxylic (mmol g^{-1})	Basic (mmol g^{-1})	H/C	O/C
2	0.012^{a}	0.059^{b}	0.356^{a-b}	0.113^{a}
7	0^{b}	0.115^{a}	0.271^{b}	0.100^{a}
17	0.011^{a-b}	0.026^{c}	0.382^{a-b}	0.070^{b}
30	0.012^{a}	0.012^{c}	0.545^{a}	0.088^{a-b}

6.3.4. Effect of biomass compactness

Fig. 6.3A shows the correlation between the pH and the biomass compactness (Adj. R^2=0.91). As the biomass compactness increased from 0 to 3 kg, the pH of the biochar decreased from 12.0 to 0.95. The reaction temperature was positively correlated with the pH (R^2=0.69) that increased with the temperature, Fig. 6.3B. As a result, the carboxylic functional groups of the biochar increased from 0 to 0.016 mmol g^{-1} while the formation of basic functional groups was discouraged. Thus it decreased from 0.115 to 0.073 mmol g^{-1} (Table 6.4). This variation of the functional groups of biochar was highly correlated with the reaction temperature and pH. The carboxylic and basic functional groups showed R^2 of 0.91 and 0.95 as the reaction temperature increased, respectively. Similarly, the pH was correlated with the

carboxylic and basic functional groups with R^2 of 0.85 and 0.87, respectively. The increase in the biomass compactness indicated that more biomass was available per unit area within the top-lit updraft gasifier. Consequently, less air was available for the incomplete gasification reactions, and the reaction temperature was reduced. This can be observed in the O/C ratio that was significantly reduced from 0.1 to 0.063 when increasing the compactness from 0 to 1 kg. The reduction in the O/C ratio indicated that the reactions were driven in a less oxidative atmosphere. Moreover, further compacting the biomass (>2 kg) did not significantly affected the O/C ratio. The decrease in the O/C ratio in the carbonization of biomass in pyrolysis processes represents carbonization due to aromatization and dehydrogenation reactions that commonly occurs due to changes in the reaction temperature (Kim et al., 2013). Therefore, in the top-lit updraft gasification, the decrease in the O/C ratio might be further encouraged by the reduced oxygen relative to the amount of biomass.

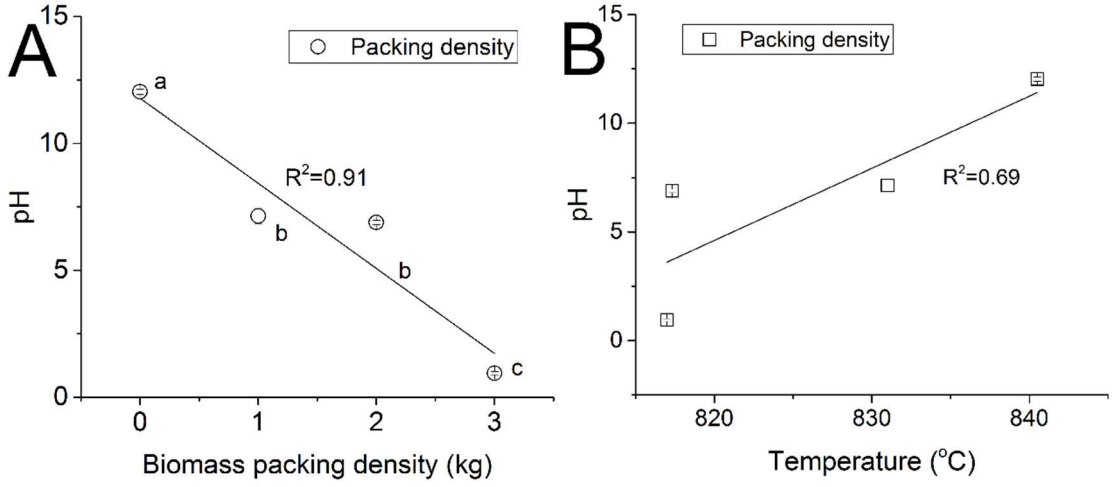

Fig. 6.3. (A) pH of biochar from wood chips produced at different biomass compactness (moisture content 10%, particle size 7 mm), and (B) pH and reaction temperature.

Table 6.4. Chemical properties of biochar from wood chips produced with different biomass compactness. Different superscripts represent significant difference.

Biomass compactness (kg)	Functional groups		Atomic ratios	
	Carboxylic (mmol g^{-1})	Basic (mmol g^{-1})	H/C	O/C
0	0^{b}	0.115^{a}	0.271^{a-b}	0.100^{a}
1	0.004^{b}	0.093^{a}	0.246^{b}	0.063^{b}
2	0.011^{a-b}	0.081^{a}	0.248^{a-b}	0.067^{b}
3	0.016^{a}	0.073^{a}	0.331^{a}	0.070^{b}

6.4. Conclusions

The effect of operational parameters and biomass physical properties on the biochar surface chemistry was investigated. When increasing the airflow rate, the basic functional groups of the biochar increased up to 0.115 mmol g^{-1} due to increase in the reaction temperature, but no acidic functional groups were observed because of the oxidative nature of the process. The CEC of biochar was found to increase when the airflow rate increased, and it reached a maximum of 6.33 cmole kg^{-1} at 20 lpm. This increase was driven by the degree of oxidation in the top-lit updraft gasifier that was accompanied by increase in the reaction temperature. The variation in the physical properties of the biomass were found to significantly affect the surface chemistry of the biochar. The increase in moisture content from 10 to 14% was found to reduce the pH of biochar from 12 to 7 due to reduced oxidative effects in the reactor. Furthermore, increasing woodchips particle size from 3 to 7 mm increased biochar pH from 1.1 to 12; whilst further increase in particle size from 7 to 30 mm reduced the pH from 12 to 2.3. As a result, the carboxylic functional groups increased with pH and the basic functional group decreased. Likewise, the increase in biomass compactness caused a proportional decrease in the pH of biochar that reached the minimum reported in this work of 0.95. This extreme decrease in the pH was the result of the reduced air for combustion

compared to the amount of biomass in the gasifier chamber that caused a less aggressive oxidation. Therefore, increase in compactness increased the carboxylic functional groups and reduced the basic functional groups.

6.5. References

Ahmad, M., Rajapaksha, A. U., Lim, J. E., Zhang, M., Bolan, N., Mohan, D. Ok, Y. S. (2014). Biochar as a sorbent for contaminant management in soil and water: A review. Chemosphere, 99, 19-33. doi:http://dx.doi.org/10.1016/j.chemosphere.2013.10.071

Bagreev, A., Adib, F., & Bandosz, T. J. (2001). pH of activated carbon surface as an indication of its suitability for H2S removal from moist air streams. Carbon, 39(12), 1897-1905. doi:http://dx.doi.org/10.1016/S0008-6223(00)00317-1

Bagreev, A., Bandosz, T. J., & Locke, D. C. (2001). Pore structure and surface chemistry of adsorbents obtained by pyrolysis of sewage sludge-derived fertilizer. Carbon, 39(13), 1971-1979.

Bazuła, P. A., Lu, A., Nitz, J., & Schüth, F. (2008). Surface and pore structure modification of ordered mesoporous carbons via a chemical oxidation approach. Microporous and Mesoporous Materials,108(1–3), 266-275. doi:http://dx.doi.org/10.1016/j.micromeso.2007.04.008

Brewer, C. E., Schmidt-Rohr, K., Satrio, J. A., & Brown, R. C. (2009). Characterization of biochar from fast pyrolysis and gasification systems. Environmental Progress & Sustainable Energy, 28(3), 386-396. doi:10.1002/ep.10378

Brick, S., & Lyutse, S. (2010). Biochar: Assessing the promise and risks to guide US policy. Natural Resources Defense Council Issue Paper.Available at: Http://www.Nrdc.org/energy/files/biochar_paper.Pdf (Accessed 3 November 2012),

Brown, R. (2009). Biochar production technology. Biochar for Environmental Management: Science and Technology, 127-146.

Bryden, K., & Ragland, K. (1997). Combustion of a single wood log under furnace conditions. Developments in thermochemical biomass conversion (pp. 1331-1345) Springer.

Cheng, C., Lehmann, J., & Engelhard, M. H. (2008). Natural oxidation of black carbon in soils: Changes in molecular form and surface charge along a climosequence. Geochimica Et Cosmochimica Acta,72(6), 1598-1610. doi:http://dx.doi.org/10.1016/j.gca.2008.01.010

Cheng, C., Lehmann, J., Thies, J. E., Burton, S. D., & Engelhard, M. H. (2006). Oxidation of black carbon by biotic and abiotic processes. Organic Geochemistry, 37(11), 1477-1488. doi:http://dx.doi.org/10.1016/j.orggeochem.2006.06.022

Coleman, N., Weed, S., & McCracken, R. (1959). Cation-exchange capacity and exchangeable cations in piedmont soils of North Carolina. Soil Science Society of America Journal, 23(2), 146-149.

Das, L., Kolar, P., Classen, J. J., & Osborne, J. A. (2013). Adsorbents from pine wood via K2CO3-assisted low temperature carbonization for adsorption of p-cresol. Industrial Crops and Products, 45, 215-222. doi:http://dx.doi.org/10.1016/j.indcrop.2012.12.010

Das, L., Kolar, P., Classen, J. J., & Osborne, J. A. (2013). Adsorbents from pine wood via K2CO3-assisted low temperature carbonization for adsorption of p-cresol. Industrial Crops and Products, 45, 215-222. doi:http://dx.doi.org/10.1016/j.indcrop.2012.12.010

Dumroese, R. K., Heiskanen, J., Englund, K., & Tervahauta, A. (2011). Pelleted biochar: Chemical and physical properties show potential use as a substrate in container nurseries. Biomass and Bioenergy,35(5), 2018-2027. doi:http://dx.doi.org/10.1016/j.biombioe.2011.01.053

Huangfu, Y., Li, H., Chen, X., Xue, C., Chen, C., & Liu, G. (2014). Effects of moisture content in fuel on thermal performance and emission of biomass semi-gasified cookstove. Energy for Sustainable Development, 21, 60-65. doi:10.1016/j.esd.2014.05.007

Jameel, H., Keshwani, D. R., Carter, S., Treasure, T., & Cheng, J. (2010). Thermochemical conversion of biomass to power and fuels. Biomass to Renewable Energy Processes, , 437-491.

Kim, K. H., Kim, J., Cho, T., & Choi, J. W. (2012). Influence of pyrolysis temperature on physicochemical properties of biochar obtained from the fast pyrolysis of pitch pine (pinus rigida). Bioresource Technology, 118, 158-162. doi:http://dx.doi.org/10.1016/j.biortech.2012.04.094

Kim, W., Shim, T., Kim, Y., Hyun, S., Ryu, C., Park, Y., & Jung, J. (2013). Characterization of cadmium removal from aqueous solution by biochar produced from a giant

miscanthus at different pyrolytic temperatures. Bioresource Technology, 138, 266-270. doi:http://dx.doi.org/10.1016/j.biortech.2013.03.186

Kloss, S., Zehetner, F., Dellantonio, A., Hamid, R., Ottner, F., Liedtke, V., . . . Soja, G. (2012). Characterization of slow pyrolysis biochars: Effects of feedstocks and pyrolysis temperature on biochar properties. Journal of Environmental Quality, 41(4), 990-1000.

Lawrinenko, M. (2014). Anion exchange capacity of biochar Retrieved from http://lib.dr.iastate.edu/cgi/viewcontent.cgi?article=4692&context=etd

Lehmann, J. (2007). Bio-energy in the black. Frontiers in Ecology and the Environment, 5(7), 381-387. Retrieved from http://www.jstor.org/stable/20440704

Liang, B., Lehmann, J., Solomon, D., Kinyangi, J., Grossman, J., O'neill, B., . . . Petersen, J. (2006). Black carbon increases cation exchange capacity in soils. Soil Science Society of America Journal, 70(5), 1719-1730.

Moreno-Castilla, C., López-Ramón, M. V., & Carrasco-Marín, F. (2000). Changes in surface chemistry of activated carbons by wet oxidation. Carbon, 38(14), 1995-2001. doi:http://dx.doi.org/10.1016/S0008-6223(00)00048-8

Mukherjee, A., Zimmerman, A. R., Hamdan, R., & Cooper, W. T. (2014). Physicochemical changes in pyrogenic organic matter (biochar) after 15 months of field aging. Solid Earth, 5(2), 693-704. doi:10.5194/se-5-693-2014

Mukherjee, A., Zimmerman, A. R., & Harris, W. (2011). Surface chemistry variations among a series of laboratory-produced biochars. Geoderma, 163(3–4), 247-255. doi:http://dx.doi.org/10.1016/j.geoderma.2011.04.021

Nguyen, B. T., & Lehmann, J. (2009). Black carbon decomposition under varying water regimes. Organic Geochemistry, 40(8), 846-853. doi:http://dx.doi.org/10.1016/j.orggeochem.2009.05.004

Nsamba, H. K., Hale, S. E., Cornelissen, G., & Bachmann, R. T. (2014). Improved gasification of rice husks for optimized biochar production in a top lit updraft gasifier. Journal of Sustainable Bioenergy Systems, 4(04), 225. doi:10.4236/jsbs.2014.44021

Qian, K., Kumar, A., Patil, K., Bellmer, D., Wang, D., Yuan, W., & Huhnke, R. L. (2013). Effects of biomass feedstocks and gasification conditions on the physiochemical properties of char. Energies, 6(8), 3972-3986. doi:10.3390/en6083972

Qian, K., Kumar, A., Patil, K., Bellmer, D., Wang, D., Yuan, W., & Huhnke, R. L. (2013). Effects of biomass feedstocks and gasification conditions on the physiochemical properties of char. Energies, 6(8), 3972-3986.

Shafizadeh, F., & Sekiguchi, Y. (1983). Development of aromaticity in cellulosic chars. Carbon, 21(5), 511-516. doi:http://dx.doi.org/10.1016/0008-6223(83)90144-6

Zhu, L., Lei, H., Wang, L., Yadavalli, G., Zhang, X., Wei, Y. Ahring, B. (2015). Biochar of corn stover: Microwave-assisted pyrolysis condition induced changes in surface functional groups and characteristics. Journal of Analytical and Applied Pyrolysis, 115, 149-156. doi:http://dx.doi.org/10.1016/j.jaap.2015.07.012

CHAPTER 7 - Modeling product distribution of a top-lit updraft biomass gasifier at varying operating conditions

Abstract

In this study, a kinetic model for the prediction of the products of top-lit updraft (TLUD) biomass gasification was developed. The three main zones within the TLUD gasifier, the pyrolysis, incomplete combustion and reduction reaction zones were incorporated in the model and were solved sequentially. The validation of the model was performed with experimental data from chapters 1 and 3 and was found qualitatively accurate in predicting product distribution of biochar, hydrogen, carbon monoxide, and tar in syngas at different airflow rates, moisture contents and particles sizes under isothermal condition. For wood chips and rice hulls, the model was able to predict the yield of biochar that had a difference of 0.32% and 0.64% at 20 lpm with the experimental data, respectively. Likewise, the model was able to predict the higher heating value with difference of 0.05 and 0.12 MJ/m^3 for wood chips and rice hulls, respectively. Similarly, the model had a close prediction of the biochar yield and higher heating value that presented differences with the experiments of 0.49% and 0.63 MJ/m^3 at 10% moisture content, respectively. However, when the particle size was varied, the model estimated lower yields of biochar (e.g., 4.3% less with particle size of 17 mm) than the experimental result. The model was evaluated with different biomass compactness, and it showed to predict the biochar yield (e.g. difference of 0.49% at 2 kg). Similarly, the model predicted the higher heating value of the syngas that varied from 3.98 to 3.45 for the model, and from 3.67 to 3.61 for the experimental results. The model predicted the qualitative tendency of the gas composition and tar content in all cases. Therefore, this model can be

implemented as a tool to evaluate the outputs of biomass gasification in a top-lit updraft gasifier.

7.1. Introduction

Agricultural residues and municipal wastes are some examples of raw materials that are being used to produce energy and biomaterials (Yahya et al., 2015). The conversion of biomass into useful products can take place through different processes such as chemical, biological and thermal conversion (Raheem et al., 2015; Azman et al., 2015; Kumar et al., 2015). Biomass gasification is the incomplete oxidation of biomass that produces syngas and biochar (Gomez-Barea and Leckner, 2010). Syngas is a gas mixture of H_2 and CO that can be used to generated electricity by direct combustion, and hydrocarbons including diesel and gasoline via FischerTropsch process (Jameel et al., 2010). Whereas biochar is a carbon-rich material that can be used to improve water and nutrients retention in soils, absorb pollutants and produce H_2 via steam reforming reactions (James et al., 2014; Winsley, 2007). Although gasifiers can produce biochars, they are designed and optimized to improve the yield of gas products by improving the carbon conversion efficiency that results in the nearly complete utilization of the carbon from the biomass (Sharma, 2008). Therefore, there is not extensive work focused on the production of biochar using gasification processes (Brown, 2009).

Top-lit updraft biomass gasifiers produce relatively high yield of biochar when compared with other gasification units such as fluidized bed, downdraft and updraft gasifiers (Nsamba et al., 2014). However, current available literature presents little attention to the combined production of syngas and biochar from this reactor. For instance, Huangfu et al.

(2014) studied the effect of the moisture content on the thermal performance and emissions of a top-lit updraft gasifier. However, the H_2 content of the syngas was not reported and the potential of the produced biochar was not addressed. Similarly, Saravanakumar (2007) studied the production of syngas from long stick wood in a top-lit updraft gasifier. However, the production of biochar from this process was not considered. The utilization of top-lit updraft gasification can not only help to efficiently produce biochar, but it also can simultaneously generate syngas (Nsamba et al., 2015). Extensive work has been made on the prediction of syngas from biomass gasification (Yang et al., 2004; Puig-Arnavat et al., 2010; Gobel et al., 2007). Several approaches have been implemented. These include equilibrium models, kinetic models and computer models (e.g. ASPEN, Computational fluid dynamics, etc.) (Gomez-Barea and Leckner, 2010; Patra and Seth, 2015). Syngas composition, tar content and carbon conversion were often considered in the modelling process (Tinaut et al., 2008). However, these models did not consider carbon as a product of gasification. It was rather associated with the prediction of conditions at which low gasification efficiency was expected (Fiaschi and Michelini, 2001). In contrast, pyrolysis models can effectively predict the yield of biochar from a wide number of biomasses (Sharma et al., 2015; Koufopanos et al., 1989). However, they are unsuitable for the prediction of biochar from biomass gasification because of the oxygen-free nature of the pyrolysis process that is contrary to the thermochemical oxidation of biomass gasification. As a result, a model that considers the prediction of biochar and syngas as products of gasification is needed.

The goal of this work was to develop a kinetic model for the prediction of the products of top-lit updraft biomass gasification. The production of biochar, syngas and tar were

considered in the model with two biomasses at varying airflow rates. In addition, the products of gasification were predicted when biomass with different particle sizes, moisture content and biomass compactness were used in the process. This approach can help to identify the expected output of the gasifier at different conditions.

7.2. Model

A model for the prediction of biochar (carbon), hydrogen, carbon monoxide, higher heating value and tar content was developed. The model considered chemical properties of the biomass as well as the moisture content and particle size. Similar to experiments in chapter 1, the products of biomass gasification were estimated for wood chips and rice hulls at 8, 12, 16 and 20 lpm; the equivalent superficial velocities for the airflow rates were 0.83, 1.25, 1.66 and 2.08 cm/s, respectively. Additionally, the effect of the moisture content and particle size in the gasification of wood chips was tested at 20 lpm, as it was presented in chapter 3.

The following assumptions were considered when modelling the top-lit updraft biomass gasifier:

- Tar fueled the incomplete combustion reaction and it occurred instantaneously.
- The concentration of reactants and products did not vary in the radial direction of the tubular reactor.
- The reactor operated in isothermal and adiabatic steady state mode.
- The pressure differential in the reactor was not significant.
- Ash did not react during thermochemical reactions.
- The control volume analyzed was 1 dm3.

- All gases were considered ideal gases.
- Heterogeneous reactions were not reversible.

In order to understand the gasification of biomass in a top-lit updraft biomass gasifier, it is important to picture the mechanisms of reaction within the gasifier chamber. It has been expressed in chapter 1 that as the flaming pyrolysis was displaced from the top to the bottom of the gasifier, several reactions took place. The heat from the combustion zone devolatilized the biomass located below this zone as part of pyrolysis reactions (Saravanakumar et al. 2007). Moreover, on the top of the combustion zone, biochar and gases generated reacted due to reduction reactions (Patra and Seth, 2015). Therefore, the model here described considered these three major zones in the following order: pyrolysis, incomplete combustion and reduction. The pyrolysis reactions were represented by the molar balance of equation (1) in which carbon, CO2, CH4 and tar (CH1.03O 0.03) are the products of the thermal decomposition of biomass (pyrolysis) at high temperature (Palma, 2013). Where α and β are the moles of hydrogen and oxygen in the biomass, respectively; and x1, x2, x3 and x4 are the moles of individual products generated during the pyrolysis of biomass.

$$CH_\alpha O_\beta \overset{\Delta T}{\rightarrow} x_1 C + x_2 CO_2 + x_3 CH_4 + x_4 CH_{1.03} O_{0.03} \qquad (1)$$

The initial yield of biochar was calculated based on the maximum amount of biochar generated when considering the carbon yield from cellulose, hemicellulose, and lignin as presented by Sharma (2011). Moreover, the incomplete combustion of tars took place with the corresponded air/fuel ratio for the selected airflow rates. Equation (2) shows the reaction of the incomplete combustion of tar that produces CO and H_2 (Tinaut et al, 2008).

$$CH_{1.03}O_{0.03} + 0.483\,O_2 \rightarrow CO + 0.516\,H_2 \quad (2)$$

The concentrations of products from the first two stages were used to feed the reduction reactions. Heterogeneous (solid/gas) reactions of the biochar and the gases from previous reactions were considered and presented in equations (3) – (5). Similar approach have been widely implemented in the literature (Babu and Sheth, 2006; Giltrap et al. 2003; Li-da et al., 2009).

$$C + CO_2 \rightarrow 2CO \quad (3)$$

$$C + 2H_2 \rightarrow CH_4 \quad (4)$$

$$C + H_2O \rightarrow CO + H_2 \quad (5)$$

Despite the fact that top-lit updraft gasification is often associated with downdraft biomass gasification (Perez et al, 2012), the characteristic reaction mechanisms of this reactor makes it able to produce biochar. Reed et al. (1988) presented an empirical equation for the prediction of the flaming pyrolysis time experienced by a biomass particle in a top-lit updraft gasification unit. This equation accounts for the moisture content, biomass density, reaction temperature, molar fraction of oxygen in the air, and shape of the biomass particles, equation (6). In this model, since the time for incomplete combustion of tars was considered instantaneous, the time for flaming pyrolysis was used to estimate the reaction time for the reduction reactions.

$$t_{fp} = \frac{0.207\,\rho\,F_s\,D\,(1+1.76\,F_m)(1+0.61D)e^{\left(\frac{9369}{RT}\right)}}{(1+3.46\,F_{O_2})} \quad (6)$$

where,

t_{fp} – Flaming pyrolysis time (min)

ρ – Density of the biomass particle (g/cm^3)

Fs – Sphericity of biomass materials (for biomass materials, Fs = 0.2, de Souza-Santos, 2004)

D – Diameter of biomass particle (cm)

F_m – Weight fraction of moisture content in biomass (g/g)

R – Ideal gas constant (J/mol/K)

T – Temperature (K)

F_{O_2} – Molar fraction of oxygen in the gasification agent (0.21 for air).

The reaction rates for the kinetic model are presented in equations (7)-(10). The reaction rate for the incomplete combustion of tar (7) was adopted from Tinaut et al. (2008). Moreover, the reaction rates for the reduction reactions were calculated based on reactions that obey the elementary rate law (Fogler, 2006), and they were considered to be no reversible, equations (8)-(9).

$$r_{Com} = T\ k_t C_{char} C_t^{0.5} \quad (7)$$

$$r_{gas1} = k_1 C_{char} C_{CO_2} \quad (8)$$

$$r_{gas2} = k_2 C_{char} C_{H_2O} \quad (9)$$

$$r_{gas3} = k_3 C_{char} C_{H_2}^2 \quad (10)$$

The kinetic constant k_i was calculated according to Arrhenius equation (11) that considers the temperature dependence of chemical reactions (Fogler, 2006).

$$k_i = A_i e^{-\frac{E_i}{RT}} \quad (11)$$

where k is the kinetic constant for reaction i, A - pre-exponential factor (1/s), E - activation energy (kJ/mol/K), T - reaction temperature (K) and R- ideal gas constant (KJ/mol). Table 7.1 presents the activation energy and pre-exponential factors for the rate reactions.

Table 7.1. Activation energy (E) and pre-exponential factors (A)

Reaction	A (1/s)	E (KJ/mol/K)	Reference
Tar	59.8	101.43	[1,2]
gas1	3.42 T	129.7	[1,2]
gas2	4.18E-3	129.7	[1,2,3]
gas3	7.301E-2	129.7	[1,2,3]

[1] Tinaut et al., 2008; [2] Perez, 2007; [3] Wang and Kinoshita, 1993

The differential equations presented below describe the production and disappearance of carbon, gases and tar due to incomplete combustion and reduction reactions. They were defined based on the fundamental equation (12) for batch reactors (Speight, 2002).

$$\frac{dC_j}{dt} = \sum_{i=1}^{R} \alpha_{i,j}\, r_i \quad (12)$$

where, *Cj* (moles/m3) is the concentration of a substance (j= Carbon, H2, CO, CH4, CO2, CO, H2O and tar), $\alpha_{i,j}$ is the stoichiometric coefficient for corresponding reactions, r_i is the reaction rate for individual reactions (equations 7, 8, 9 and 10), and t (seconds) is the reaction time.

Differential equations for the incomplete combustion of tar, equations (13) – (16):

$$\frac{dC_{tar}}{dt} = -r_t \quad (13)$$

$$\frac{dC_{O_2}}{dt} = -0.483\, r_t \quad (14)$$

$$\frac{dC_{H_2}}{dt} = 0.517\, r_t \quad (15)$$

$$\frac{dC_{CO}}{dt} = -r_t \qquad (16)$$

Differential equations for reduction reactions, equations (17) – (22):

$$\frac{dC_{Carbon}}{dt} = -r_{gas} - r_{gas2} - r_{gas3} \qquad (17)$$

$$\frac{dC_{CO_2}}{dt} = -r_{gas1} \qquad (18)$$

$$\frac{dC_{CH_4}}{dt} = r_{gas2} \qquad (19)$$

$$\frac{dC_{CO}}{dt} = 2\,r_{gas1} + r_{gas2} \qquad (20)$$

$$\frac{dC_{H_2O}}{dt} = -r_{gas2} \qquad (21)$$

$$\frac{dC_{H_2}}{dt} = r_{gas2} - 2r_{gas3} \qquad (22)$$

7.3. Calculations of kinetic model

The differential equation for tar combustion was solved in MATLAB® using the integrated ordinary differential equation solver ODE15s. The biomass concentration within the gasifier and the concentration of oxygen in the gasification agent were used as the initial reactants in the tubular reactor. Then, the outputs of modelling the incomplete combustion of tars were used as the initial reactants for the reduction reactions that were also solved using an ODE15s code.

7.4. Validation of model

The resulting concentrations of the products of gasification were compared with the experimental results presented in chapters 1 and 3. Biochar yield, hydrogen, carbon monoxide, higher heating value and tar content were analyzed for wood chips and rice hulls at different

airflow rates. In addition, the effect of varying the moisture content, biomass compactness and particle size of wood chips was examined.

7.4.1. Effect of airflow rate

Fig. 7.1 presents the prediction and experimental yield of biochar for rice hulls and wood chips at different airflow rates. Regardless of the biomass type, the yield of biochar decreased as the airflow rate increased. This trend was also presented by the model in close approximation to the experimental data for both biomasses. However, the consideration of the ash content in the calculation of the yield of biochar of rice hulls was crucial to predict the biochar yield. This was because of the high ash content in rice hulls (23%) and the configuration of the model to predict carbon content after it reacted in the solid/gas reactions within the reduction zone of the gasifier. In contrast, little difference was observed when considering the ash content of wood chips due to its low inorganic composition (0.57%).

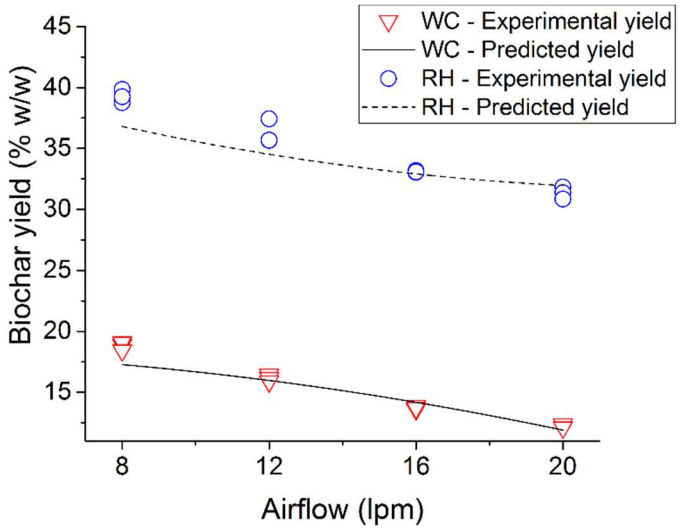

Fig. 7.1. Biochar yield of wood chips and rice hulls at varying levels of airflow rate. WC – wood chips, RH – rice hulls.

Table 7.2 presents the predicted and experimental results of H_2, CO, HHV and tar content of wood chips and rice hulls. For wood chips, the model presented accurate estimation of the HHV, but when comparing the predicted H_2 composition with the experimental results, it was over estimated at low airflow rates. However, the CO composition was under predicted at low airflow rates. In addition, the tar content showed by the experiments at low airflow was 60 g/m^3 higher than that predicted by the model, but at higher airflows little difference was presented between the model and experimental data. Likewise, the prediction of the products of rice hulls gasification showed that H_2 and tar content were over estimated by the model. However, a better estimation of HHV and CO was presented.

Table 7.2. Experimental and model comparison of gas properties and tar content from wood chips and rice hulls at different airflow rates. Particle size 2 mm, moisture content 10%, compactness 0 kg.

	Experimental results				Model results			
Airflow rate (lpm)	H_2(%) v/v	CO(%) v/v	HHV (MJ/m^3)	Tar (g/m^3)	H_2(%) v/v	CO(%) v/v	HHV (MJ/m^3)	Tar (g/m^3)
Wood chips								
8	3.31	13.72	3.17	86.24	6.37	7.04	3.45	26.13
12	4.68	14.27	3.50	49.30	6.59	8.31	3.42	20.88
16	5.43	14.23	3.57	22.19	6.65	11.99	3.77	17.85
20	6.61	14.97	3.93	12.99	6.68	14.59	3.98	15.25
Rice hulls								
8	2.83	14.22	3.12	16.56	6.91	9.95	2.73	68.40
12	3.69	15.09	3.34	6.62	7.01	13.19	3.05	54.63
16	4.26	15.97	3.49	2.95	7.11	15.40	3.30	48.73
20	4.23	15.80	3.37	2.76	7.23	15.26	3.25	41.32

7.4.2. Effect of particle size

The comparison of the predicted and experimental yield of biochar produced with different particle sizes is presented in Fig. 7.2. The biochar yield of the experimental results presented a similar tendency than that presented by the model. However, the predicted biochar yield at small (<7 mm) and larger (>7 mm) particle sizes was lower than that presented by the experiments. This could be related to the fact that the reactor was assumed to be isothermal. As result an overall higher temperature was presented in the reduction zone that lead to the utilization of more carbon in the solid /gas reactions (Babu and Seth, 2006; Wang and Kinoshita 1993).

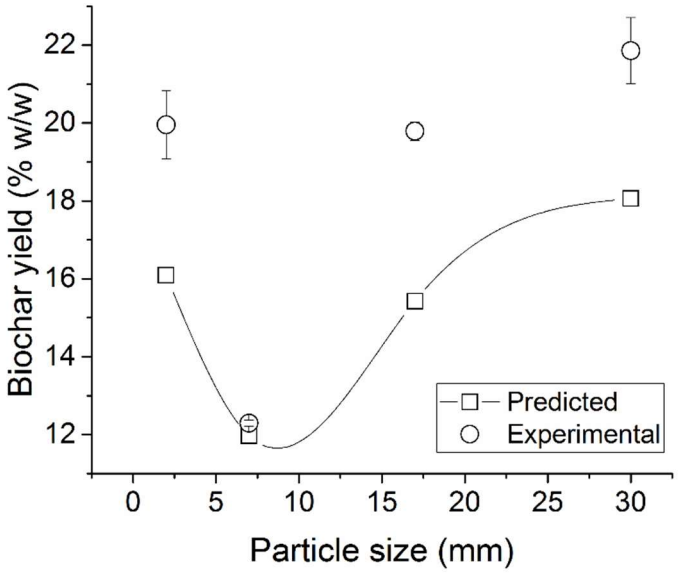

Fig. 7.2. Biochar yield of wood chips at different levels of particle size. Moisture content 10%, compactness 0 kg.

The prediction of syngas composition and tar content when varying the particle size also showed challenges in the prediction, Table 7.3. Even with the adjustment of the flaming

pyrolysis time at different diameters of particles, H_2 was not properly estimated since it showed to decrease with the particle size. This differed from the experimental data that presented a peak in the H_2 concentration at particle size of 7 mm. Furthermore, the CO and tar content were under estimated at small (<7 mm) and large (>7 mm) particle sizes, but the model performed a better estimation of the HHV of syngas.

Table 7.3. Experimental and model results comparison of gas properties and tar content from wood chips at different particle sizes. Airflow rate 20 lpm, moisture content 10%, compactness 0 kg.

	Experimental results				Model results			
Particle size (mm)	H_2(%) v/v	CO(%) v/v	HHV (MJ/m^3)	Tar (g/m^3)	H_2(%) v/v	CO(%) v/v	HHV (MJ/m^3)	Tar (g/m^3)
2	4.26	14.71	3.26	79.43	6.90	7.61	3.22	17.13
7	6.61	14.97	3.67	12.99	6.68	14.59	3.98	15.25
17	3.59	12.80	2.94	69.71	6.71	9.39	3.49	19.52
30	2.89	11.84	2.71	93.51	6.52	4.25	2.90	21.42

7.4.3. Effect of moisture content

The addition of the moisture content to biochar was found to decrease the biochar yield, Fig. 7.3. This tendency was also described by the model. However, at moisture contents higher that 18%, the biochar yield was under estimated by the model. This can be related to the fact that the increase of the moisture content increased the flaming pyrolysis time since additional energy was needed to devolatilize the biomass particles. As a result, the produced carbon was longer exposed to reduction reactions. Thus the yield of biochar was further decreased (Huangfu et al., 2014).

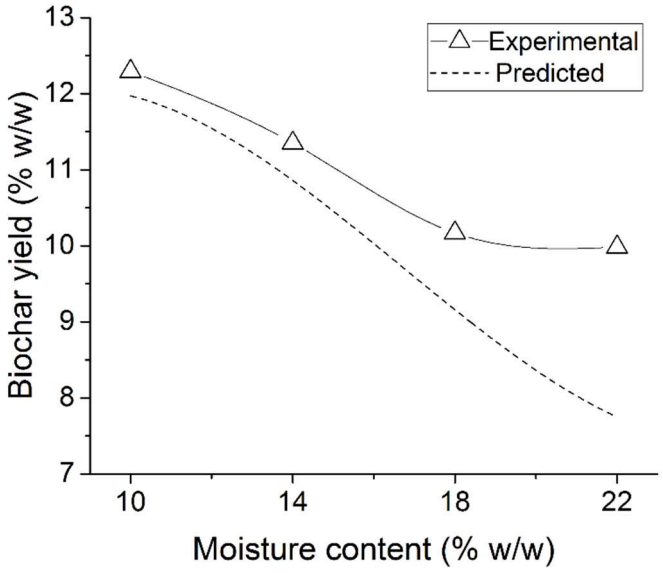

Fig. 7.3. Biochar yield of wood chips at different levels of moisture content. Particle size 7 mm, compactness 0 kg.

The developed kinetic model over predicted the H_2, CO and HHV of the syngas produced when moisture was added to the biomass, Table 7.4. In spite of this, it closely predicted the yield of tar at all levels of moisture content. The over prediction of H_2 could be related to the improved estimation of the tar. This is because more tar would have to be reacted in the incomplete combustion reaction for the tar content to reduce (Milne et al., 1998). Therefore, more H_2 was generated. Similarly, the over estimation of CO was the result of the additional carbon used in the reduction reactions due to the increase of the flaming pyrolysis time when the biomass contained more water.

Table 7.4. Experimental and model results comparison of gas properties and tar content from wood chips at different moisture contents. Airflow rate 20 lpm, particle size 7 mm, compactness 0 kg.

	Experiment				Model			
Moisture content (%)	H_2(%) v/v	CO(%) v/v	HHV (MJ/m^3)	Tar (g/m^3)	H_2(%) v/v	CO(%) v/v	HHV (MJ/m^3)	Tar (g/m^3)
10	6.61	14.97	3.67	12.99	6.68	14.59	3.98	15.25
14	5.73	12.92	3.13	7.56	6.99	14.07	3.76	10.40
18	5.62	10.51	2.65	6.18	7.07	15.35	3.84	8.39
22	6.02	11.16	2.84	6.24	7.17	15.92	3.85	6.37

7.4.4. Effect of biomass compactness

The biochar yield at different biomass compactness levels is presented in Fig. 7.4. The increase of the biochar yield when the biomass compactness increased was closely predicted by the model from 0 to 2 kg. However, the model under predicted the yield of biochar by 1.86% at biomass compactness of 3 kg. This can be due to the fact that despite the increase in the density of biomass; the reaction temperature and flaming pyrolysis time did not vary. As a result, little difference in the yield of biochar was achieved at biomass compactness of 3 kg.

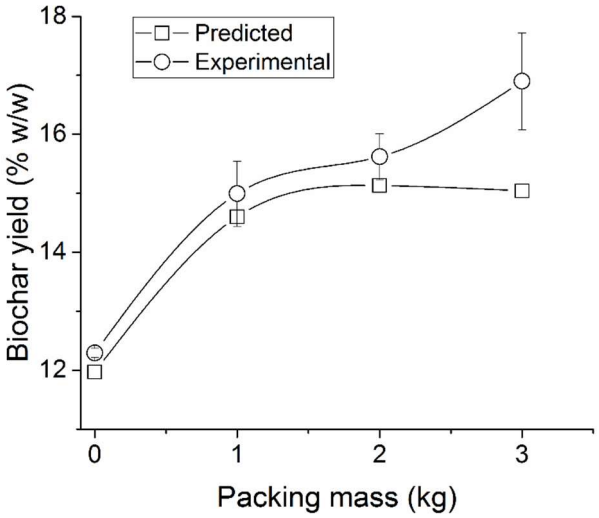

Fig. 7.4. Biochar yield of wood chips at different levels of compactness. Particle size 7 mm, moisture content 10%.

Table 7.5 shows the experimental and predicted syngas properties and tar content at different biomass compactness. The model was able to accurately predict the H_2 and HHV of the syngas. However, it under predicted the CO and tar content at high levels of compactness. For instance, it presented a difference of 30.64 g/m^3 in tar content between experimental and predicted result at 3 kg compactness.

Table 7.5. Experimental and model results comparison of gas properties and tar content from wood chips at different compactness. Airflow rate 20 lpm, particle size 7 mm, moisture content 10%.

	Experiment				Model			
Packing mass (kg)	H_2(%) v/v	CO(%) v/v	HHV (MJ/m^3)	Tar (g/m^3)	H_2(%) v/v	CO(%) v/v	HHV (MJ/m^3)	Tar (g/m^3)
0	6.61	14.97	3.67	12.99	6.68	14.59	3.98	15.25
1	5.91	14.50	3.49	24.87	6.89	9.71	3.37	14.61
2	5.73	14.82	3.52	20.42	6.91	8.89	3.31	15.00
3	5.80	15.25	3.61	47.51	6.79	9.61	3.45	16.87

7.4.5. Overall biochar yield

Fig. 7.5 shows the prediction and experimental values of biochar yield from wood chips when the airflow rate, particle size, moisture content and biomass compactness were considered. It is evident that a strong prediction of the biochar was achieved by the model at low biochar yields. However, at high experimental yields of biochar, the model under predicted their value. This can be explained by what was previously addressed in chapter 1. The reaction temperature was associated with the yield of biochar which decreased as the reaction temperature increased (Demirbas 2004; Demirbas 2001; Sun et al., 2014). Therefore, it can be stated that the proposed model can effectively predict the yield of biochar at high reaction temperatures (low biochar yield). However, it lacks of precision at low reaction temperatures

since higher values of biochar yield were shifted when they were compared with the experimental data.

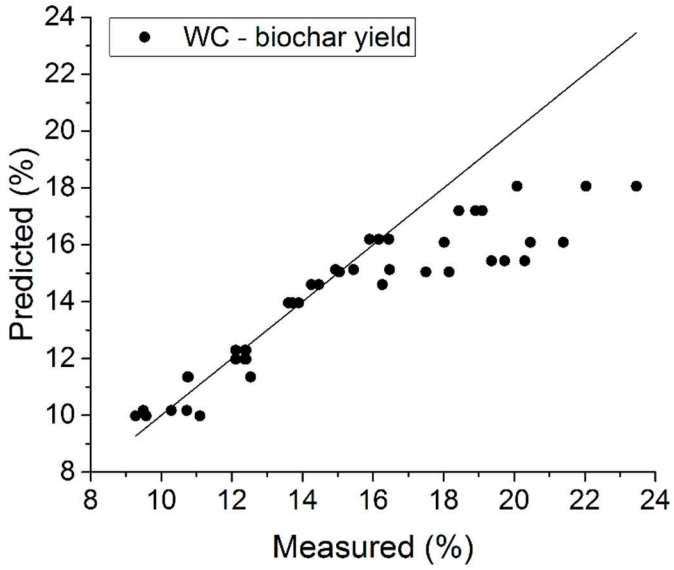

Fig. 7.5. Comparison of prediction and measure yield of biochar from wood chips (WC).

7.5. Conclusions

A model for prediction of the products of top-lit updraft biomass gasification was developed and validated with experimental data. The model showed accurate prediction of the biochar yield of wood chips and rice hulls at different airflow rates. Similarly, the model was able to predict the yield of biochar when the moisture content and compactness of wood chips was increased. However, when the particle size varied, the model underestimated the yield of biochar. The prediction of H_2 and CO compositions in syngas qualitatively matched experimental results. It could also predict the higher heating value at different airflow rates, particle sizes, moisture contents, and biomass compactness. In addition, the model predicted

the tar content in syngas when different moisture contents were used. However, it did not show accurate quantitative estimation of the tar content at varying airflow rates, particles sizes or biomass compactness, although the predicted tendency of the tar content matched the experimental results.

7.6. References

Azman, S., Khadem, A. F., van Lier, J. B., Zeeman, G., & Plugge, C. M. (2015). Presence and role of anaerobic hydrolytic microbes in conversion of lignocellulosic biomass for biogas production. *Critical Reviews in Environmental Science and Technology, 45*(23), 2523-2564. doi:10.1080/10643389.2015.1053727

Babu, B. V., & Sheth, P. N. (2006). Modeling and simulation of reduction zone of downdraft biomass gasifier: Effect of char reactivity factor. Energy Conversion and Management, 47(15–16), 2602-2611. doi:http://dx.doi.org/10.1016/j.enconman.2005.10.032

Brown, R. (2009). Biochar production technology. Biochar for Environmental Management: Science and Technology, , 127-146.

Demirbas, A. (2004). Effects of temperature and particle size on bio-char yield from pyrolysis of agricultural residues. Journal of Analytical and Applied Pyrolysis, 72(2), 243-248. doi:10.1016/j.jaap.2004.07.003

Demirbas, A. (2001). Carbonization ranking of selected biomass for charcoal, liquid and gaseous products. Energy Conversion and Management, 42(10), 1229-1238. doi:10.1016/S0196-8904(00)00110-2

Fiaschi, D., & Michelini, M. (2001). A two-phase one-dimensional biomass gasification kinetics model. Biomass and Bioenergy, 21(2), 121-132. doi:http://dx.doi.org/10.1016/S0961-9534(01)00018-6

Fogler, H. S. (2006). Elements of chemical reaction engineering. Upper Saddle River, NJ: Prentice Hall PTR. Retrieved from http://www2.lib.ncsu.edu/catalog/record/DUKE004662137

Font Palma, C. (2013). Modelling of tar formation and evolution for biomass gasification: A review. Applied Energy, 111, 129-141. doi:http://dx.doi.org/10.1016/j.apenergy.2013.04.082

Giltrap, D. L., McKibbin, R., & Barnes, G. R. G. (2003). A steady state model of gas-char reactions in a downdraft biomass gasifier. Solar Energy, 74(1), 85-91. doi:http://dx.doi.org/10.1016/S0038-092X(03)00091-4

Gøbel, B., Henriksen, U., Jensen, T. K., Qvale, B., & Houbak, N. (2007). The development of a computer model for a fixed bed gasifier and its use for optimization and control. Bioresource Technology,98(10), 2043-2052. doi:http://dx.doi.org/10.1016/j.biortech.2006.08.019

Gómez-Barea, A., & Leckner, B. (2010). Modeling of biomass gasification in fluidized bed. Progress in Energy and Combustion Science, 36(4), 444-509. doi:http://dx.doi.org/10.1016/j.pecs.2009.12.002

Huangfu, Y., Li, H., Chen, X., Xue, C., Chen, C., & Liu, G. (2014). Effects of moisture content in fuel on thermal performance and emission of biomass semi-gasified cookstove. Energy for Sustainable Development, 21, 60-65. doi:10.1016/j.esd.2014.05.007

Jameel, H., Keshwani, D. R., Carter, S., Treasure, T., & Cheng, J. (2010). Thermochemical conversion of biomass to power and fuels. Biomass to Renewable Energy Processes, , 437-491.

James R, A. M., Yuan, W., Boyette, M. D., Wang, D., & Kumar, A. (2014). In-chamber thermocatalytic tar cracking and syngas reforming using char-supported NiO catalyst in an updraft biomass gasifier.International Journal of Agricultural and Biological Engineering, 7(6), 91-97.

Koufopanos, C. A., Lucchesi, A., & Maschio, G. (1989). Kinetic modelling of the pyrolysis of biomass and biomass components. The Canadian Journal of Chemical Engineering, 67(1), 75-84. doi:10.1002/cjce.5450670111

Kumar, A., Kumar, N., Baredar, P., & Shukla, A. (2015). A review on biomass energy resources, potential, conversion and policy in india. Renewable and Sustainable Energy Reviews, 45, 530-539. doi:http://dx.doi.org/10.1016/j.rser.2015.02.007

Li-Da Zhong, Wang-Hong Mei, & Zhu Hong. (2009). Kinetic model establishment and verification of the biomass gasification on fluidized bed. Paper presented at the Machine Learning and Cybernetics, 2009 International Conference on, , 4 2112-2117. doi:10.1109/ICMLC.2009.5212211

Milne, T. A., Abatzoglou, N., & Evans, R. J. (1998). Biomass gasifier" tars": Their nature, formation, and conversion National Renewable Energy Laboratory Golden, CO.

Nsamba, H. K., Hale, S. E., Cornelissen, G., & Bachmann, R. T. (2015). Designing and performance evaluation of biochar production in a top-lit updraft up-scaled gasifier. Journal of Sustainable Bioenergy Systems, 5(02), 41.

Nsamba, H. K., Hale, S. E., Cornelissen, G., & Bachmann, R. T. (2015). Designing and performance evaluation of biochar production in a top-lit updraft up-scaled gasifier. Journal of Sustainable Bioenergy Systems, 5(02), 41.

Patra, T. K., & Sheth, P. N. (2015). Biomass gasification models for downdraft gasifier: A state-of-the-art review. Renewable and Sustainable Energy Reviews, 50, 583-593. doi:http://dx.doi.org/10.1016/j.rser.2015.05.012

Pérez, J. F. (2007). One dimensional model of the biomass gasification process in concurrent fixed bed: Experimental validation with inverted gasifiers.

Pérez, J. F., Melgar, A., & Benjumea, P. N. (2012). Effect of operating and design parameters on the gasification/combustion process of waste biomass in fixed bed downdraft reactors: An experimental study. Fuel, 96, 487-496.

Puig-Arnavat, M., Bruno, J. C., & Coronas, A. (2010). Review and analysis of biomass gasification models. Renewable and Sustainable Energy Reviews, 14(9), 2841-2851.

Raheem, A., Wan Azlina, W. A. K. G., Taufiq Yap, Y. H., Danquah, M. K., & Harun, R. (2015). Thermochemical conversion of microalgal biomass for biofuel production. Renewable and Sustainable Energy Reviews, 49, 990-999. doi:http://dx.doi.org/10.1016/j.rser.2015.04.186

Reed, T. B., Levie, B., & Graboski, M. S. (1988). Fundamentals, Development and Scaleup of the Air= Oxygen Stratified Downdraft Gasifier,

Saravanakumar, A., Haridasan, T. M., Reed, T. B., & Bai, R. K. (2007). Experimental investigation and modelling study of long stick wood gasification in a top lit updraft fixed bed gasifier. Fuel, 86(17–18), 2846-2856. doi:http://dx.doi.org/10.1016/j.fuel.2007.03.028

Sharma, A., Pareek, V., & Zhang, D. (2015). Biomass pyrolysis—A review of modelling, process parameters and catalytic studies. Renewable and Sustainable Energy Reviews, 50, 1081-1096. doi:http://dx.doi.org/10.1016/j.rser.2015.04.193

Sharma, A. K. (2008). Equilibrium and kinetic modeling of char reduction reactions in a downdraft biomass gasifier: A comparison. Solar Energy, 82(10), 918-928.

Sharma, A. K. (2011). Modeling and simulation of a downdraft biomass gasifier 1. model development and validation. Energy Conversion and Management, 52(2), 1386-1396.

Sun, Y., Gao, B., Yao, Y., Fang, J., Zhang, M., Zhou, Y. Yang, L. (2014). Effects of feedstock type, production method, and pyrolysis temperature on biochar and hydrochar properties. Chemical Engineering Journal, 240, 574-578.

Tinaut, F. V., Melgar, A., Pérez, J. F., & Horrillo, A. (2008). Effect of biomass particle size and air superficial velocity on the gasification process in a downdraft fixed bed gasifier. an experimental and modelling study. Fuel Processing Technology, 89(11), 1076-1089. doi:http://dx.doi.org/10.1016/j.fuproc.2008.04.010

Wang, Y., & Kinoshita, C. M. (1993). Kinetic model of biomass gasification. Solar Energy, 51(1), 19-25.

Winsley, P. (2007). Biochar and bioenergy production for climate change mitigation. New Zealand Science Review, 64(1), 5-10.

Yahya, M. A., Al-Qodah, Z., & Ngah, C. W. Z. (2015). Agricultural bio-waste materials as potential sustainable precursors used for activated carbon production: A review. Renewable and Sustainable Energy Reviews, 46, 218-235.

Yang, Y. B., Sharifi, V. N., & Swithenbank, J. (2004). Effect of air flow rate and fuel moisture on the burning behaviours of biomass and simulated municipal solid wastes in packed beds. Fuel, 83(11–12), 1553-1562. doi:http://dx.doi.org/10.1016/j.fuel.2004.01.016

CHAPTER 8 - Conclusions and Future work

8.1. Conclusions

The simultaneous production of biochar and syngas from Top-lit updraft biomass gasification was investigated. After evaluating gasification product distribution, physiochemical properties of biochar, properties of syngas and the effect of physical properties of biomass on gasification, the following conclusions have be drawn:

1. Increase in the airflow rate in the top-lit updraft gasifier caused increase of the reaction temperature regardless of the biomass type and insulation condition. As a result, the yield of biochar decreased and the hydrogen content increased. Similarly, the increase in airflow increased the biomass burning rate within the gasifier. Little difference was presented in the CO and higher heating value of syngas when using the insulation and increasing the airflow. However, the tar content decreased at higher airflows, but tar production in the syngas was encouraged by the addition of insulation. In addition, large amount of tars were observed in the biochar when the reactor was not insulated, but they were significantly reduced at higher airflows and with the addition of insulation. Rice hulls presented higher biochar yields than wood chips; this was associate with the high ash content of rice hulls since a considerable part of the biomass remained unreacted.
2. The airflow rate and the insulation had significant effect of the physiochemical properties of biochar from top-lit updraft biomass gasification. The oxygen content of biochar from rice hulls decreased as the airflow increased. However, the carbon,

hydrogen, nitrogen, fixed carbon and higher heating value were reduced as the airflow increased as a result of the predominated oxidation reactions because of the high ash content in the unreacted biomass. Moreover, no significant effect on the biochar chemical properties was presented by the insulation. In contrast, biochar from wood chips increased in carbon and fixed carbon as the airflow rate increased due to aromatization of biochar as the reaction temperature increased. The volatile matter of the two biomasses was significantly reduced after carbonization indicating that volatiles contributed to fuel the combustion zone. In addition, the BET surface area of the biochar from both biomasses was found to increase as the airflow rate increased because of the increase in the reaction temperature. Furthermore, the use of insulation presented higher BET surface areas due to the increase of the overall temperature in the gasifier.

3. The gasification process and the physiochemical properties of the biochar were affected by the moisture content, particle size and compactness of wood chips. The effect of the particle size displayed to two main behaviors. Particle sizes below 7 mm promoted increase in the yield of biochar, but they affected the physiochemical composition (e.g. BET surface area decrease) of biochar because of the reduction in the reaction temperature. Similarly, particles with size larger than 7 mm also increased the yield of biochar and decrease the reaction temperature. The increase in the moisture content caused considerable decrease in the burning rate, but it did not significantly change the combustion temperature. As result, the tar content of syngas was reduced to its minimum for wood chips of 6.24 g/m^3 because of reforming and cracking reaction in

the gasifier. The increase in density by compacting the biomass increased the yield of biochar, but it stimulated the formation of excessive tars in the syngas. This was because the additional biomass per unit area that was reacted with the same amount of air than when no compacted. Finally, the physical properties of the biomass can strongly affect the properties of the biochar because of the changes in reaction temperature.

4. The biochar surface chemistry was changed by the airflow rate and the variation of the physical properties of wood chips. The increase of the airflow rate caused increase in the basic functional groups, AEC and the CEC surface charge of biochar. This was the result of the oxidative nature of the gasification process and the increase in the reaction temperature. No acid functional groups were detected by varying the airflow because of the high pH of biochar (>10.3). The increase in the particle size showed two tendencies. Particles lower than 7 mm exhibited pH as low as 1.1. As a result, the carboxylic functional group was detected in the biochar. In a similar way, increase in the particle size higher than 7 mm also presented lower pH level that also resulted in the presence of carboxylic functional group in the biochar. These lower pH were achieved because of the reduced combustion temperature at small (<7 mm) and large (>7 mm) particle sizes. The addition of moisture to the biomass decrease the pH of the biochar from 12 to 7, and it increased the basic functional group, but no acidic functional groups were identified. In addition, the increase in compactness also reduced the pH of the biochar that decreased to 0.95. This decrease in pH was the result of the reduced oxidation effect of biomass due to excessive biomass relatively to the air for

combustion when the biomass was compacted. Moreover, the reduction of pH below 7.0 resulted in increase in the carboxylic functional group of biochar and decrease in the basic functional group.

5. A model for the prediction of the products of top-lit updraft biomass gasification was developed and validated. The model was designed to predict the products at different airflow rates, particle size, moisture content, and biomass compactness. The model was able to quantitatively predict the yield of biochar and higher heating value of syngas at all conditions, except when varying the particle size that presented under prediction of the biochar yield. In addition, the model did not quantitatively estimated the H_2, CO and tar produced in the reactor when different conditions were tested. However, it showed the tendencies of the tar content at different conditions. Therefore, this model can be an effective tool for the determination of products from biomass gasification in a top-lit updraft gasifier.

8.2. Contributions

This research covered the evaluation of biochar, syngas, and tar production in a top-lit updraft gasifier. It additionally investigated the chemical and physical properties of biochar at different gasification conditions. Therefore, the conclusions of this work can be used to further investigate the utilization of biochar from top-lit updraft gasification for potential biochar applications. For example, biochar produced from this process can be implemented in waste water treatments, removal of air pollutants, soils conditioning and to improve soil

nutrient retention. This work can also serve as the base to implement biochar surface chemistry and charge modification techniques for targeted applications in one step process via top-lit updraft gasification.

8.3. Future work

1. The characterization of tars produced with different gasification operational parameters and biomass physiochemical properties in a top-lit updraft gasifier needs to be considered. This study would identify and quantify tar components generated under different gasification conditions. It would also contribute to investigate the effect of the physical and chemical properties of biomass on the concentration of different tar components. Therefore, correlations between the different gasification conditions and tar composition can be made in order to predict specific tar components in top-lit updraft biomass gasification. This could help to understand tar production in this gasifier and diagnose the best tar cracking and reforming methods to reduce to minimum tars generation.
2. The effect of chemical pre-treatment of biomass for biochar production in a top-lit updraft gasifier is a topic that needs to be studied. The use of chemicals for biomass pre-treatment might modify the physiochemical properties and the surface chemistry of biochars. As a result, correlations between biomass pre-treatment and properties of the biochar can be established. This can help to identify and implement procedures for production of biochar with required properties for specific applications.

APPENDICES

Appendix A - Calculation of Orthogonal Coefficients

Calculation of Orthogonal Coefficients for Unequal Intervals according to:
Grandage, A. "130. Query: Orthogonal Coefficients for Unequal Intervals." *Biometrics* 14.2 (1958): 287-289.

Linear orthogonal coefficient:

X_i	$\varepsilon_{1i} = X_i + a_1$	ε_{1i}
2	$2 + a_1$	-12
7	$7 + a_1$	-7
17	$17 + a_1$	3
30	$30 + a_1$	16
Sum:	$56 + 4\ a_1 = 0$	0
	$a_1 = -14$	

Quadratic orthogonal coefficient:

X_i	ε_{1i}	$\varepsilon_{2i} = X^2_i + b_2\ X_i + a_2$	$\varepsilon_{1i}\ (X^2_i = b_2\ X_i + a_2)$	ε_{2i}
2	-12	$4 + 2\ b_2 + a_1$	$- 48 - 24\ b_2 - 12\ a_1$	83.289
7	-7	$49 + 7\ b_2 + a_1$	$- 343 - 49\ b_2 - 7\ a_1$	-34.122
17	3	$289 + 17\ b_2 + a_1$	$867 + 51\ b_2 + 3\ a_1$	-118.948
30	16	$900 + 30\ b_2 + a_1$	$14400 + 480\ b_2 + 16\ a_1$	69.779
Sum:	0	$1242 + 56\ b_2 + 4\ a_1$	$14877 + 458\ b_2 + 0 = 0$	0
		$a_1 = 144.255$	$b_2 = - 14877/458$	

Appendix B – Multiple linear regression

Considerations for multiple linear regression:

1. Backward selection
2. Use of coefficient of orthogonal polynomials for equally spaced intervals
3. In case of major violations of the assumptions, use a correction method for the dependent variable was implemented. As result, tar content was adjusted to Ln(tar), natural logarithm of tar.
4. Use of collinearity diagnostics to determine instability of the model and high standard errors. See SAS/STAT® 9.2 User's guide, Second Edition. "Collinearity Diagnostics". Last accessed: August 2015.
5. Model assumptions: Error is random and identically distributed normal random variables that contain mean of 0 and variance σ^2.

General model code:

```
%let depvar= lntar; /* indicate the variable of interest */

data a;
 input
airflow     insulation ps     wt    pack  yield Htemp tar   sqrttar
      lntar       unosqrttar  br    sqrtbr      lnbr  unosqrtbr   h2    co
      synhhv      charwt      volatile    ash         fixcar      carbon
      C2    Hydrogen    N     S     O     charhhv;
AFL = (-3)*(airflow=8)+(-
1)*(airflow=12)+(1)*(airflow=16)+(3)*(airflow=20);
AFQ = (1)*(airflow=8)+(-1)*(airflow=12)+(-
1)*(airflow=16)+(1)*(airflow=20);
WTL = (-3)*(WT=10)+(-1)*(WT=14)+  (1)*(WT=18) + 3*(WT=22);
WTQ = ( 1)*(WT=10)+(-1)*(WT=14)+ (-1)*(WT=18) + 1*(WT=22);
PKL = (-3)*(PACK=0)+(-1)*(PACK=1)+  (1)*(PACK=2) + 3*(PACK=3);
PKQ = ( 1)*(PACK=0)+(-1)*(PACK=1)+ (-1)*(PACK=2) + 1*(PACK=3);
PSL = (-12)*(PS=2)+(-7)*(PS=7)+  (3)*(PS=17) + 16*(PS=30);
PSQ = ( 83.289)*(PS=2)+(-34.122)*(PS=7)+ (-118.948)*(PS=17) +
69.779*(PS=30);
datalines;

Copy data here
;

ods graphics on;
proc reg data=a;
  mod1: model &depvar = AFL AFQ WTL WTQ PSL PSQ PKL PKC insulation/vif stb
tol COLLIN;
 run;
```